COMPOUND SPECIFIC ISOTOPIC ANALYSIS TO INVESTIGATE SOURCES AND DEGRADATION OF GLYPHOSATE

Dissertation

der Mathematisch-Naturwissenschaftlichen Fakultät

der Eberhard Karls Universität Tübingen

zur Erlangung des Grades eines

Doktors der Naturwissenschaften

(Dr. rer. nat.)

Vorgelegt von
Emmanuel Onyonka Mogusu
aus Kenia

Tübingen
2015

*"Penye nia kuna njia" Where there is a will, there is a wa***y – African proverb**

"Education is not the learning of facts, but it is the training of the mind to think" **–Albert Einstein**

"*The fear of the Lord is the beginning of knowledge*" - **Proverbs 1:7**

Tag der mündlichen Qualifikation: 18.12.2015

Dekan:	Prof. Dr. Wolfgang Rosenstiel
1. Berichterstatter:	PD. Dr. Martin Elsner
2. Berichterstatter:	Prof. Dr. Stefan Haderlein

TABLE OF CONTENTS

Acknowledgement x

Summary xii

Zusammenfassung xv

1.1 Introduction

1.1.1 Pesticides 2

1.1.2 Pesticides in the environment 2

1.1.3 Glyphosate herbicide 4

1.1.4 Physical properties 5

1.1.5 Glyphosate degradation in the environment 6

1.1.6 Glyphosate herbicide in groundwater 9

1.2 Compound specific isotopic analysis 9

1.2.1 Expected stable isotope fractionation of glyphosate and AMPA 12

1.2.2 Practical challenges of glyphosate analysis 12

1.3 Scope of the study 12

1.3.1 Objective 1: 12

1.3.2 Objective 2: 13

1.3.3 Objective 3: 13

Dual Element ($^{15}N/^{14}N$, $^{13}C/^{12}C$) Isotope Analysis of Glyphosate and AMPA: Derivatization-Gas Chromatography Isotope Ratio Mass Spectrometry (GC/IRMS) Combined with LC/IRMS

Abstract: 15

2.1 Introduction 16

2.2 Experimental section 20

2.2.1 Materials 20

2.2.2 Derivatization with trimethyl silyl diazomethane (TMSD) 20

2.2.3 pH Optimization 21

2.2.4 GC-MS conditions 21

2.2.5 Nitrogen isotope analysis by GC/IRMS 22

2.2.6 Carbon isotope analysis by LC/IRMS 22

2.2.7 Elemental analysis / isotope ratio mass spectrometry (EA/IRMS) 23
2.2.8 Standard and sample measurement 24
2.2.9 Abiotic degradation of glyphosate with MnO_2 24
2.3 Results and discussion 25
2.3.1 Derivatization of glyphosate and AMPA 25
2.3.2 Optimum pH conditions for accurate isotope analysis 26
2.3.3 Effects of glutamate (amino acids) during derivatization with iso-PCF 28
2.3.4 Variability of excess derivatization agent 30
2.3.5 Validation of the method 32
2.3.6 Glyphosate analysis of different commercial herbicides. 33
2.3.7 Nitrogen isotope ratios during abiotic degradation 34
2.4 Conclusions 35
Compound-specific Isotope Fractionation during Biodegradation of Glyphosate with *Ochrobactrum sp.* FrEM
Abstract 39
3.1 Introduction 40
3.2 Experimental Methods 41
3.3 Results and discussion 44
3.3.1 Isolation and biodegradation of glyphosate 44
3.3.2 Stable isotope fractionation of glyphosate during biodegradation 46
3.3.3 Stable isotope fractionation of glyphosate during abiotic degradation 48
3.3.4 Dual isotope plot 49
3.4 Environmental significance 50
Extraction of Glyphosate from Water with Activated Alumina: Parameter Optimization and Preliminary Isotope Measurements
Abstract 53
4.1 Introduction 54
4.2 Experimental Methods 56
4.2.1 Materials 56
4.2.2 Batch adsorption experiment 56
4.2.3 Desorption efficiency 58
4.2.4 Extraction of glyphosate on packed alumina column 58

4.2.5 LC-MS/MS measurements 58
4.2.6 Nitrogen isotope analysis by GC/IRMS 59
4.2.7 Carbon isotope analysis by LC/IRMS 60
4.2.8 Elemental analysis / isotope ratio mass spectrometry (EA/IRMS) 60
4.3 Results and Discussions 61
4.3.1 Adsorption isotherm 61
4.3.2 Expected effect of pH on adsorption 62
4.3.3 Desorption of glyphosate 64
4.3.4 Isotope effects of glyphosate during sorption on alumina 66
4.3.5 Glyphosate enrichment on modified column 68
4.4 Conclusion 70
5.0 Conclusion and Outlook 72
References 78
Appendices i
Appendix I: List of Tables and Figures ii
Appendix II: Chapter 2- SI vi
Appendix III: Chapter 3- SI xii
Materials ..... *xiii*
Derivatization reaction with FMOC-Cl ..... *xiii*
LC/MS-MS measurements ..... *xiii*
Derivatization of glyphosate and AMPA for nitrogen isotope analysis ..... *xiv*
Nitrogen isotope analysis by GC/IRMS ..... *xv*
EA/IRMS ..... *xv*
Practical challenges during separation on LC/IRMS ..... *xviii*
Attempts of glyphosate degradation with Ochrobactrum anthropi GPK3 ..... *xxii*
Graphic Art ..... *xxiv*
Appendix IV: Chapter 4- SI xxv
Appendix V: CURRICULUM VITAE/LEBENSLAUF xxxii

Acknowledgement

First and foremost, I take this special opportunity to greatly thank my direct supervisor PD Dr. Martin Elsner for giving me the chance to pursue my PhD dissertation in his group (Environmental isotope chemistry group). I thank him for his inspiring guidance and endless support during my PhD studies. I learnt so much during the entire time.

I also wish to thank my second advisor Prof. Dr Stefan Haderlein from the University of Tübingen for his support with my registration at the University of Tübingen and communication with the Scholarship agency officials (DAAD) during the entire time of my research.

This research thesis was supported by the German National Science Foundation (DFG) within the Priority Program SPP1315 and the DAAD (Duetsche Academic Austausche Deinest) scholarship that also supported my stay in Germany. I thank the DAAD selection committee for giving me the invaluable opportunity to conduct my research in Germany and also for further elongating my fellowship (6 months). I thank Prof. Rainer Meckenstock the former director of the Institute of ground water (IGÖE) and PD Dr Christian Griebler now the acting director for allowing me to conduct my research at the Institute. I also thank the HELENA graduate school (at the Helmholtz research center) for the financial support to attend regional and international conferences (Goldschmidt 2014 in Sacramento USA) that made it possible for me to share my research work. I appreciate the workshops that were organized by HELENA graduate school. They were very helpful for the development of my career.

Special thanks to external collaborators from the University of Duisburg-Essen: Dr. Maik Jochmann, Mr. Benjamin Wolbert, Dr. Dorothea Kujawinski and Prof. Dr Torsten Schmidt for their support and contribution towards the joint publication of chapter 2 and 3 of this thesis. I thank Dr Gwenaël Imfeld from the University of Strasbourg, France for collecting field soil samples that we used for our experiments. Thanks to Dr. Alexey A. Leontievsky from G.K. Skryabin Institute of Biochemistry and Physiology of Microorganisms, Russian Academy of Sciences for kindly sharing bacterial strains (*Ochrobactrum antropia* GPK 3 *and Achromobacter sp)* which were used at the beginning of our biodegradation experiments.

I would also thank my dearest colleagues at IGÖE: Stefan, Armin Meyer, Shiran Qui, Sviatlana, Housna, Zhenya, Clemens, Janina, Kathrin, Alfredo, Heide, Michael Stöckl, Michael Maier, Anja Wunderlich and Myriam for their support and contributions. They provided a good working atmosphere.

This work is dedicated to my parents, fiancé and all my entire family for their patience, prayers and support during the whole time. This was all made possible through Christ in us the hope of glory.

Summary

Synthetic organic pesticides have world wide applications for agriculture and livestock management for the control of pest, disease and weeds. Increasing detection of pesticides in groundwater is of concern to drinking water provides. Therefore, to assess fate and transformation of organic pesticides in the environment the first step is to address the risks of soil and water contamination. Biodegradation, or natural attenuation, is the most sustainable approach for the removal of pesticide contaminants in the environment. However, to identify this process, conventional methods (measuring changes in concentrations and identifying metabolites) is challenging and not always conclusive. In particular, transformation products are not always detected and other processes such as dilution, dispersion and sorption may also cause changes in contaminant concentrations. Complementary tools are therefore warranted. Compound-specific isotopic analysis (CSIA) is a complementary approach to investigate sources and degradation of organic pollutants based on patterns and changes in their stable isotope ratios.

This thesis focuses on glyphosate ((*N*-phosphomethylglycine)), a widely used post-emerging, non-selective herbicide that is effective against weeds. Glyphosate and its main degradation product AMPA (aminomethyl phosphonic acid) are frequently detected in surface and groundwater above the EU (European Union) general concentration threshold value of pesticides (0.1 µg/L). In addition, recently, it was classified as probably carcinogenic to humans by the World Health Organization's cancer research unit. To investigate sources and degradation of glyphosate and AMPA, we bring forward CSIA as a promising complementary tool.

The first objective of this thesis was the development and optimization of a stable isotope analysis method to analyze $^{15}N/^{14}N$ in glyphosate and AMPA. A recent study on $^{13}C/^{12}C$ analysis of glyphosate and AMPA demonstrated the potential, but also the limitations for product authentication when only isotopes of one element were analyzed [1]. My motivation was to advance isotope ratio analysis of an additional element so as to exploit the full potential of multiple elements analysis ("two-dimensional CSIA"). To this end, chapter 2 presents compound-specific $^{15}N/^{14}N$ analysis of glyphosate and AMPA by a two-step derivatization in combination with GC/IRMS. In the first step, the N-H group was derivatized with isopropyl chloroformate (iso-PCF), and in the second step the remaining acidic groups

were methylated with trimethylsilyldiazomethane (TMSD). Buffering the solution at pH 10 was crucial to obtain accurate nitrogen isotope ratios. The limits for accurate $\delta^{15}N$ analysis of glyphosate and AMPA were 150 ng and 250 ng injected, respectively. A combination of $\delta^{15}N$ and $\delta^{13}C$ analysis (i) enabled an improved distinction of commercial glyphosate products and (ii) showed that glyphosate isotope values during degradation by MnO_2 clearly fell outside the commercial product range. This highlights the potential of combined carbon and nitrogen isotopes analysis to trace sources and degradation of glyphosate.

The second objective of my thesis was to determine isotope fractionation during degradation of glyphosate. To this end, chapter 3 was dedicated to determining bulk isotope enrichment factors in laboratory experiments as a basis to characterization abiotic and biotic degradation processes (biodegradation vs. abiotic degradation of glyphosate with MnO_2). A bacterial strain was isolated from a vineyard field site (northern France, using enrichment cultivation) and showed the ability to utilize glyphosate as phosphorus source. The strain was identified by 16S rRNA sequence analysis as *Ochrobactrum* sp. FrEM 15651. AMPA was not detected during glyphosate biodegradation, however, the evidence of sarcosine confirmed an alternative degradation route – the sarcosine pathway (C-P cleavage). A small carbon and nitrogen isotope fractionation of -4.8‰ ± 0.5‰ and -0.6‰ ± 0.7‰ respectively, was observed during biodegradation of glyphosate with *Ochrobactrum sp.* FrEM. This suggests that the intrinsic isotope fractionation may have been masked. The $AKIE_{carbon}$ for biotic degradation was calculated as 1.014. In the case of abiotic degradation of glyphosate with manganese dioxide (MnO_2), the nitrogen isotope fractionations were as high as ε_N = -17‰ ±0.5‰. The strong nitrogen isotope fractionation during abiotic degradation of glyphosate would leave a robust imprint of degradation in natural systems. The $AKIE_{carbon}$ during abiotic degradation was calculated as 1.011. The dual isotopic analysis for $\Delta\ \delta^{13}C$ and $\delta^{15}N$ slope (4.6 ± 0.03, 0.4 ± 0.03) was able to distinguish abiotic and biotic degradation pathways.

The third objective of this thesis was to develop an enrichment method to extract glyphosate and AMPA from water. The Chapter 4 of this thesis describes the preliminary results of enrichment tests using activated alumina-packed columns to extract and enrich glyphosate from water. The activated alumina had an adsorption capacity and surface density of 85 mg/g and 2 µmol/m^2, respectively. The adsorption of glyphosate on activated alumina was pH dependent. Glyphosate was adsorbed at a pH value that was lower than the PZC (point of zero charge) of the alumina surface so that the surface was positively and glyphosate negatively

charged. Desorption of glyphosate, in contrast, was favored above pH 10 where glyphosate molecules and the alumina surface were both negatively charged. Preliminary isotope values ($^{13}C/^{12}C$ & $^{15}N/^{14}N$) of glyphosate after enrichment on activated alumina suggest no significant isotope effect is expected compared to the input laboratory working glyphosate standard when extraction conditions are optimized. Therefore, there is promising potential to use activated alumina for the enrichment of glyphosate and AMPA from water to enable CSIA applications to detect glyphosate degradation, and to explore the source of AMPA, in the environment.

Zusammenfassung

Synthetische organische Pestizide finden bei der Bekämpfung von Schädlingen, Krankheiten und Unkräutern in den Bereichen der Landwirtschaft und Viehzucht weltweite Anwendung. Der Nachweis dieser Pestizide in Grundwasser gewinnt immer mehr an Bedeutung bei der Trinkwasserproduktion. Daher muss zur Risikobeurteilung von möglichen Boden- und Wasserverunreinigungen das Verhalten und v.a. der Abbau der organischen Pestizide abgeschätzt werden. Der biologische Abbau, auch natürliche Attenuation genannt, stellt den nachhaltigsten Prozess dar, um Pflanzenschutzmittelverunreinigungen aus der Umwelt zu beseitigen. Allerdings kann dieser Prozess mit den momentan eingesetzten Methoden (Bestimmung von Konzentrationsänderungen und Metabolitenbestimmung) nur bedingt nachgewiesen werden, und ist nicht immer zielführend. Insbesondere besteht das Problem, dass zum einen die Abbauprodukte häufig nicht nachgewiesen werden können, und zum anderen, dass auch Prozesse wie Verdünnung, Dispersion und Sorption zu einer Abnahme der Konzentration des Pflanzenschutzmittels führen können. Aus diesem Grund braucht es zusätzliche komplementäre Herangehensweisen. Die substanz-spezifische Isotopenanalytik (CSIA) stellt eine komplementäre Vorgehensweise dar, die es ermöglicht Kontaminationsquellen und den Abbau von organischen Umweltschadstoffen anhand von deren Mustern und Veränderungen in den stabilen Isotopenverhältnissen bei natürlicher Häufigkeit, zu untersuchen.

Der Fokus meiner Doktorarbeit liegt auf dem Herbizid Glyphosat (N-Phosphomethylglycin). Es wird weitgehend in der Nacherntephase eingesetzt, gilt als nicht-selektives Herbizid und wird zur effizienten Bekämpfung von Unkräutern eingesetzt. Glyphosat und sein Hauptabbauprodukt AMPA (Aminomethylphosphonsäure, engl. aminomethyl phosphonic acid) werden häufig in Oberflächengewässern und Grundwässern detektiert und übersteigen oftmals den von der EU (Europäischen Union) für Pestizide festgelegten Grenzwert von 0.1 µg/L. Weiterhin, wurde vor kurzem, Glyphosat von der Krebsforschungsagentur der Weltgesundheitsorganisation (WHO) als „wahrscheinlich krebserzeugend beim Menschen“ eingestuft. Um Kontmainationsquellen und Abbau von Glyphosat und AMPA besser charakterisieren zu können, wird CSIA dieser beiden Zielsubstanzen, als vielversprechende komplementäre Herangehensweise erprobt.

Das erste Ziel der Arbeit bestand in der Entwicklung und der Optimierung der isotopenanalytischen Methode zur Bestimmung des $^{15}N/^{14}N$ Verhältnisses (natürliche

Häufigkeiten) von Glyphosat und AMPA. In einer kürzlich veröffentlichten Studie zur Bestimmung des $^{13}C/^{12}C$ Verhältnisses von Glyphosat und AMPA konnte das Potenzial, aber auch die Limitierung gezeigt werden, wenn zur Produktauthentifizierung nur das Isotopenverhältnis eines Elements herangezogen wird [1]. Meine Motivation bestand daher darin, die Analyse des Isotopenverhältnisses eines weiteren Elements voranzutreiben um das ganze Potenzial einer Mehrelementanalyse („zweidimensionale CSIA“) auszuschöpfen. In diesem Zusammenhang wird im zweiten Kapitel der Arbeit die substanz-spezifische $^{15}N/^{14}N$ Isotopenanalyse des Glyphosats und AMPA mittels eines zweistufigen Derivatisierungsverfahrens in Kombination mit der gaschromatographischen Isotopenverhältnis-Massenspektrometrie (GC/IRMS) vorgestellt. Im ersten Schritt wurde die N-H Bindung mit Hilfe von Isopropylchlorformiat (iso-PCF) derivatisiert. Im zweiten Schritt wurde die verbleibende Säuregruppe mit Trimehtylsilyldiazomethan (TMSD) methyliert. Um richtige Stickstoffisotopenverhältnisse bestimmen zu können, war es entscheidend, dass die gepufferten Lösung einen pH von 10 hatte. Die analytische Grenze für richtige $\delta^{15}N$ Analysen lag für Glyphosate bei injizierten 150 ng und für AMPA bei 250ng. Die Kombination von $\delta^{15}N$ und $\delta^{13}C$ Analysen ermöglichte (i) eine verbesserte Unterscheidbarkeit von kommerziell erhältlichen Glyphosatprodukten und zeigte (ii), dass die Isotopenwerte von Glyphosat nach Abbau mittels MnO_2 eindeutig außerhalb des Bereiches der kommerziell erhältlichen Produkte gewesen sind. Dies unterstreicht das Potenzial der kombinierten Kohlenstoff und Stickstoff Isotopenanalysen bei der Identifikation der Quellen und des Abbaus von Glyphosat.

Das zweite Ziel meiner Doktorarbeit war die Bestimmung der Isotopenfraktionierung während des Abbaus von Glyphosat. Dementsprechend handelt das dritte Kapitel von der Bestimmung von „bulk“ Isotopenanreicherungsfaktoren, die aus Abbaustudien im Labor gewonnen wurden. Diese Anreicherungsfaktoren dienen als Grundlage zur Charakterisierung von abiotischen und biotischen Abbauprozessen (Bioabbau vs. abiotischen Abbau von Glyphosat mittel MnO_2). Dazu wurde zuerst ein Bakterienstamm aus der Umwelt (Weinanbaugebiet, Nordfrankreich) isoliert (Anreicherungskultivierung), der die Fähigkeit hat, Glyphosat als Phoshphorquelle zu nutzen. Der Bakterienstamm wurde mittels 16S rRNA Sequenzanalysen als *Ochrobactrum* sp. FrEM 15651 charakterisiert. AMPA wurde während des biologischen Abbaus von Glyphosat nicht detektiert. Der Nachweis von Sarkosin hingegen, bestätigte einen alternativen Abbauweg- den Sarkosin Abbauweg (C-P Bindungsbruch). Mit $\varepsilon_{kohlenstoff} = -4.8‰ \pm 0.5‰$ und $\varepsilon_{Stickstoff} = -0.6‰$ fiel die detektierbare C

und N Isotopenfraktionierung, die mit dem Glyphosatabbau durch *Ochrobactrum sp.* FrEM assoziiert gewesen ist, gering aus. Dies lässt vermuten, dass die intrinsische Isotopenfraktionierung „maskiert" gewesen ist. Der daraus abgeleitete $AKIE_{Kohlenstoff}$ betrug für den biologischen Abbau 1.014. Im Falle des abiotischen Glyphosatabbaus mittels Mangandioxid (MnO_2) hingegen betrug die Stickstoffisotopenfraktionierung $\varepsilon_{Stickstoff}$ = -17‰ ±0.5‰. Die, während des abiotischen Glyphosatabbaus auftretende stark ausgeprägte Isotopenfraktionierung im Stickstoff würde vermutlich auch in natürlichen Systemen einen robusten „Fußabruck" des Abbaus hinterlassen. Der $AKIE_{Kohlenstoff}$ betrug für den abiotischen Abbau 1.011. Anhand der unterschiedlichen Steigungen (Δ_{biotic} = 4.6 ± 0.03 und$\Delta_{abiotic}$) der zweidimensionalen Isotopenplots ($\delta^{13}C$ vs $\delta^{15}N$) war es möglich den abiotischen und biotischen Abbauweg des Glyphosates zu unterscheiden.

Das dritte Ziel der Arbeit bestand in der Entwicklung einer Anreicherungsmethode um Glyphosat und AMPA aus Wasser zu extrahieren. In Kapitel 4 werden die Ergebnisse aus Anreicherungsverfahren, die mit Hilfe von aktivierten Aluminiumoxid gepackten Säulen Glyphosat und AMPA aus Wasser extrahierten und anreicherten, gezeigt und diskutiert. Das aktivierte Aluminiumoxid hatte eine Adsorptionskapazität von 85 mg/g und eine Oberflächendichte von 2 µmol/m^2. Die Adsorption des Glyphosates auf dem aktivierten Aluminiumoxid war pH abhängig. Glyphosat wurde bei einem pH, der niedriger als der PZC (Nulladungspunkt) des Aluminiumoxides gewesen ist, adsorbiert. Somit war die Oberflächenladung des Aluminiumoxides positiv und die Ladung des Glyphosates zugleich negativ. Im Gegensatz dazu, war die Desorption des Glyphosates bei einem pH über 10 begünstigt. Bei diesem pH sind sowohl die Glyphosatmoleküle als auch die Oberfläche des Aluminiumoxides negativ geladen. Bisher gemessene Isotopenwerte ($^{13}C/^{12}C$ & $^{15}N/^{14}N$) deuten darauf hin, dass nach weiterer Optimierung des getesteten Anreicherungsverfahrens signifikanten Veränderungen im ursprünglichen Isotopenverhältnis des Glyphosates nicht zu erwarten sind. Deshalb besteht das vielversprechende Potenzial, dass die Anwendung von aktiviertem Aluminiumoxid zur Anreicherung von Glyphosat und AMPA aus Wasserproben es ermöglicht, CSIA zur Erforschung der Herkunft von AMPA und dem Nachweis des Glyphosatabbaus in der Umwelt anzuwenden.

Chapter 1

Introduction

1.1 Introduction

1.1.1 Pesticides

Pesticides are substances intended to prevent, destroy or control pests. They generally represent groups of organic substances that are classified based on their target organism, mode of action, chemical structure and physical properties. They have long been used for pest and disease management and are important in agriculture [2]. An estimate one third of the world's food crop would have been destroyed during growth, harvest or storage had it not been for the use of pesticides [3]. Consequently, a raise in pesticide use is expected to match the food demand of an exponential human population growth (9 billion by 2050 according to UN –World Population Prospects report). According to the EPA market estimates, the worldwide pesticide consumption amounted to approximately 5.2 billion pounds in (2006-2007) with herbicides having the largest portion of total use, followed by other pesticides, insecticides, and fungicides (EPA 2006-2007 market report). Countries depending on agriculture as their main economic activity to a large extent depend on the use of pesticide to secure and increase productivity. 25% of Kenya's GDP is based on agricultural production both small- and largescale [4]. The Kenyan pesticide market was approximately US $ 40.4 million dollars in 1992, placing Kenya among the highest pesticide users in sub-Saharan Africa according to "Pesticide Use and Management in Kenya" which was commissioned by World Wide Fund for Nature (WWF) (PCPB annual report 1995). The major active substance imported were glyphosate, mancozeb, dimethoate, imiprotrin, deltametrin, alphacypermetrin, amitraz, 1,3 dichloropropene, sulphur, and metam sodium in order of decreasing volume that accounted to a total of 10,000 tons annually [5].

The dependency of pesticides for food production is clearly not in question. However, the question as to what happens to the pesticides (toxic organic compounds) after they are released into the environment desires close attention.

1.1.2 Pesticides in the environment

Pesticides are released into the environment mainly through the large-scale agricultural crop management practice and also from non-agricultural application (for example in railway tracks or urban garden management). Precipitation leads to the transport and leaching of pesticides into surface and groundwater. The agricultural sources can be divided into two categories (1) diffuse and (2) point sources. Diffuse sources are the result of the pesticides

applied, washed from the fields and transported (or leached) into surface and groundwater via various ways. Depending on the soil type and conditions, the pesticides flow rapidly or slowly through the unsaturated zone. In sandy soils (unstructured soils) contaminants flow slower and this is known as matrix flow. In structured soils (clay soils), however, preferential flow is observed. It referred to the uneven and often rapid movement of water through macropores, cracks, and warm holes allowing faster transport. On the other hand, point sources are the results from the farmer's improper handling (cleaning of farm tools), storage and disposal of the chemicals [6].

Pesticides are typically detected in surface and groundwater at very low concentrations of few µg/L. Groundwater is the source of drinking water for most countries in the world. The concentrations of the majority of pesticides (Atrazin, Bentazon, Mecoprop (MCPP), Diuron, 1,2-Dichloethan, AMPA) in groundwater exceed the stipulated European Union (EU) general threshold value for pesticides and metabolites of 0.1 µg/L (Council Directives 98/83/EC and 2006/118/EC) [7]. Therefore, groundwater monitoring campaigns are routinely done to determine the concentration of pesticides and their metabolites together with restricting the use of pesticides near groundwater catchment areas in order to maintain the drinking water quality.

Pesticides that are released into the environment are subjected to various physical, chemical and biological processes. These processes govern the fate of pesticides in the environment. Physical processes leave the chemical structure of the compound (pesticide) unchanged (such as sorption, dispersion, sedimentation, diffusion and volatilization). They results in the mass transfer between different phases or transport and mixing of the substance within an environmental system. Conversely, chemical and biological processes such as biodegradation lead to the transformation of the pesticide into products (metabolites) of different environmental behavior (see Figure S7 in the appendix III) [8].

Biodegradation is a process where organic contaminants (pesticides) are broken down by the help of microorganisms. Biodegradation, a natural attenuation processes in groundwater, is considered as the only effective process in removing contaminants of many compound classes [9]. The efficiency of biodegradation depends on (i) reactivity of the substances [10] (ii) stimulating conditions (for example soil type, precipitation, presence of degradation microorganism, pH , temperature and nutrient status of the field) and (iii) crop management practices (application method and timing) [11,12].

The persistence of pesticides is expressed in terms of half-life (the length of time required for one-half the original amount to be degraded). Pesticide persistence in soil and water can be estimated based on substance chemical properties

The use of pesticides is clearly inevitable, however, there is a growing concern on the increased detection of pesticides and their metabolite (sub-µg/L) in surface and groundwater. Therefore, it is important to develop new approaches that will assess and monitor their fate in the environment to protect and safeguard our threatened groundwater resources [13]. However, assessing groundwater contamination of pesticides is complex since they are continuously introduced annually (every growing season) into the environment. This thesis focuses on glyphosate a widely used herbicide for weed control in sugar, soya and maize plantations and its main metabolite AMPA (that are common groundwater contaminants).

1.1.3 Glyphosate herbicide

Glyphosate is the active ingredient (substance) of the widely used herbicide "Roundup" introduced by Monsanto in the early 1970s. It is a systematic, broad-spectrum, post-emerging herbicide effective against weeds [14]. In the last decade, application of glyphosate have experienced an exponential increase because: (1) It has been considered as environmentally benign; (2) it strongly sorbs to soil particles, limiting the potential for transport and leaching [15]; (3) it has a short half-life in soil that means it is easily degraded by soil micro-organisms; (4) introduction of glyphosate (generic glyphosate-resistance crops (*Zea mays L.*) to cotton (*Gossypium Hirsutum L.*) and soya beans (*Glycine max L.*)) has resulted in a reduction in the application of other herbicides to control weeds and finally (5) its low toxicity to mammals, birds and most aquatic fauna [16] and mode of action (inhibition of the enzyme Enylpyrvylshikimate-3-phosphate synthase (EPSPS) in the Shikimate-3-phosphate pathway (important in the synthesis of essential aromatic amino acid) is present only in plants, algae, bacteria and fungi) [17] [18-20].

However, there are concerns on the use of glyphosate herbicide. First and foremost, the evolution of glyphosate- resistant weeds, due to heavy use of glyphosate which has lead it to be used together with other herbicides [21]. In literature there are different opinions regarding the health effects of this herbicide. Some studies have shown that it disrupts the gut bacteria in animals, preferentially killing beneficial bacteria and causing an overgrowth of pathogens [22,23]. It also chelates with minerals such as iron and cobalt, and may interference with cytochrome P450 (CYP) enzymes [24,25].

In 2007, EPA selected glyphosate for further screening into its endocrine screening program. Selection for this program is based on a compound's prevalence of use and does not imply particular suspicion of endocrine activity (EPA, Federal registry 2007). Recently, the World Health Organization's cancer research unit has classified glyphosate as "**probably carcinogenic to humans**- Group 2A". This category is used when there is limited evidence of carcinogenicity in humans and sufficient evidence of carcinogenicity in experimental animals [26]. These findings were based on a review of years of scientific research where glyphosate has been detected in the air during spraying, in water, and in food [26].

1.1.4 Physical properties

Glyphosate is an organophosphorus compound. Even though it is a simple molecule with (carboxylic, amino and phosphonate functional groups) and a low molecular weight (MW 169), but its analysis is challenging. Glyphosate and its metabolite AMPA are highly water-soluble (10.1 g/L at 20°C, 5.81 g/L at 25°C respectively) with a low K_{OW} (Log K_{OW} = -3.5, -1.9, respectively)[27] .They have several acidic functionalities (pK_a = 0.8, 2.3, 6.0, 11.0 and pK_a= 0.9, 5.6, 10.2 for glyphosate and AMPA, respectively), contributing to their zwitterionic character [28,29] .The summary of the physical properties of glyphosate and AMPA are shown in Table1-1

Parameter	Glyphosate (Roundup)	Interpretation	AMPA	Interpretation
Chemical structure	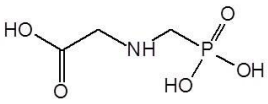	**Polar**	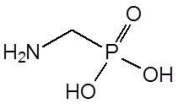	**Polar**
Molar mass(g/mol)	169.08		111.01	
Half-life (days)	34-44	Non-persistent	151	**Persistent**
GUS	-0.54	Low leachability	0.2	Low leachability
K_{OC}	27621	Non-volatile	2002	**slightly mobile**
Log Kow	-3.5	Low	-1.3	Low
Solubilty (mg L^{-1})	11500	High	5810	High
Vapour Pressure (mPa)	0.000001	Non-volatile	-	-
Henry's law constant (dimensonless)	2.0×10^{-19}	Non-volatile	0.16	**Moderate volatile**
pKa	0.8; 2.6; 6; 10.9	zwitterionic	0.9; 6; 10.2	zwitterionic

GUS: Groundwater Ubiquity score
Kow Octanol-water Coefficient
Koc Soil adsorption Coefficient
Sources Schuette et al 1998, Pesticide properties Database U. of Hertfordshire

Table 1-1 Common name, molar mass half-life, GUS value (groundwater ubiquity score), sorption coefficient (K_{oc}), water solubilty, vapour pressure index, Henry's constant index and pKa for glyphosate and metabolite AMPA

1.1.5 Glyphosate degradation in the environment

In the environment glyphosate is strongly bound to soil (see sorption coefficient in table 1-1) through its phosphate moiety [13]. Glyphosate is broken down through two degradation pathways- i) abiotic degradation and ii) biotic degradation. Biodegradation is the main degradation route in the environment. But, it is considered stable to hydrolytic abiotic degradation indicated by minimum hydrolysis in a study conducted at various pH [30,31]. Glyphosate biodegradation follows two degradation pathways 1) AMPA formation by the cleavage of a C-N bond (N-dealkylation reaction) and 2) intermediate formation of sacrosine and glycine [13] as shown in Figure 1-1. Several studies have isolated bacterial strains that were capable of degrading glyphosate from soil. By now, only aerobic bacteria have been isolated from soil or sediment. Earlier studies were able to isolate *Pseudomonas* sp. strain

PG2982, *Arthrobacter* sp. strain GLP-1 that utilized glyphosate as phosphorus source. These organisms were shown to cause the cleavage of the C-P bond, resulting in the formation of sarcosine [32]. Another strain *Arthrobacter* sp. strain ATCC 13752 was capable of metabolizing glyphosate to AMPA, and the carbon of AMPA was completely converted to CO_2 [32]. Several years later, the metabolism of glyphosate in 163 environmental bacterial strain isolated under non-selective conditions showed that 26 strains metabolized glyphosate via C-P bond cleavage forming sarcosine [33]. Most recently, bacterial strains *Ochrobactrium anthropi GPK3*, *Achromobacter* sp isolated from soil were able to degrade glyphosate through two alternative degradation pathways which are AMPA and sarcosine pathways (C-N bond and C-P bond cleavage, respectively) [34-36]. The postulated degradation pathway of glyphosate (complete pathway described in [34]) is shown in Figure 1-1.

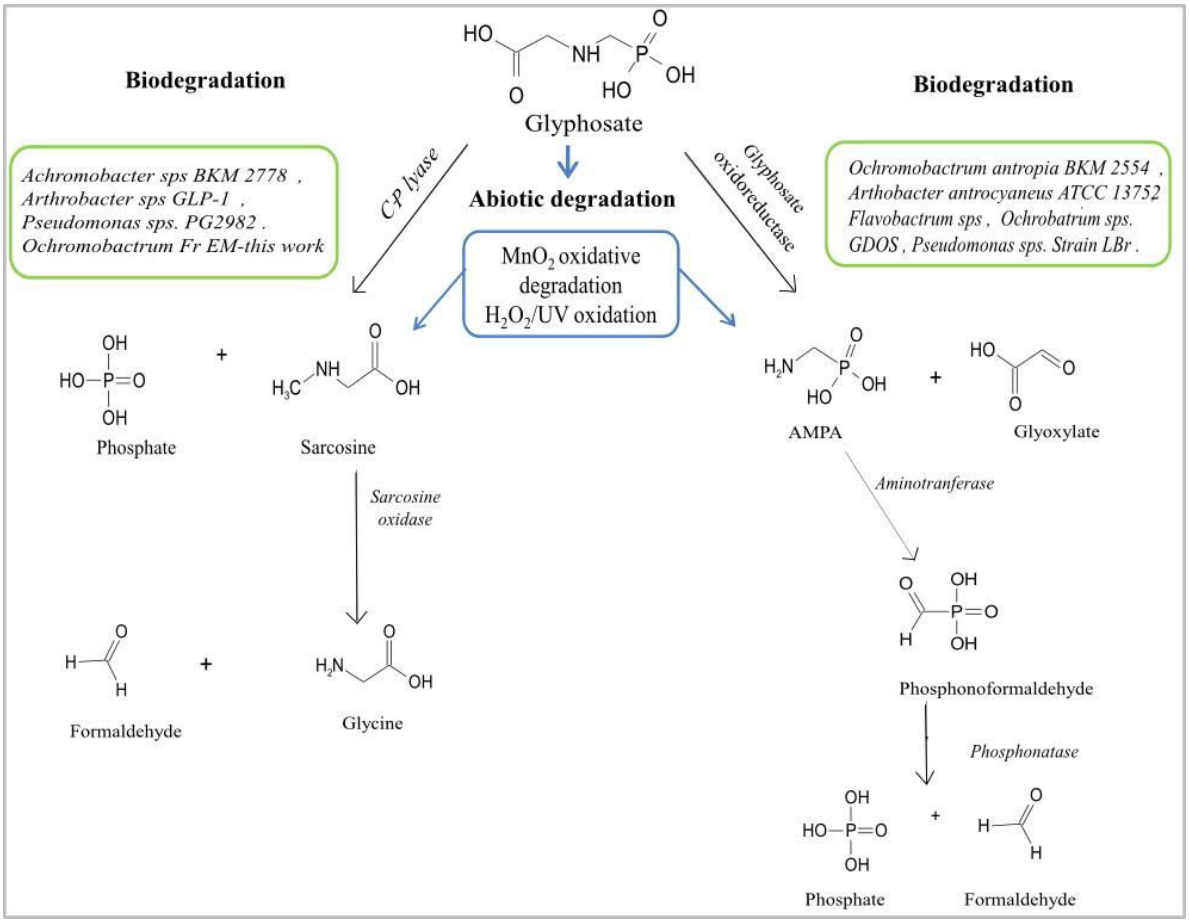

Figure 1-1: Postulated glyphosate degradation (biotic & abiotic) pathways leading to its metabolites AMPA and sarcosine. Strains isolated from soil, wastewater and sediment with glyphosate degradation activity. Oxidative abiotic degradation with MnO_2 and advanced oxidation by H_2O_2/UV

Barrett et *al* [37] reported the first study on the oxidative abiotic degradation of herbicide glyphosate with MnO_2. They proposed that glyphosate is first adsorbed to manganese via its phosphate group and then transfers an electron to facilitate reduction of Mn(IV) to Mn(III). C-P bond cleavage results in formation of sarcosine which is further transformed into glycine and formic acid. Evidence of C-N bond cleavage has been confirmed in later studies [38].

Transition metal oxides present in soils contribute to the natural degradation of organic compounds present in soil. Birnessite (δ-MnO_2), is a manganese mineral present in soils. Oxidation of organic compounds such as phenol, chloroaniline, diclofenac, glyphosate, atrazine and carbamazepine with MnO_2 has been reported [39-42].

Early studies on photolysis of glyphosate in either water or soil suggested that it is not readily photo-degraded [43,44]. This is because glyphosate does not display absorption bands in UV/VIS range that would enable an excitation of the molecule and lead to direct photolysis. However, advanced oxidation processes (AOPs) have been reported to degrade glyphosate and therefore offering a potential option to reduce glyphosate concentration in water to acceptable limits. This indicates that, in contrast to direct photolysis, indirect photolysis (i.e reaction with the OH radicals) does take place [45,46]. A different reaction pathway was proposed where the $^{\cdot}OH$ radical formed attacks glyphosate leading to a carbon centered radical and phosphate (C-P bond cleavage as first step). The radical reacts with molecular oxygen to give a new radical (step 2). This then react with water to form glycine, formaldehyde and $HO_2^{\cdot}$ radical.

In soil, glyphosate is considered to be moderately persistent with a field dissipation of 44-60 days and the half-life ranging from several weeks to years, but averages to two months. Field studies conducted at sandy and two loamy sites indicated that both glyphosate and AMPA can leach through structured soils [43]. Leaching and degradation of glyphosate differs from soil to soil. This variability and uncertainty makes it difficult to conclude its behavior in soil [13]. In another study, soil columns treated with glyphosate and *S*-metolachlor under two different rainfall regimes (light frequent rainfall and heavy short rainfall) observed that glyphosate remained in the surface soil layer because of its strong adsorption capacity, whereas AMPA leached down in small amounts in both rainfall regimes [47]. It has also been shown that the transport of glyphosate was influenced by the soil type and that the phosphate concentration contributes to its leaching through stratified soils [48].

1.1.6 Glyphosate herbicide in groundwater

Glyphosate and its metabolite AMPA are frequently detected in surface and groundwater above the EU general threshold level of 0.1 µg/L [49-51]. AMPA has a high potential to leach into groundwater than glyphosate based on a study that reported that AMPA are more mobile and persistent in aquatic environment than earlier research and monitoring suggested [52]. The groundwater Ubiquity score (0.2) of AMPA (a number derived from its half-life and sorption coefficient and Henry's law constant) predicts a slight leachability into groundwater (shown in table 1-1).

However, the fate and sources of AMPA in groundwater is poorly understood as phosphonates used in laundry products also form AMPA as main transformation metabolite, which makes the assessment of AMPA even more complex [53,54].

To this end, assessing the sources and degradation processes of glyphosate and AMPA by conventional methods is challenging and sometime inconclusive. This is because: (i) metabolites are often not detected, (ii) an attempt to close mass balances requires exhaustive sampling bringing about the installation and operation of expensive and labor-intensive sampling networks and (iii) the transformations of glyphosate can proceed simultaneously along competing pathways thus making the characterization of these processes difficult. The transformation products may be further degraded and their physiochemical behavior (sorption, retardation) may be different from the glyphosate compound hence may not always be detected

Therefore, this thesis aims to pursue an alternative approach to investigate the sources and degradation of glyphosate and AMPA. This approach is CSIA (compound specific isotope analysis) as explained below.

1.2 Compound specific isotopic analysis

Assessment of the transformation of organic compounds with compound-specific isotope analysis (CSIA) makes use of the stable isotope composition of organic compounds at their natural isotopic abundance. This composition can be measured by gas chromatography-isotope ratio mass spectrometry (GC/IRMS) or liquid chromatography-isotope ratio mass spectrometry (LC/IRMS scheme shown in Appendix –AII). It is expressed as an isotopic ratio ($R= E/E_{sample}$), where ^{h}E is the heavy isotope and ^{l}E the lighter isotope of an element E (e.g.,

$^{h}E/^{l}E= {}^{13}C/^{12}C$, $^{15}N/^{14}N$). Isotope ratios are reported as difference in per mil with respect to an international reference standard:

$$\delta^{13}C_{sample,VPBD} = \frac{R\left(^{13}C/^{12}C\right)_{sample} - R\left(^{13}C/^{12}C\right)_{VPBD}}{R(^{13}C/^{12}C)_{VPBD}} \quad (1\text{-}1)$$

$$\delta^{15}N_{sample,N_2-AIR} = \frac{R\left(^{15}N/^{14}N\right)_{sample} - R\left(^{15}N/^{14}N\right)_{N_2-AIR}}{R(^{15}N/^{14}N)_{N_2-AIR}} \quad (1\text{-}2)$$

The use of the per mil notation is important because the natural abundance of isotopes and the variations in isotope ratios of these elements are generally very small. By reporting isotopes ratios relative to standards of known isotopic composition, one ensures that several possible errors (chemical conversion and mass spectrometer performance) cancel out if the results are presented as a ratio (eq. 1-2). The use of reliable isotope standards or reference materials is critical to compare results between runs on a single machine, but also to relate them to other isotope instruments and laboratories. Gas chromatography-isotope ratio mass spectrometry analysis of organic compounds is possible for hydrogen ($^{2}H/^{1}H$), carbon ($^{13}C/^{12}C$), nitrogen ($^{15}N/^{14}N$), oxygen ($^{18}O/^{16}O$) and ($^{37}Cl/^{35}Cl$) [55] elements.

The Rayleigh model for a closed system is used to quantify the isotopic fractionation (eq 1-3), where the enrichments factor (ε) describes the relationship between the change in isotopic composition (R_t/R_o) and the change in concentration ($f = C_t/C_o$).

$$\ln\frac{R_t}{R_0} = \ln\left(\frac{1+\delta^h E}{1+\delta^h E_0}\right) = \varepsilon \ln f \quad (1\text{-}3)$$

Such isotopic data can give different types of information: (i) Isotope ratios can be used like fingerprints to distinguish different contaminant sources and to identify a liable party in cases of environmental forensics [56] (ii) In addition, abiotic or biotic transformation reactions of organic compounds can be detected and distinguished from each other based on kinetic isotope fractionation. The reason is the kinetic isotope effect associated with degradation reactions: light isotopes (e.g.,^{12}C) typically react slightly faster causing an enrichment of heavy isotopes (e.g.,^{13}C) in the remaining organic compound. This is mainly the result of ZPE (zero point energy level) differences of the two isotopes. A significant isotopic fractionation is

expected at reactive positions involving the elements, where the covalent bond is broken or formed during the rate determining step of the process. Conversely, other physical processes (dilution, adsorption, advection) typically result in a negligible isotopic fractionation as observed in batch and chromatographic experiments [57]. Detection of such enrichments in the field samples makes it possible to monitor degradation and provide an additional line of evidence of natural attenuation even in the absence of mass balances

Estimations of the extent of (bio) degradation (B) can also be obtained according to the equations:

$$B = 1 - f = \left(\frac{R}{R_0}\right)^{\left(\frac{1}{\varepsilon}\right)} = \left(\frac{\delta^h E + 1}{\delta^h E_0 + 1}\right)^{\left(\frac{1}{\varepsilon}\right)} \qquad (1\text{-}4)$$

where R_0 and R are the isotope ratios of element E in the compound at the source and at a specific location in the field respectively, and *f* is the fraction of the remaining contaminant at the given location [58]. Finally, (iii) Multi-element isotope analysis ("multidimensional") makes it even possible to identify different degradation pathways. The reason is that different transformation reactions typically involve different bonds and different elements leading to characteristically different trends in dual element isotope plots [59]. Therefore, the more elements are included in isotopic analysis the better is the chance to delineate a reaction mechanism. While these approaches are well-established for point source priority pollutants [60], investigations of agricultural organic chemicals are recently emerging [61-64].

To date, CSIA is a widely accepted routine analysis to monitor degradation of volatile hydrocarbons (BTEX) and chlorinated hydrocarbons (PCE (tetrachloroethylene),TCE (trichloroethylene), cDCE (cis-1,1-dichloroethylene)) in contaminated aquifers (groundwater). This is because of automated sample handling [65,66] and environmental concentrations that lie above the limits of precise isotope analysis [67,68]. In recent years, research studies on the degradation of chemical micropollutants such as pesticides, detergents and pharmaceuticals using CSIA have increased [69-72]. CSIA, therefore, is a potential complementary tool to assess compound transformation of glyphosate and its metabolite AMPA, which are common micropollutants in groundwater.

1.2.1 Expected stable isotope fractionation of glyphosate and AMPA

As already mentioned (in Section 1.1.3), glyphosate strongly sorbs to soil which making it not bioavailable to soil bacteria as shown in Figure 1-2 (a).The insights into the expected during degradation of glyphosate and AMPA might provide some insights into the fate of AMPA in groundwater similar to other studies [69]. The microbial degradation of glyphosate in soil forms AMPA (cleavage of the C-N bond) which is expected to show no changes in the $^{13}C/^{12}C$ isotope ratio.

1.2.2 Practical challenges of glyphosate analysis

Analysis of glyphosate and AMPA are very challenging because of their physical properties (see Table 1-1). Their analyses are tedious because numerous steps are necessary during purification and often derivatization is required for GC-MS, LC-MS/MS and HPLC/UV. This is because: (i) they lack a chromophore or fluorophore for detection and (ii) the polar groups need to be converted into volatile derivatives for GC analysis. Several studies have developed sensitive methods that analyzed glyphosate in river water after derivatization with FMOC-Cl and LC-MS/MS analysis (Hanke et al 2008, Einhorn et al 2007). Direct HPLC analysis was reported using ion chromatography with electrochemical or mass spectrometry detection (Hao et al 2011). CSIA of polar compound like glyphosate and AMPA is even more challenging because of (1) the introduction of additional carbon atoms during derivatization which potentially causes an isotope fractionation during derivatization (2) the additional atoms "dilute" isotope changes in the target compound and 3) To enable CSIA glyphosate analysis at environmental concentrations (< 0.1 µg/L) sensitive enrichment method is needed.

1.3 Scope of the study

This thesis focuses on assessing the transformation of glyphosate and its main metabolite (AMPA) using CSIA. The objectives were: (i) to develop and optimize a method for stable isotope analysis (CSIA) of glyphosate and AMPA, (ii) to investigate the associated isotope fractionation of glyphosate during degradation and (iii) to develop an enrichment method for glyphosate and AMPA extraction from natural water.

1.3.1 Objective 1:

In chapter 2, a method to measure nitrogen isotope analysis was developed. The objective was to advance isotope ratio analysis of an additional element (besides carbon) for dual element isotope analysis Different conditions during derivatization of glyphosate and AMPA, which

include pH, the variability of excess derivatization agent and vortexing time, were optimized. A dual element isotope approach ($^{13}C/^{12}C$ and $^{15}N/^{14}N$) was used to distinguish different glyphosate products and oxidative abiotic degradation.

1.3.2 Objective 2:

In chapter 3, a specific bacterial strain that showed the ability to degrade glyphosate was isolated from a soil collected from a vineyard. The objective was to use this strain as a reference to investigate the isotope fractionation during biodegradation of glyphosate. In addition, abiotic degradation of glyphosate with MnO_2 was performed. The objectives were to understand the mechanism during abiotic degradation of glyphosate at a MnO_2 surface and to distinguish the degradation pathway using multi-element isotope analysis.

1.3.3 Objective 3:

In chapter 4, a method to extract and enrich glyphosate from water was developed. This was to advance the application of CSIA towards field analysis of glyphosate and AMPA. Sorption conditions and sorption effects induced during sorption on alumina was investigated. This was to ensure that the enrichment method does not induce any isotope fractionation.

Chapter 2

Stable Isotopic Method Development and Optimization

Dual Element ($^{15}N/^{14}N$, $^{13}C/^{12}C$) Isotope Analysis of Glyphosate and AMPA: Derivatization-Gas Chromatography Isotope Ratio Mass Spectrometry (GC/IRMS) Combined with LC/IRMS

Emmanuel O. Mogusu, J. Benjamin Wolbert, Dorothea M. Kujawinski,

Maik A. Jochmann and Martin Elsner

Abstract:

To assess sources and degradation of the herbicide glyphosate (*N*-(phosphonomethyl) glycine) and its metabolite AMPA (aminomethylphosphonic acid), concentration measurements are often inconclusive and even $^{13}C/^{12}C$ analysis alone may give limited information. To advance isotope ratio analysis of an additional element, we present compound-specific $^{15}N/^{14}N$ analysis of glyphosate and AMPA by a two step derivatization in combination with gas chromatography/isotope ratio mass spectrometry (GC/IRMS). The N-H group was derivatized with isopropyl chloroformate (iso-PCF), and remaining acidic groups were subsequently methylated with trimethylsilyldiazomethane (TMSD). Iso-PCF treatment at pH <10 gave too low $^{15}N/^{14}N$ ratios indicating an incomplete derivatization; in contrast, too high $^{15}N/^{14}N$ ratios at pH >10 indicated decomposition of the derivative. At pH 10, and with an excess of iso-PCF by 10-24, greatest yields and accurate $^{15}N/^{14}N$ ratios were obtained (deviation from elemental analyzer-IRMS: -0.2 ‰ ± 0.9 ‰ for glyphosate; -0.4 ‰ ± 0.7 ‰ for AMPA). Limits for accurate $\delta^{15}N$ analysis of glyphosate and AMPA were 150 ng and 250 ng injected, respectively. A combination of $\delta^{15}N$ and $\delta^{13}C$ analysis (i) enabled an improved distinction of commercial glyphosate products and (ii) showed that glyphosate isotope values during degradation by MnO_2 clearly fell outside the commercial product range. This highlights the potential of combined carbon and nitrogen isotopes analysis to trace sources and degradation of glyphosate.

2.1 Introduction

Glyphosate (*N*-(phosphonomethyl) glycine) is a systemic, non-selective, broad-spectrum, post-emerging herbicide that is highly effective in weed control for agricultural and domestic applications [73]. Its degradation follows two alternative pathways: (1) C-N bond cleavage leading to AMPA (amino methylphosphonic acid) and glyoxylate formation (main pathway): (2) C-P bond cleavage forming sarcosine (N-methylglycine) and inorganic phosphate [13,34,36,37]. Glyphosate and its main degradation product AMPA have been detected in surface as well as in groundwater [49,74,75]. An additional source for AMPA are phosphonates from domestic laundry, which may form AMPA as a key metabolite making assessments even more complex [76]. The increasing detection of glyphosate and AMPA in surface and groundwater has therefore driven much research on their sources and environmental fate [74].

So far, concentration measurements have been the prime focus for glyphosate analysis, and analytical efforts have targeted method sensitivity and reproducibility for the monitoring of glyphosate and AMPA in different matrices (soil, water, food) [77-85]. To this end, glyphosate and AMPA are typically derivatized because (1) in the underivatized form, they lack a chromophore or fluorophore for high performance liquid chromatography/ultraviolet analysis (HPLC/UV), (2) for gas chromatography-mass spectrometry (GC-MS) analysis, polar groups need to be converted into a stable volatile derivative and (3) the introduction of non-polar group has the additional advantage that it facilities the extraction from aqueous solution [83].

Concentration measurements alone, however, are often not sufficient to adequately assess sources and degradation of glyphosate and its metabolite AMPA, because mass balances need to be established and an extensive sampling network is typically needed [86,87], which is often not possible. Also, one cannot distinguish a different provenance of the same chemical, for example for product authentication or source allocation. New approaches are, therefore, warranted to enable a more comprehensive understanding of the sources and transformation of glyphosate and AMPA in natural systems.

Here, compound-specific isotope analysis (CSIA) provides an alternative approach to investigate sources and degradation of organic pollutants [88,89]. In case of CSIA the stable isotope composition of organic compounds by gas chromatography/isotope ratio mass spectrometry (GC/IRMS) or liquid chromatography-isotope ratio mass spectrometry

(LC/IRMS) is analyzed. Such measurements can provide various types of information. (i) Isotope ratios can be used as fingerprints to distinguish contaminant sources or a different provenance of the same substance in chemical products [90,91]. (ii) In addition, it is possible to distinguish between abiotic or biotic transformation reactions of organic compounds based on kinetic isotope fractionation [56,9]. The reason is that isotopes of lower mass (e.g., ^{12}C) typically react slightly faster in biotic and abiotic degradation processes causing an isotope enrichment of those with higher mass (e.g.,^{13}C) in the remaining organic compound (kinetic isotope effect, *KIE*). If such enrichment is detected in field samples, degradation can be demonstrated even in the absence of mass balances [92,58]. Thus, there is a considerable potential of CSIA to characterize sources and degradation for glyphosate and its metabolite AMPA in analogy to other studies [69,93].

However, CSIA is challenging for these compounds, because glyphosate and AMPA are highly water-soluble (10.1 gL^{-1} at 20°C, 5.81 gL^{-1} at 25°C respectively), do not partition into organic solvents and are not directly amenable to gas chromatography [16,15]. For that reason, the first method for compound-specific $\delta^{13}C$ analysis of glyphosate and AMPA, which has recently been published [1], is based on LC/IRMS. Even with such "one-dimensional" isotopic information alone the benefit of CSIA to distinguish glyphosate in different commercial samples could already be clearly demonstrated. However, to exploit the full potential of compound-specific isotope information it is well recognized that analysis of multiple elements ("two-dimensional CSIA") is mandatory for improved source identification and a more reliable assessment of degradation [89,94-96,58,97,98] Besides $\delta^{13}C$ measurements, also a method to accomplish $\delta^{15}N$ isotope analysis is therefore warranted.

Such nitrogen isotope analysis is not possible by LC/IRMS, because a method is missing to quantitatively produce N_2 from nitrogen-containing compounds in the liquid phase of LC/IRMS, and to measure this contribution against the high background of atmospheric N_2. For dual element isotope analysis, carbon isotope analysis by LC/IRMS therefore needs to be combined with a complementary GC/IRMS-based approach for nitrogen isotope analysis. Kataoka *et al*. [83] presented a derivatization scheme which introduces small substituting groups facilitating subsequent gas chromatographic analysis (Figure 2-1).

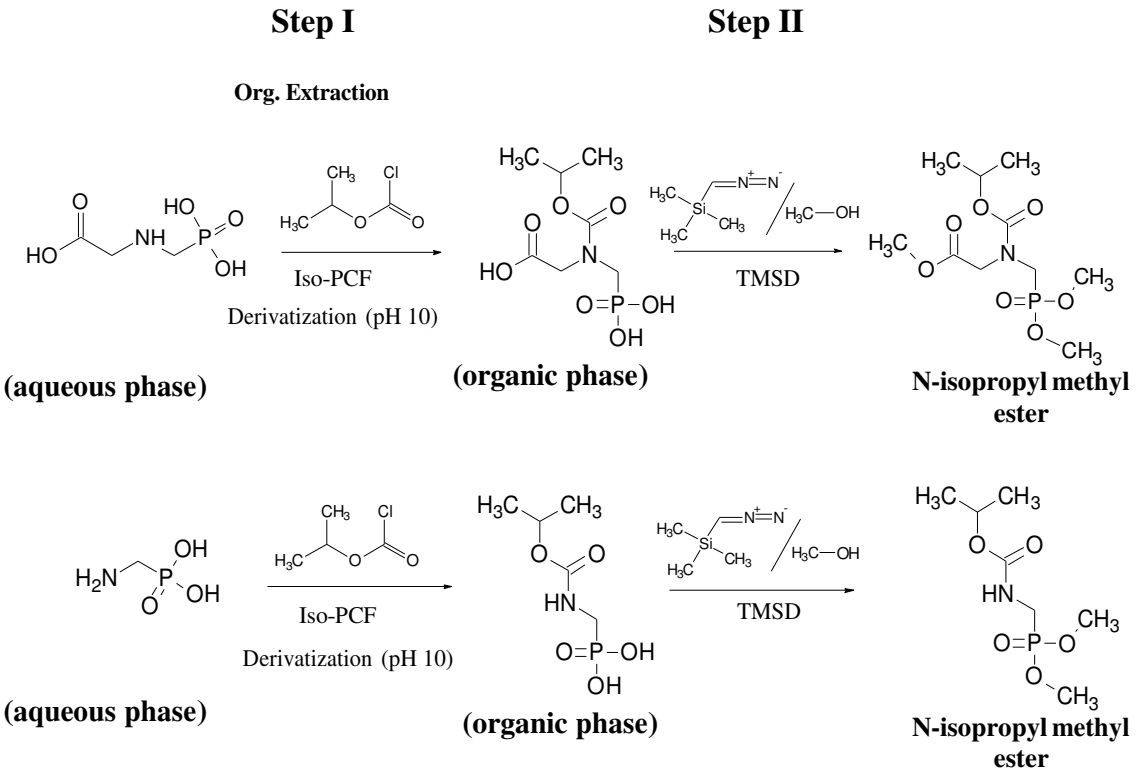

Figure 2-1. Derivatization reaction of glyphosate and AMPA with isopropyl chloroformate (iso-PCF) and trimethyl silyl diazomethane (TMSD).

In a first step, the amino group in glyphosate and AMPA molecules is acylated. This step facilitates the extraction of glyphosate and AMPA from the water phase into an organic solvent. In this organic medium, trimethylsilyl diazomethane (a strong methylating agent) is used to methylate the remaining acidic groups (carboxyl and phosphate) in a second step. The speciation diagram for glyphosate and AMPA in Figure 2-2 illustrates that for the first step, an optimization of the pH is crucial for the following reasons. The N-H group must first be derivatized before the compound can be extracted into an organic solvent. This derivatization (and, for that matter, any kind of alternative derivatization approach) only works with deprotonated N-H groups and is, therefore, complicated by the fact that the N-H group is protonated until pH 9 or 10 for both glyphosate and AMPA. Accordingly, Kataoka *et al*. [83] reported complete derivatization (yields 98% and higher) for pH values greater than 10. However, a delicate balance is required between a pH that is sufficiently high to deprotonate the N-H group, but sufficiently low to prevent decomposition of the derivative, which is labile to attack by OH^- at high pH. The latter aspect was not addressed in the previous study [83].

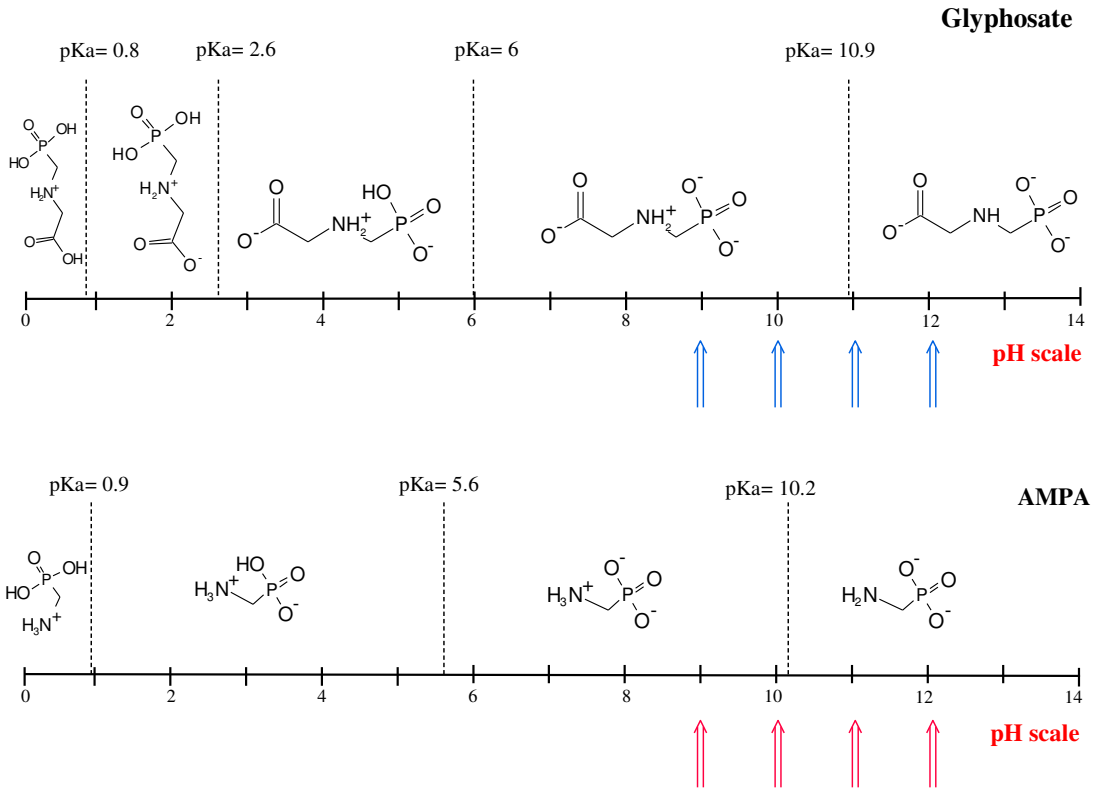

Figure 2-2: An illustration of the speciation of glyphosate and AMPA dependence to pH showing the different pKa values for glyphosate and AMPA (pKa = 0.8, 2.6, 6, 10.9; 0.9, 5.6,10.2) [99,100] respectively. The blue and red arrows represent the pH values at which derivatization with iso-PCF were tested.

The objectives of the chapter were: (1) to test whether the derivatization method of Kataoka *et al*. [83] (Figure 2-1) can be adapted and validated to accomplish accurate $\delta^{15}N$ values of glyphosate and AMPA by GC/IRMS; (2) specifically, to investigate at which pH $\delta^{15}N$ values measured by GC/IRMS match those of EA/IRMS; (3) to test the effect of excess derivatization agent (iso-PCF) on isotope values of glyphosate and AMPA; (4) to validate the method by testing linearity (ensuring that there is no amount-dependency of isotope values), and by determining the lower limits of precise and true isotope analysis; (5) finally, to investigate the potential of a dual element isotope approach to distinguish glyphosate from different commercial herbicides and to trace degradation of glyphosate in abiotic transformation by MnO_2 as a model reaction.

2.2 Experimental section

2.2.1 Materials

Glyphosate (in-house standard (CAS No. 1071-83-6), AMPA (CAS No. 1066-51-9) with purities of 99%, 1.0 M Iso-PCF (isopropyl chloroformate) in hexane, 2.0 M TMSD (trimethyl silyl diazomethane) in ethyl ether, as well as diethyl ether, methanol, ethyl acetate and *tert*-butanol (with purities <99%) were all purchased from Sigma-Aldrich (GmbH Steinheim, Germany). A total of thirteen different commercial products containing glyphosate as active ingredient were purchased from a local market and sixteen additional formulations from a previous study [1] were investigated. Sodium peroxodisulfate ($Na_2S_2O_8$), potassium hydroxide (KOH), phosphoric acid (H_3PO_4) and monosodium phosphate (KH_2PO_4) (all with purities <99% from Fluka; Steinheim; Germany) were used as LC eluents and oxidation reagents. Stock glyphosate and AMPA standards were prepared in MilliQ water and stored in 50 mL plastic falcon tubes (supplied by Greiner, Germany) at 4°C.

2.2.2 Derivatization with trimethyl silyl diazomethane (TMSD)

The derivatization of glyphosate and AMPA followed the procedure described previously [83], but instead of the highly explosive diazomethane gas, trimethyl silyl diazomethane was used as less hazardous alternative. The derivatization reaction (Figure 1) involved a three-step procedure. (1) 500 µL of glyphosate solution containing 30 mM / 5000 ppm (corresponding to 15 µmol absolute) was transferred to a reaction tube and adjusted to pH 10 with 50 µL of a Borate/NaOH buffer (see below). Immediately after adding 100 µL of 1.0 M isopropyl chloroformate (iso-PCF) (100 µmol absolute) in hexane, the solution was mixed for two minutes (min) by a mini-vortexer. Subsequently, 50-100 µL of 2 M HCl (100-200 µmol absolute) were added to lower the pH to 1-2. (2) The excess of derivatization agent was extracted with 3 mL ethyl ether and the organic layer was discarded. The aqueous solution was saturated with sodium chloride and extracted twice with 20% *tert*-butanol in ethyl ether. The ethereal solutions were then combined. (3) Subsequently, 200 µL methanol were added to the ethereal extract together with 50 µL of 2.0 M TMSD (absolute 100 µmol) in ether and the mixture was allowed to react at room temperature (25 °C) for 1 h until a visual disappearance of the yellow color indicated that no diazomethane remains. Under these conditions, Kataoka *et al*. reported an analyte conversion of up to 98% [83]. Finally, the solution was evaporated under a gentle stream of nitrogen to dryness. The residue was dissolved in 1 mL ethyl acetate and 1 µL of the formed N-isopropyl carbonyl methyl ester derivative in ethyl acetate was used for further analysis. To test how an excess of derivatization agent in the first step of Figure 1

influences the isotopic composition of glyphosate and AMPA, the iso-PCF-to-analyte ratio was varied between 2 and 34 corresponding to adding between 50 µL and 500 µL of 1.0 M iso-PCF in hexane (between 50 and 330 µmol absolute) to 500 µL of 30 mM / 5000 ppm glyphosate (15 µmol absolute) and 45 mM / 5000 ppm AMPA (22.5 µmol absolute). The derivatization reaction was conducted under the fume hood because of the toxic nature of trimethyl silyl diazomethane.

2.2.3 pH Optimization

To determine the optimum pH in the first step of the derivatization sequence (i.e., introduction of the isopropyl formate group) different pH values from 9 to 12 were tested. To this end, 50 µL of the different buffer solutions were added to 500 µL of 30 mM (5000 ppm) glyphosate solution (15 µmol absolute). The respective buffer solutions had the following compositions. For pH 9: 250 mL of 0.3 M sodium borate adjusted to pH 9 with phosphoric acid (corresponding to 15 µmol borate in 50 µL), for pH 10: 100 mL of 0.08 M sodium borate mixed with 20 mL of 4 M NaOH (corresponding to 3.4 µmol borate and 34 µmol NaOH in 50 µL), for pH 11: 100 mL of 0.08 M sodium borate mixed with 20 mL of 8.0 M NaOH (corresponding to 3.4 µmol borate and 66 µmol NaOH in 50 µL), for pH 12: 100 mL of 0.04 M $NaHCO_3$ mixed with 20 mL of 4.0 M NaOH (corresponding to 1.7 µmol $NaHCO_3$ and 34 µmol NaOH in 50 µL). In theory, 200 µmols of buffer capacity would be needed to neutralize all HCl that can be formed from 100 µL 1.0 M iso-PCF (100 µmol absolute). In practice, our result at pH 10 indicates that a much smaller neutralization capacity of NaOH + borate in the order of 35 µmols was sufficient. This indicates that of the iso-PCF molecules present in hexane, only a limited number partitioned into the aqueous phase. This amount was sufficient to effectively derivatize glyphosate in the aqueous phase, but small enough not to affect the pH within the vortex time of 2 min.

2.2.4 GC-MS conditions

A gas chromatograph (Agilent 7890A, Waldbron, Germany) connected to an quadrupole mass spectrometer (Agilent 5975C, Waldbron, Germany) with Chemstation mass data system (Agilent 5975C, Waldbron, Germany), was used to analyze samples during the optimization of the derivatization procedure and to confirm the identity of the derivative. The injector temperature was set to 250°C and the samples were injected in a splitless mode. The helium (grade 5.0, supplied by Linde, Germany) carrier gas flow was set to 1.56 mL min^{-1} After 1 min, the split ratio was switched to 1:10. Separation of the derivatives of glyphosate and AMPA was achieved by a DB-5 column (30 m, 0.25 mm i.d. and 0.25 µm film thickness

Agilent, Waldbron, Germany). The oven temperature was programmed as follows: the initial temperature was 80°C for 1 min and increased to 140°C at 10°C min^{-1}, ramped to 230°C at 10°C min^{-1}, which was held for 8 min. The overall run time was 24 min. The MS was operated in selected ion monitoring mode (SIM) detecting 2-3 ions at 100 msec dwell time of both derivatives, where the ion source temperature was set to 230°C.

2.2.5 Nitrogen isotope analysis by GC/IRMS

The GC/IRMS system consisted of a Trace GC ultra-gas chromatograph (Thermo Fisher Scientific, Milan, Italy) linked to a Finnigan MAT 253 (Thermo Fisher Scientific, Bremen, Germany) by a Finnigan GC combustion III interface (Thermo Fisher Scientific, Bremen, Germany). The emission was set to 2 mA for nitrogen analysis. Helium (grade 5.0, supplied by Linde, Germany) was used as carrier gas at a flow rate of 1.4 mL min^{-1}. The samples (1 µL of N-isopropyl carbonyl methyl ester derivative) were injected by a GC CombiPal autosampler (CTCAnalytik, Zwingen, Switzerland) in splitless mode at constant injector temperature of 250°C and after 1 min, the split ratio was switched to 1:10. Separation was achieved on a 30 m DB-5 column (Agilent Technologies, USA) with 0.25 mm i.d. and 1.0 µm film thickness. The oven temperature was programmed as follows: the initial temperature of 80°C was held for 1 min. Then the temperature was increased to 140°C with 10°C min^{-1} and ramped to 230°C at 10°C min^{-1}. The final temperature was held for 8 min. The separated glyphosate and AMPA N-isopropyl methyl ester derivatives were combusted online to N_2 with a NiO tube/CuO-NiO reactor operated at 1000°C (Thermo Fisher Scientific, Bremen, Germany). A liquid nitrogen trap was employed to eliminate CO_2 for N_2 measurement. The N_2 was subsequently transferred online to the IRMS.

2.2.6 Carbon isotope analysis by LC/IRMS

Carbon isotope analysis of glyphosate was conducted by LC/IRMS according to the method by Kujawinski *et al*. [1]. Analysis of commercial herbicide products from different manufactures was conducted on a LC/IRMS system at the Helmholtz Zentrum München consisting of a Finnigan Surveyor HPLC system including a Surveyor MS pump and a Surveyor autosampler coupled to a Finnigan MAT 253 IRMSvia a Finnigan LC isolink interface (all instruments Thermo Fisher Scientific Bremen, Germany). In contrast, carbon isotope analysis of samples taken during an abiotic degradation experiment of glyphosate with manganese dioxide (MnO_2) were measured on an LC/IRMS Instrument in the Duisburg-Essen laboratory consisting of a Rheos Allegro binary pump (Flux Instruments, Buchs, Switzerland) and a HTC PAL autosampler (CTC Analytics, Idstein, Germany) coupled to a Delta V

Advantage (Thermo Scientific, Bremen, Germany) IRMS via a LC-IsoLink (Thermo Scientific, Bremen, Germany).

In both cases a Hypercarb column 100 × 4.6 mm, 3 µm particle size (Thermo Scientific, Langerwehe, Germany) was used to separate glyphosate from its by-products. The eluent was a 2.5 mM NaH_2PO_4 solution adjusted to pH 1.9 with conc. H_3PO_4. The flow rate was 300 µL min^{-1} in isocratic mode. The injected sample volume was 25 µL (München) and 20 µL (Essen), respectively. The reagents to convert the HPLC effluent to CO_2 were phosphoric acid (1.5 M) and sodium peroxodisulfate (0.84 M). For all experiments the flow rate of each reagent was 50 µL min^{-1}. The wet chemical oxidation was performed at a reactor temperature of 99.9°C. The helium (grade 5.0) flow rate of the separation unit to transfer CO_2 to the IRMS was set to 2.3 $mLmin^{-1}$. Before use, the reagent solutions and eluents were degassed in an ultrasonic bath under vacuum for 30 min. To avoid re-uptake of CO_2, all solutions were continuously sparged with helium.

2.2.7 Elemental analysis / isotope ratio mass spectrometry (EA/IRMS)

Carbon and nitrogen isotopic ratios of reference materials of glyphosate and AMPA ("laboratory working standards") were determined by an EA/IRMS consisting of a EuroEA (EuroVector, Milano, Italy) coupled to a FinniganTM MAT253 IRMS (Thermo Fisher Scientific, Bremen, Germany) by a FinniganTM ConFlow III interface (Thermo Fisher Scientific, Bremen, Germany). The materials were calibrated against the reference materials USGS 40 (L-glutamic acid), USGS 41 (L-glutamic acid), IAEA 600 (caffeine) provided by the International Atomic Agency (IAEA, Vienna, Austria) [101]. The $\delta^{13}C$ and $\delta^{15}N$ isotope values were reported in per mille relative to PeeDee Belemnite (VPDB) and N_2-AIR, respectively.

$$\delta^{13}C_{sample,VPDB} = \frac{R\left(^{13}C/^{12}C\right)_{sample} - R\left(^{13}C/^{12}C\right)_{VPDB}}{R\left(^{13}C/^{12}C\right)_{VPDB}} \quad (2.1)$$

$$\delta^{15}N_{sample,N_2-AIR} = \frac{R\left(^{15}N/^{14}N\right)_{sample} - R\left(^{15}N/^{14}N\right)_{N_2-AIR}}{R(^{15}N/^{14}N)_{N_2-AIR}} \quad (2.2)$$

where ${}^{h}E$ *and* ${}^{l}E$ denote the heavy isotope and the light isotope of an element E (e.g., ${}^{h}E/{}^{l}E$= $^{13}C/^{12}C$, $^{15}N/^{14}N$), respectively.

For more detailed information on IRMS measurements (see Appendix II).

2.2.8 Standard and sample measurement

Samples of derivatized glyphosate (30 mM) and AMPA (45 mM) were prepared by dissolving the pure in-house laboratory reference material in MilliQ water and derivatizing it at pH 10 as described above. As described below, nitrogen isotope values of the derivatives were tested for precision, trueness and limit of precise nitrogen CSIA. Commercial samples were diluted in MilliQ water to 15 mM for GC/IRMS measurements and 2 mM for LC/IRMS measurements based on the concentration of active ingredient specified on the commercial herbicide products. Samples for GC/IRMS measurements were then derivatized at pH 10 using an excess of iso-PCF over glyphosate ratio of ten-fold. Samples were bracketed with derivatized glyphosate and AMPA in-house reference materials ("external laboratory standards") as a quality control for nitrogen isotope analysis by GC/IRMS. In the case of carbon isotope analysis by LC/IRMS, non-derivatizd samples were bracketed with non-derivatized laboratory reference materials.

2.2.9 Abiotic degradation of glyphosate with MnO_2

An abiotic degradation experiment of glyphosate was conducted with MnO_2 synthesized according to the HCl-$KMnO_4$ procedure by McKenzie et al. [102]. Briefly, the Birnessite (δ-MnO_2) was prepared by slowly pouring 6 M HCl into a boiling solution of 1 M $KMnO_4$. After 10 min of boiling, the mixture was filtered and washed with pure water until the pH of the residue was neutral. The solid residue was dried and stored over P_2O_5 as desiccant in an evacuated desiccator until further use. In the abiotic degradation experiment, 3 g δ-MnO_2 were suspended in 100 mL of a solution containing 1.5 mM glyphosate and 0.01 M sodium nitrate as background electrolyte. The experiment was conducted in 250 mL amber glass bottles where the mixture was continuously stirred with a Teflon-coated magnetic stir bar and the temperature was kept at 20°C on a water bath. Samples of 2 mL were withdrawn by a polypropylene single-use syringe (5 mL, B.Braun Melsungen AG, Melsungen, Germany) and filtered by hydrophobic PTFE syringe filters of 0.22 µm pore size (BGB Analytik AG, Rheinfelden, Germany). Carbon isotope analysis was performed in triplicate immediately after sampling. Samples were further stored at 4°C until they were derivatized for nitrogen isotope analysis (see above).

2.3 Results and discussion

2.3.1 Derivatization of glyphosate and AMPA

The derivatization of glyphosate and AMPA according to [83] is shown in Figure 2-3. As described in the experimental section, in a first step, target compounds were converted into their N-isopropylcarbonyl derivatives. Subsequently, these derivatives were extracted into an organic solvent and methylated by TMSD to form the desired methyl ester derivatives. When complete conversion occurs, no nitrogen fractionation is expected because: (1) all atoms are transformed to derivative (complete conversion) and (2) during the derivatization process no nitrogen atoms are introduced.

A gas chromatogram of the glyphosate and AMPA derivatives is shown in Figure 3 where the AMPA derivative elutes first followed by the glyphosate derivative and where the average peak widths were 47 s and 38 s, respectively. The peak resolution (R) for glyphosate and AMPA was 3.9 and 3.2, respectively, where R is defined as retention time difference divided by the mean peak width.

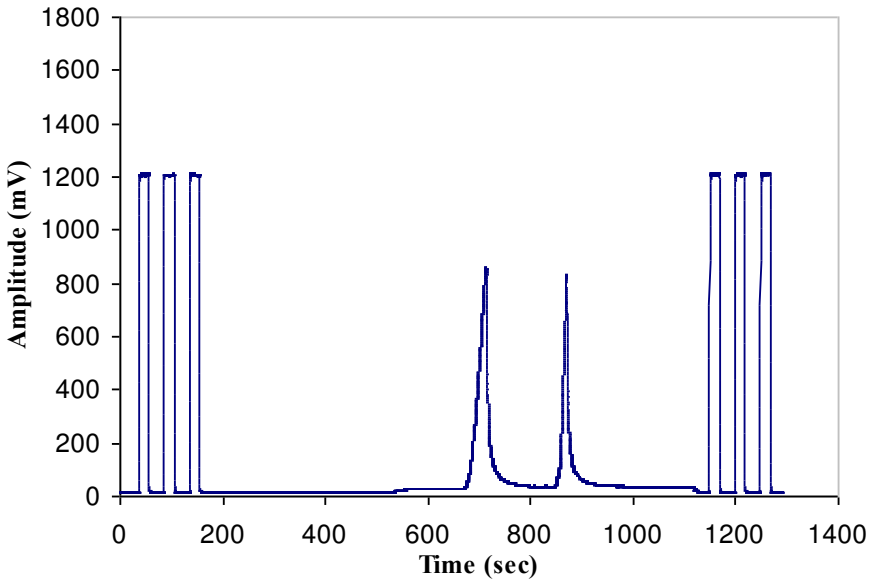

Figure 2-3: GC/IRMS chromatogram of derivatized in-house laboratory standards (amplitudes represent *m/z* 28): AMPA N-isopropyl methyl ester (720 s) and glyphosate N-isopropyl methyl ester (920 s) at concentrations of 20 mM and 13 mM, respectively. The three peaks at the beginning and the end of the chromatogram are from N_2 monitoring gas.

2.3.2 Optimum pH conditions for accurate isotope analysis

Different pH values (arrows in Figure 2-4) were tested in step 1 of the derivatization to investigate when the yield of the derivative was greatest. Figure 4a shows that GC/IRMS amplitudes of the derivative (m/z 28) were highest at pH 10. The yield was not significantly improved when increasing the excess of derivatization agent ratio from 4 to 7. Conversely, lower amplitudes were observed at pH 9, 11 and 12 suggesting that conversion of substance to its derivative was incomplete. This lower yield could also not be improved by increasing the excess of derivatization agent. Figure 4b shows that these observations were reflected in characteristic trends of δ^{15}N values which may be expected to be indicative of the underlying processes that led to incomplete conversion.

(a)

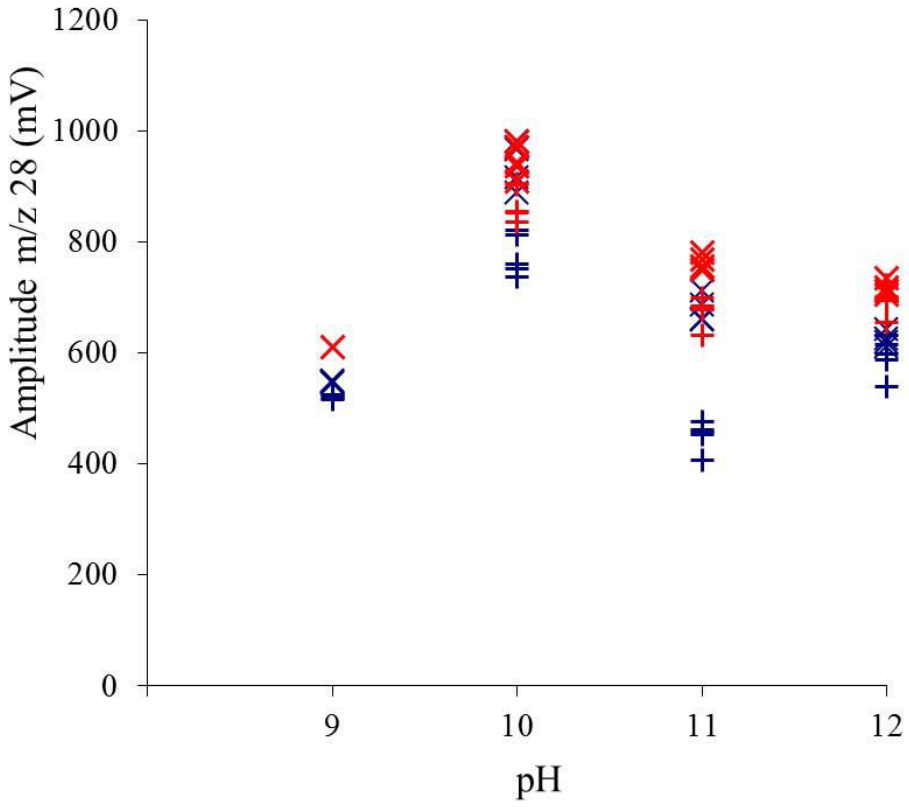

(b)

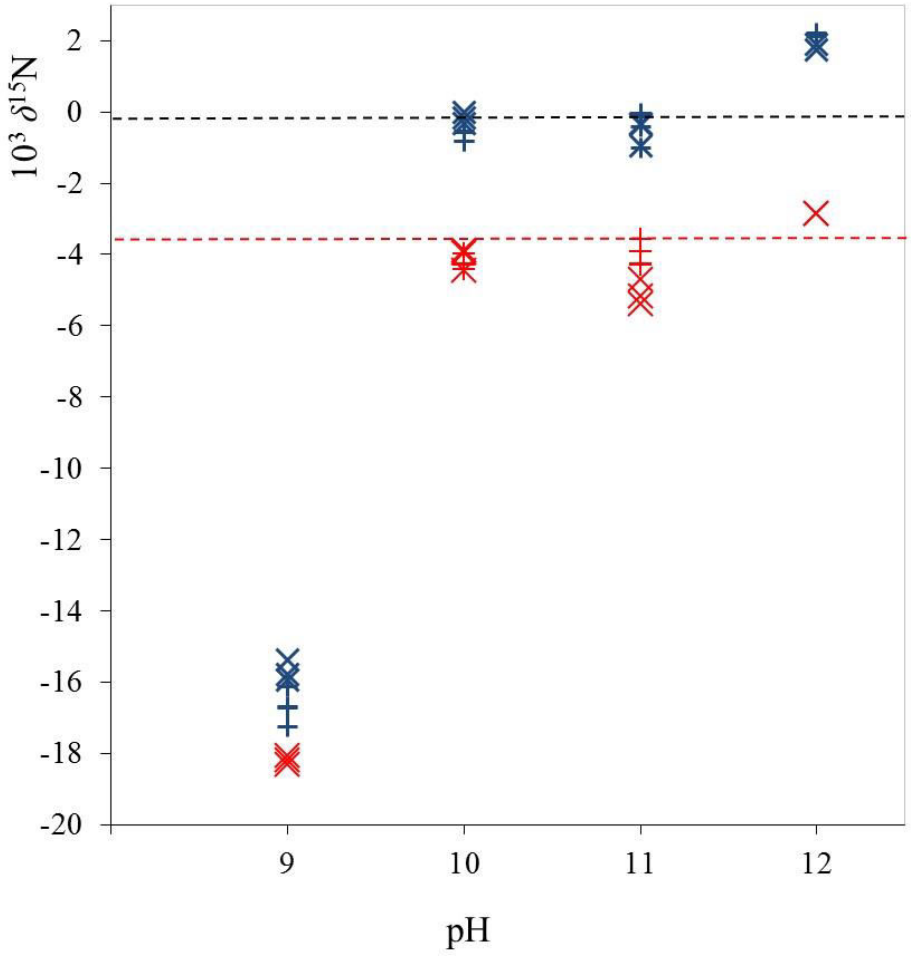

Figure 2-4 (a) Amplitudes of glyphosate and AMPA derivatives (m/z 28) vs. pH. (b) δ^{15}N isotope ratios of the derivatives depending on pH. Blue and red crosses "×" indicate the excess ratio of the isopropyl chloroformate derivatization agent to glyphosate and AMPA of 7. (iso-PCF: Analyte = 7). Blue and red "+" indicate the excess ratio of iso-PCF to glyphosate and AMPA of 4. (iso-PCF: Analyte = 4). The solid line and red dashed lines represent the δ^{15}N ratios measured by EA-IRMS of glyphosate and AMPA standard (-0.3 ‰, -3.7 ‰, respectively).

At pH 10 amplitudes were greatest, and the observed δ^{15}N value (-0.3 ‰ ± 0.8 ‰) of the glyphosate derivative was close to the target EA/IRMS value (-0.3 ‰ ± 0.1 ‰). These observations are consistent with results by Kataoka *et al*. [83] who reported an analyte conversion of >98% under these conditions. Hence, derivation at pH 10 was adequate for complete conversion and accurate nitrogen isotope analysis.

At pH values greater than 10, however, GC/IRMS amplitudes of the derivative became smaller and at pH 12, δ^{15}N values became more positive meaning that $^{15}N/^{14}N$ ratios increased in the derivative. These observations are indicative of a subsequent alkaline decomposition of the derivative. In such alkaline hydrolysis ^{14}N-containing molecules are preferentially hydrolysed [103] so that $^{15}N/^{14}N$ ratios increase in the remaining derivative molecules, consistent with the observations at pH 12. Hence, during derivatization the pH value should not become too high.

δ^{15}N values for derivatization at pH 9, finally, (a) showed a trend to more negative values, which was opposite to the trend to more positive values at pH 12, and (b) this trend towards negative values was in addition remarkably strong (-15 ‰). Both observations may be explained by incomplete derivatization at pH 9. (a) According to the kinetic isotope effect of derivatization ^{14}N-containing glyphosate molecules are preferentially converted so that the $^{15}N/^{14}N$ ratio in the derivative molecules is smaller (δ^{15}N values be more negative) than in the original glyphosate unless complete conversion has occurred. (b) While this explains the trend to more negative δ^{15}N values, it does not yet explain the magnitude of the particularly strong changes that were observed at pH 9 (-15 ‰). As further explanation it may be considered that at this pH only about 1% of all the glyphosate (pK_a = 10.9) is present in deprotonated form and can be derivatized. According to the well-established equilibrium isotope effect (EIE) of 20 ‰ between [$-N^+H_2^-$] (protonated) versus [$–NH^-$] (deprotonated) amino groups [104,105], the δ^{15}N values of this deprotonated [$–NH^-$] glyphosate are by 20 ‰ more negative compared to co-occurring protonated [$-N^+H_2^-$] gyphosate. Hence, the derivatization reaction already starts with molecules of particularly low $^{15}N/^{14}N$ values leading to even more negative δ^{15}N values as long as the derivatization reaction is not complete. Therefore, our results show that buffering solutions at pH 10 is critical for obtaining accurate nitrogen isotope ratios.

2.3.3 Effects of glutamate (amino acids) during derivatization with iso-PCF

The following additional optimization of our method was accomplished for samples containing a high background (10 gL^{-1}) of glutamate, corresponding to an excess of $2 \cdot 10^4$ of a foreign nitrogen-containing compound. (i) To adjust the pH to 10, 300 µL instead of 50 µL borate buffer were added in order to provide sufficient buffer capacity to counter the effect of glutamate. (ii) To provide also a sufficient excess of derivatization agent, 400 µL of 1.0 M isopropyl chloroformate in hexane were added. (iii) As vortex time, 6 minutes instead of 2 minutes were chosen to allow additional time for glyphosate molecules to partition into the aqueous phase as shown in Figure 2-5. This extra time was found to be necessary to

compensate for the slower reaction of glyphosate due to competition by glutamate (for partitioning into the organic phase and reaction). (iv) In the subsequent second derivatization step, 300 µl instead of 50 µL of 2.0 M trimethyl silyl diazomethane (absolute 600 µmol) were added to provide again a sufficient excess of derivatization agent. (v) To enable, finally, separation of glyphosate- and AMPA-derivatives from the interfering glutamate-derivative, a Rtx-5 Amine column (supplied by Restek, Germany) (30 m; 0.32 µm inner diameter; 1µm film thickness, was used with the following temperature program: the initial temperature of 80°C was held for 1 min. Then the temperature was increased to 150°C at 10°C min^{-1} held for 1 min and then ramped to 230°C at 3°C min^{-1}. The final temperature was held for 2 min as shown in the GC chromatogram in Figure 2-6)

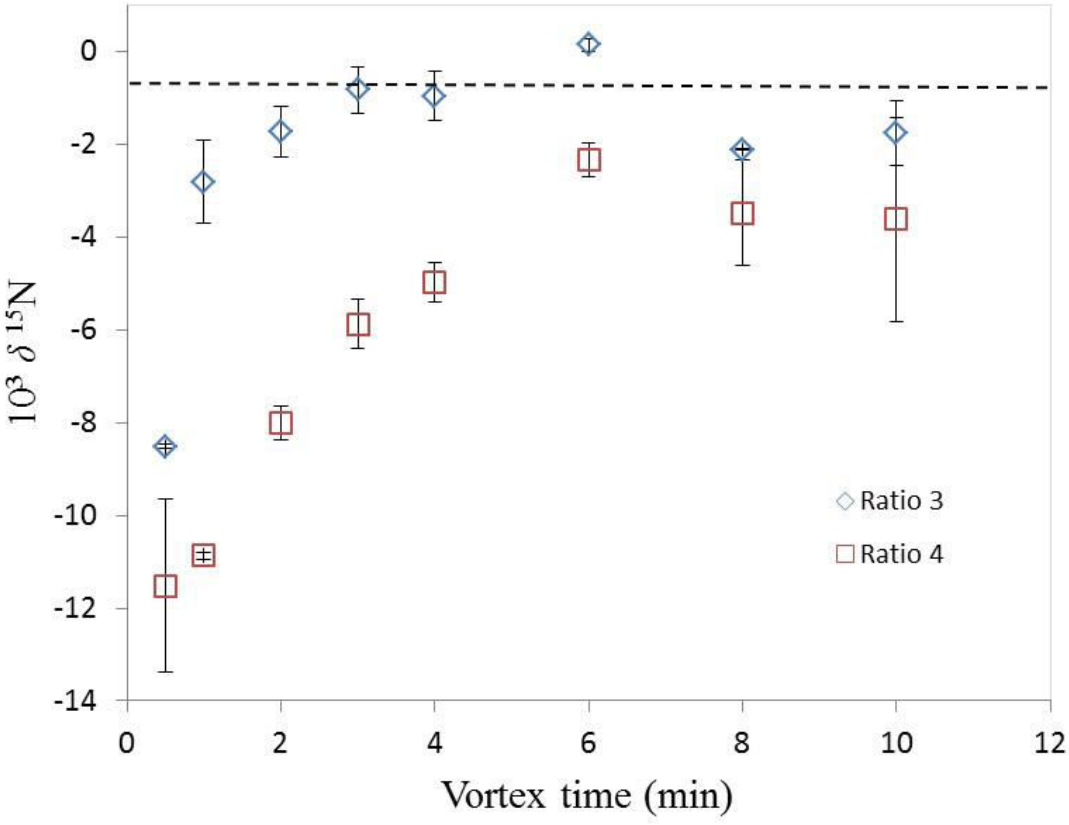

Figure 2-5: $\delta^{15}N$ values of glyphosate with increased vortex time (minutes). Blue diamonds and red rectangles represent an excess of iso-PCF to glutamate of 3 and 4, respectively. The dashed line represents the EA-IRMS $\delta^{15}N$ value of the glyphosate standard (-0.3‰). Error bars represent the standard deviation of duplicate measurements

(a)

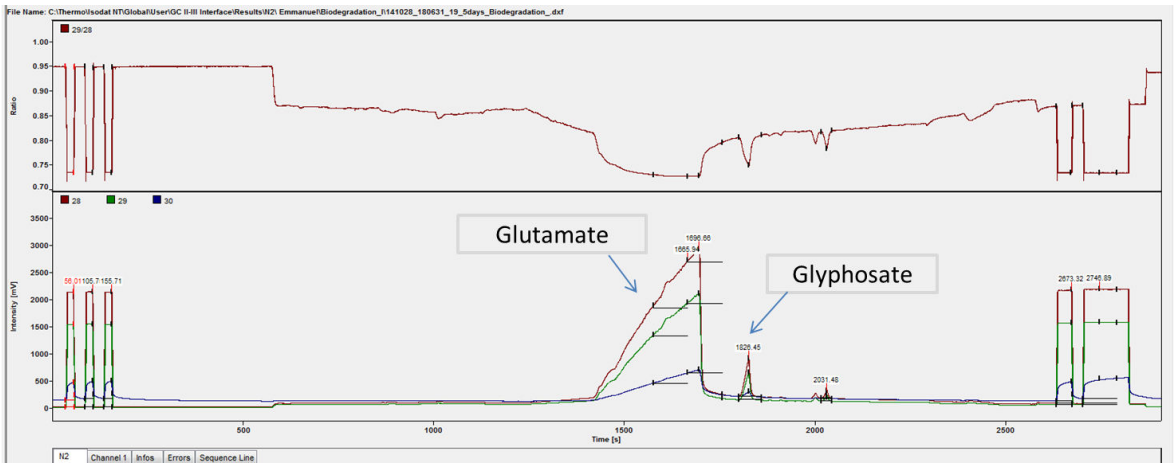

(b)

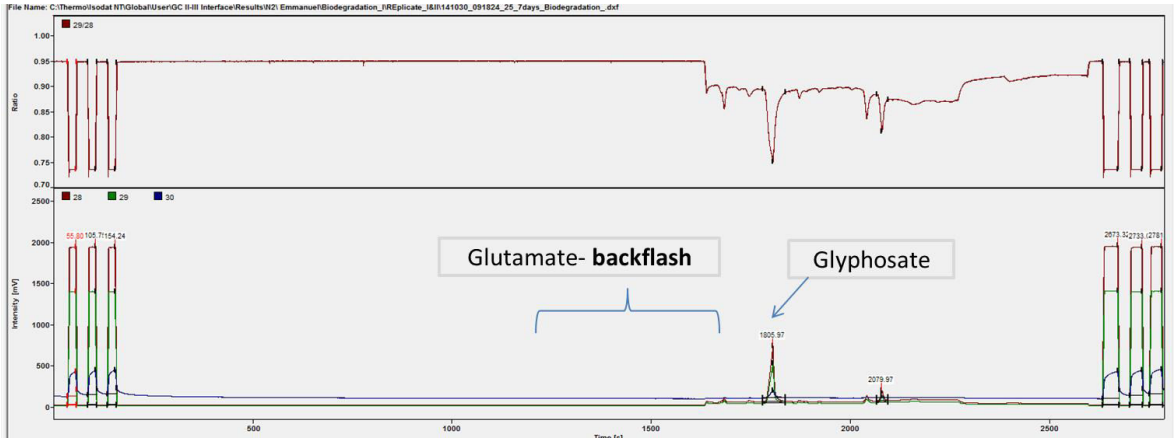

Figure 2-6 (a) GC chromatogram for nitrogen isotope analysis of glyphosate derivative (1820 sec) and glutamate derivative (1696 sec) separation on Rtx-5 Amine column. Three reference N_2 gas pulse at the beginning and end of chromatogram. Blue line (m/z 30), green line (m/z 29), brown line (m/z 28). (b) GC chromatogram after backflash mode and straight mode -glyphosate

2.3.4 Variability of excess derivatization agent

The effect of a variability of excess derivatization agent on glyphosate and AMPA is shown in Figure 2-7a and b. Results at iso-PCF:glyphosate ratios from 7 to 34 gave reproducible $\delta^{15}N$ values close to the EA/IRMS $\delta^{15}N$ target value (-0.3 ‰). A similar scenario for AMPA was observed. At iso-PCF: AMPA ratios between 7 and 24, $\delta^{15}N$ values were reproducible, albeit slightly more negative than the EA/IRMS $\delta^{15}N$ value (-3.7 ‰). An additional test with commercial herbicide samples (isoPCF:glyphosate ratio from 7 to 24) gave similar

observations (see Electronic Supplementary Material AII Figure S1) confirming that an excess of the derivatization agent 7 to 24 was adequate to produce accurate δ^{15}N values.

(a)

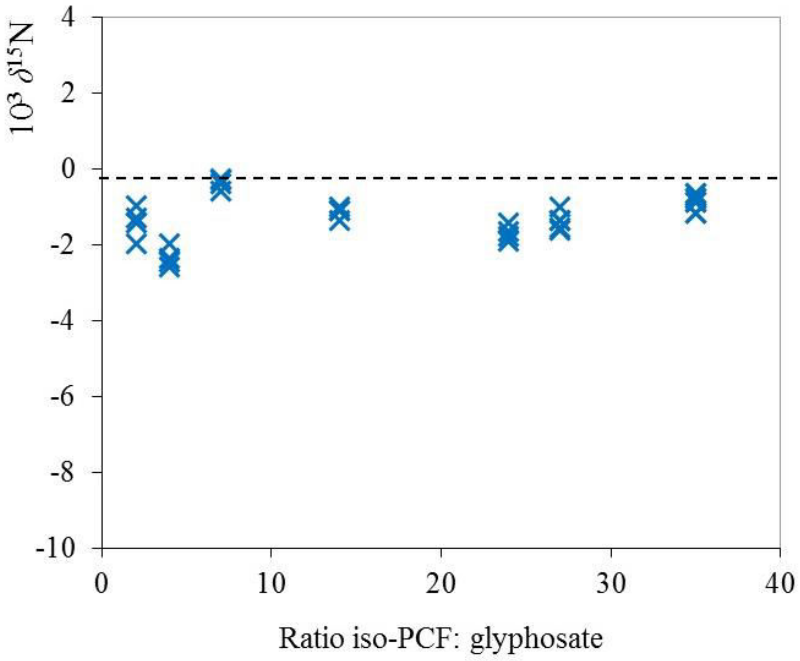

(b)

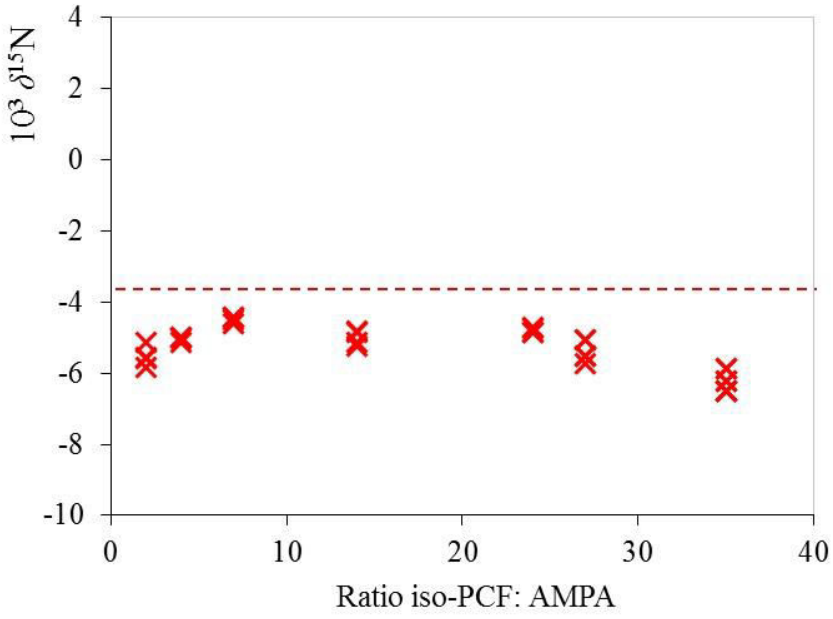

(c)

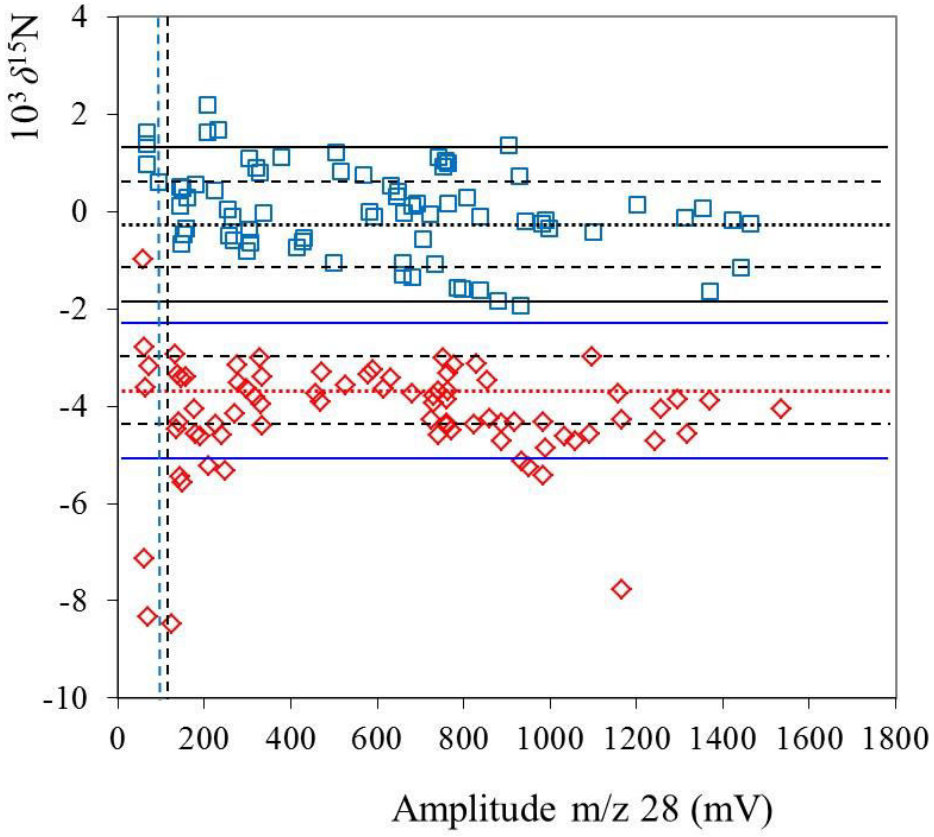

Figure 2-7 (a) δ^{15}N values of glyphosate (blue crosses) in dependence on iso-PCF: glyphosate ratios. EA-IRMS determined δ^{15}N value of glyphosate standard (-0.3 ‰) is represented by the black dashed line. (b) δ^{15}N values of AMPA (red crosses) in dependence on iso-PCF: AMPA ratios. EA-IRMS determined δ^{15}N value of glyphosate standard (-3.7 ‰) is represented by the red dashed line. (c) δ^{15}N values of glyphosate (blue rectangle) and AMPA (red diamonds) vs. peak amplitudes (m/z 28) from measurements of in-house laboratory standards in concentrations between 0.6 mM to 13 mM and 0.9 mM to 20 mM, respectively. The blue rectangle and red triangle represent the N-isopropyl methyl ester derivative of glyphosate and AMPA, respectively. The dashed lines represent the respective standard deviations (SD) (both ±0.8 ‰). The bold lines indicate the 95% confidence interval. The vertical dashed lines (blue and black) indicate the limit of precise δ^{15}N isotope analysis of glyphosate and AMPA (100 mV, 133mV) respectively.

2.3.5 Validation of the method

Figure 2-7c shows δ^{15}N values in dependence on amplitudes (m/z 28) for measurements of laboratory standards in concentrations between 0.6 mM (100 ppm) to 13 mM (2200 ppm) for glyphosate and 0.9 mM (100 ppm) to 20 mM (2200 ppm) for AMPA. The standard deviation of nitrogen isotope analysis was 0.9 ‰ (n=77; 95 % confidence interval CI= 2 σ) for glyphosate and 0.8‰ (n=77; 95 % CI= 2 σ) for AMPA. To test the trueness of the method the

nitrogen isotope ratio of the standards was compared to their EA/IRMS values. The method showed average nitrogen isotope ratios of -0.1 ± 0.4 ‰ (n=77) for glyphosate and -4.1 ± 0.3‰ (n=77) for AMPA derivatives which were close to (with a deviation of 0.2 ‰, 0.4 ‰) the expected ratios of the EA/IRMS (-0.3 ± 0.1 ‰ and -3.7 ± 0.1 ‰ respectively).

The lower limit of precise nitrogen isotope analysis was defined as the lowest amplitude that produced accurate nitrogen isotope ratios: 100 mV for glyphosate and 133 mV for AMPA respectively (see cut-off in Figure 2-7 c). This corresponds to a limit for accurate δ^{15}N values of 150 ng injected for glyphosate and 250 ng injected for AMPA respectively.

2.3.6 Glyphosate analysis of different commercial herbicides.

In order to test our method and to explore the variability of isotope ratios as a result of industrial glyphosate production, 29 samples from different manufacturers were analyzed. The δ^{15}N and δ^{13}C values of glyphosate are expected to be mainly influenced by the raw material and the production process. Production of commercial glyphosate involves three alternative processes: (1) the HCN (hydrogen cyanide) process - beginning with HCN synthesis from natural gas and ammonia catalyzed by platinum via the Andrusson process [106]; (2) the DEA (diethanolamine) process - where ethylene oxide and liquid ammonia are the starting raw materials and (3) the glycine process - where glycine is the raw material [107]. Even though two of these processes have liquid ammonia as nitrogen raw material, δ^{15}N isotope values of the glyphosate do not only depend on the initial ammonia isotopic signature, but are also affected by the production process. Therefore, in all the three processes different δ^{15}N values can be expected [106].

The δ^{15}N and δ^{13}C isotope values of the different commercial herbicides measured by GC/IRMS and LC/IRMS, respectively, are listed in (see Appendix II Table SI and SII) and shown in Figure 2-8a. The survey includes samples of previous work by Kujawinski *et al.* [1], which were for the first time characterized for δ^{15}N, and in addition includes thirteen new samples from pesticide products of a local market. The range of δ^{15}N of the commercial samples was from +3.3 ‰ to -1.5 ‰ while δ^{13}C values ranged from -24.6 ‰ to -33.7 ‰. The majority of the commercial samples had δ^{15}N ratios within ±1 ‰ of our laboratory glyphosate standards (I-III) (-0.3 ‰, -0.3 ‰ and -0.2 ‰, respectively). A dual element isotope plot of δ^{13}C versus δ^{15}N in Figure 2-8a, however, shows that more products could be distinguished when isotopes from carbon and nitrogen were considered together, compared to carbon isotope analysis alone. The dual plot therefore demonstrates the improved potential for source

distinction for different commercial glyphosate products when isotopic information on $\delta^{15}N$ and $\delta^{13}C$ becomes available in combination.

2.3.7 Nitrogen isotope ratios during abiotic degradation

To enable the use of multi-element isotope analysis to trace sources and degradation of glyphosate, an abiotic degradation experiment with manganese dioxide (MnO_2) as model reaction was conducted. The dual isotope plot ($\delta^{15}N$ vs. $\delta^{13}C$) combines the carbon and nitrogen isotope ratios of glyphosate herbicide samples from the different manufactures and the abiotic glyphosate degradation as shown in Figure 2-8b. The glyphosate isotope values during the abiotic oxidative degradation by MnO_2 showed a characteristic trend leading to values that were clearly outside of the glyphosate product range. This result demonstrates the superiority of the dual element isotope approach to trace sources and degradation of glyphosate.

(a)

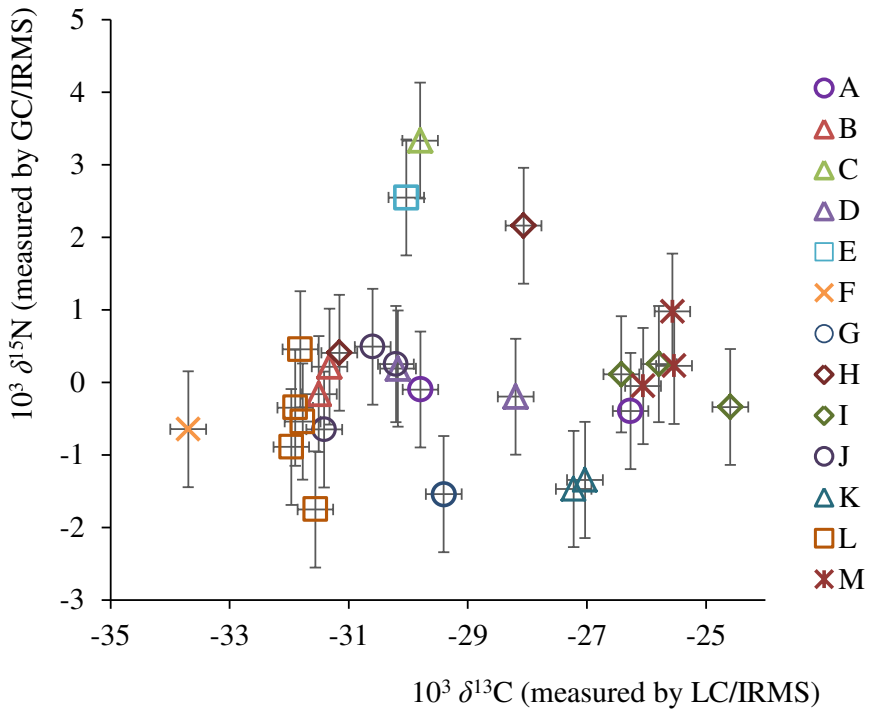

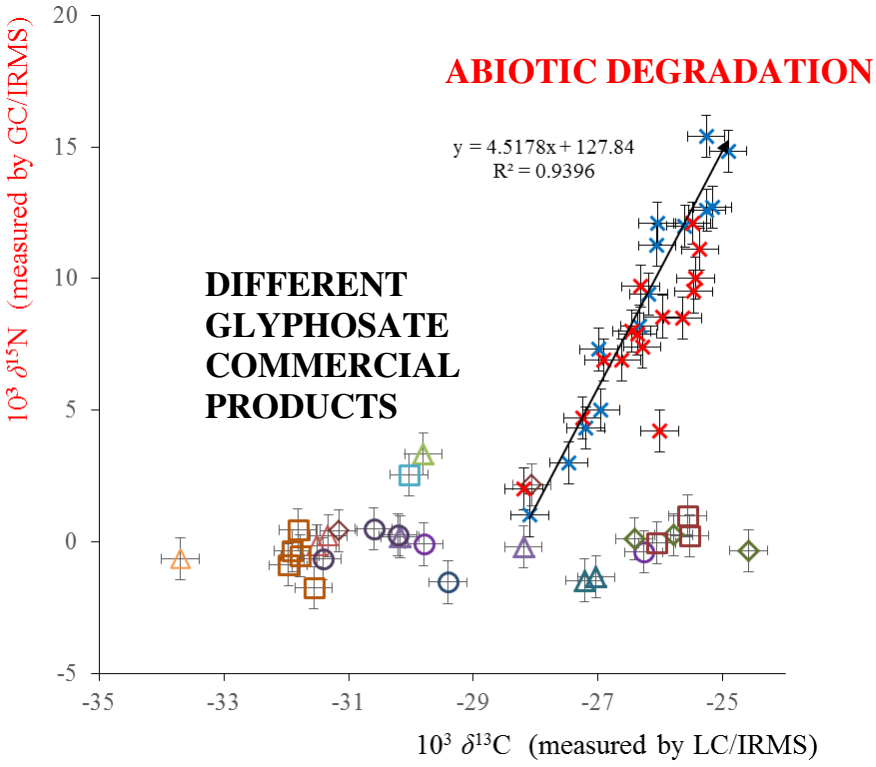

(b)

Figure 2-8 (a) Dual isotope plot (δ^{13}C vs. δ^{15}N) of glyphosate for different commercial herbicide samples. The letters A-M represent commercial herbicides products with glyphosate as active ingredient (see Appendix A2 Table SII shows the trade names). (b) Dual isotope plot (δ^{13}C vs. δ^{15}N) of the same products from different manufactures together with values measured during oxidative abiotic degradation of glyphosate with MnO_2 (red and blue crosses representing replicate experiments). Error bars given correspond to standard deviations of the methods (± 0.8‰ for δ^{15}N analysis, ± 0.3‰ for δ^{13}C analysis).

2.4 Conclusions

Compound-specific isotope analysis of glyphosate and AMPA was recently brought forward for δ^{13}C as a promising, but limited approach to authenticate commercial products and detect degradation [1]. This work introduces for the first time δ^{15}N isotope analysis for these compounds by derivatization - GC/IRMS and, thereby, unlocks the full potential of dual element isotope investigations with its superior resolution for distinguishing manufacturers and the possibility of identifying different transformation pathways [94]. For this breakthrough, a selection of optimum pH conditions in the first derivatization step by isopropyl chloroformate (iso-PCF) was found to be crucial, due to the delicate balance between incomplete conversion (leading to strongly negative δ^{15}N) and further decomposition of the derivative (causing shifts towards more positive δ^{15}N). Clear differences between

values obtained during abiotic glyphosate degradation and values measured from different glyphosate industrial products demonstrate the superiority of the dual element isotope plot for tracing sources and degradation. If suitable preconcentration methods from natural samples become available, the low limits of precise nitrogen isotope analysis presented in this study (150 ng and 250 ng for glyphosate and AMPA, respectively) may even enable a combined use of $\delta^{13}C$ and $\delta^{15}N$ analysis in future studies of environmental relevance. On the one hand, it may allow investigating different sources of AMPA – besides glyphosate, also phosphonates form AMPA as a key metabolite – and on the other hand it may provide novel insights into competing environmental transformation pathways of glyphosate.

Chapter 3

Biodegradation and Isotope fractionation of Glyphosate with *Ochrobactrum sp*. FrEM

Compound-specific Isotope Fractionation during Biodegradation of Glyphosate with *Ochrobactrum sp.* FrEM

Emmanuel O. Mogusu[1], Benjamin Wolbert[2], Maik Jochmann[2] Torsten Schmidt[2] and Martin Elsner[1]

[1]Helmholtz Zentrum München, Institute of Groundwater Ecology, Ingolstädter Landstrasse 1, 85764 Neuherberg, Germany.

[2] University of Duisburg-Essen, Instrumental Analytical Chemistry, Universitätstraße 5, 45141 Essen, Germany

Abstract

Compound-specific isotope analysis has recently been brought forward as a new opportunity to investigate sources and degradation of glyphosate. This work investigates for the first time the isotope fractionation associated with biodegradation of glyphosate. A bacterial strain was isolated from a vineyard soil sample using enrichment cultivation method. The bacteria were rod-shaped and were identified as *Ochrobactrum sp.* FrEM with 16S RNA sequencing. The strain utilized glyphosate as phosphorus source. A small carbon and nitrogen isotope fractionation of -4.8‰ ± 0.5‰ and -0.6‰ ± 0.7‰ respectively, was observed during biodegradation of glyphosate with *Ochrobactrum sp.* FrEM. The $AKIE_{carbon}$ for biotic degradation was calculated as 1.014. On the other hand, a strong nitrogen isotope fractionation of -17‰ during the abiotic degradation with MnO_2 was observed which could leave a significant imprint of degradation in natural systems. The combination of carbon isotope and nitrogen (dual element isotope plot) was able to differentiate between the abiotic degradation and biodegradation of glyphosate that had different slopes $\Delta = \delta^{15}N/\ \delta^{13}C = 4.6$ and 0.1, respectively.

3.1 Introduction

Glyphosate (*N*-phosphomethylglycine) is a systemic, non-selective, broad-spectrum, post-emerging herbicide effective in weed control for cultivation of corn, soya and sugar beet[14,51,108]. The worldwide market share of glyphosate is estimated at USD $ 5.6 billion, with production of 620,000 tonnes in 2008[109,19,20]. Recently, the World Health Organization's cancer research unit has classified glyphosate as probably carcinogenic to humans ("Group 2A"). This category is used when there is limited evidence of carcinogenicity in humans and sufficient evidence of carcinogenicity in experimental animals [26]. Additional concern about frequent detections of glyphosate and AMPA (aminomethyl phosphonic acid) in surface and groundwater motivates research into their environmental fate [49] [50,51,110,111].

Biodegradation is the main degradation pathway responsible for the mass removal of glyphosate in the environment[112,13,113]. Microbial degradation follows two degradation pathways. 1) AMPA formation by the cleavage of a C-N bond (N-dealkylation reaction) and 2) intermediate formation of sarcosine and glycine (C-P bond cleavage) [13]. Earlier studies isolated *Pseudomonas* sp. strain PG2982 and *Arthrobacter* sp. strain GLP-1, which both utilized glyphosate as sole phosphorus source. They formed sarcosine by C-P bond cleavage catalyzed by the enzyme C-P lyase [32]. Recently, the bacterial strains *Ochrobactrum anthropi GPK3* and *Achromobacter* sp, were isolated from soil. They showed the capability to degrade glyphosate through two alternative degradation pathways: by formation of AMPA (C-N bond cleavage) and sarcosine (C-P bond cleavage), respectively [34-36,114].

Compound-specific isotope analysis has recently been brought forward as new opportunity to investigate sources and degradation of glyphosate[115,1]. It takes advantage of the stable isotopic composition of an organic compound at natural abundance[98,94]. Abiotic or biotic transformation reactions of organic compounds can be detected based on kinetic isotope fractionation[59,116]. In addition, the isotope ratios can be used like fingerprints to distinguish different contaminant sources[56,117], and a characteristic evolution of these ratios during degradation reactions can give evidence of different transformation pathways.

Though first results on dual element (C, N) isotope analysis of glyphosate look promising to distinguish sources and degradation pathways[115] , additional research is necessary before the next step can be taken to investigate glyphosate in natural systems. In particular, two questions are of central relevance. (a) Can suitable enrichment methods be validated for

sensitive isotope analysis of glyphosate at low concentrations? (b) Can laboratory degradation studies demonstrate significant isotope fractionation associated with biodegradation of glyphosate, the main degradation pathway in nature?

This contribution focusses on exploring the second research gap. The specific objectives of this chapter were (1) to isolate and characterize strains capable of degrading glyphosate; (2) to measure carbon isotope fractionation associated with biodegradation; (3) to probe for the magnitude of nitrogen isotope fractionation in biodegradation; (4) to compare dual element isotope trends to preliminary data on abiotic degradation by MnO_2; (5) to use these results to assess the prospects of using isotope fractionation for investigating biodegradation of glyphosate.

3.2 Experimental Methods

A list of reagent chemicals and a detailed description of the analytical methods can be found in the appendix AIII (as supporting information chapter 3). The soil samples were collected from different plots (and later combined) on a vineyard field site in northern France (Agricultural and Viticultural College of Rouffach – Rouffach soil) where glyphosate was the most frequently used herbicide with a yearly application of between 18 and 61 kg/ha [118]. Soil samples from each plot location were then thoroughly mixed in sterile bottles, sealed, transported to the laboratory and stored at 4°C until use.

For bacterial isolation from soil, a mineral medium (MS1) (for composition see Supporting Information) with 60 mM (10 gL^{-1}) sodium glutamate as carbon source were used. Ammonium chloride was used as nitrogen source and glyphosate as sole phosphorous source. 10 g of soil sample were first sieved (> 2 mm). Then, 5 g of soil were suspended in 10 ml sterile water and centrifuged. One millilitre of sample was used to inoculate an MS1 medium containing 50 ml glyphosate in a 250 ml Erlenmeyer flask which was shaken at 160 rpm for 24 hrs. Several transfers were made and later streaked on agar plates containing 3 mM glyphosate. The single colonies formed were inoculated on agar plate (containing 60 mM glutamate as carbon source and 3 mM glyphosate) to represent the pure isolated strain. These were then identified and used for further biodegradation experiments.

The isolated bacteria were identified using 16S rRNA gene sequencing. For 16S rRNA gene amplification, the chromosomal DNA was isolated using a bacterial DNA extraction kit (Roche Applied Science, Germany) following the protocol of the manufacture. PCR amplification was performed using universal primers forward 27f and reverse 1492r. Standard PCR conditions was carried out in a 50 µL volume containing 1 × PCR buffer, 1.5 mM $MgCl_2$, 2 mM dNTP mixture, 1 µM primers, 1 µM of P*fu* DNA polymerase (Fermentas, St. Leon-Rot, Germany) and 2 ng of template DNA. DNA was purified from a gel using Agarose Gel Extraction kit (Roche Applied Sciences, Germany) and sequenced. Sequence homologies were evaluated using BLAST software (version 2.2.12). ClustalQ software was used to align the sequences. A neighbour-joining tress was constructed using Molecular Evolution Genetic Analysis (MEGA) software (version 6.0). The strain was identified as *Ochrobactrum sp.* strain FrEM (see Figure 4 in supporting information).

The biodegradation batch experiments were conducted (in replicates) using *Ochrobactrum sp.* strain FrEM grown on MS1 medium. Sodium glutamate 60 mM (10 gL^{-1}) was used as carbon source and 3 mM (0.5 gL^{-1}) glyphosate was used as sole phosphorus source. Fifty mililiters of nutrient medium (MS1) were inoculated with *Ochrobactrum sp.* strain FrEM and incubated at 30 °C at 160 rpm overnight. Cells were harvested by centrifugation, washed twice with minimal medium and transferred into a 250 ml Erlenmeyer flask containing 50 ml of MS1 medium without phosphorous (for cell starvation). This was incubated for 48 hrs, then 20 ml culture aliquots were centrifuged at 3000 rpm (Heraeus Megafuge 1.0R), and the pellets were inoculated into 150 ml of MS1 medium containing 120 µM glyphosate as only phosphorus source. The experiment was conducted in four replicates together with an experimental control (no bacteria). The bacterial growth was monitored (OD 590 nm) with a Varian Cary 50 Bio UV−vis Spectrophotometer. 3 ml aliquots were taken for concentration and 10 ml sample for isotope analysis ($^{13}C/^{12}C$ and $^{15}N/^{14}N$)). To prevent further degradation of the samples, 2 M NaOH was added and samples were stored at 4 °C until analysis. Samples for isotope analysis were frozen at -20°C and lyophilized for preconcentrate of the analytes.

A preliminary abiotic degradation experiment of glyphosate was conducted with MnO_2 synthesized according to the HCl-$KMnO_4$ procedure by McKenzie et al [102]. Briefly, 1.5 g of synthesized δ-MnO_2 were suspended in 100 mL of a solution containing 1.5 mM glyphosate and 0.01 M sodium nitrate as background electrolyte. The experiment was conducted in 250 mL amber glass bottles and the mixture was continuously stirred with a Teflon-coated magnetic stir bar at 20°C on a water bath. Samples of 2 mL were taken by a

polypropylene single-use syringe (5 mL, B.Braun Melsungen AG, Melsungen, Germany) and filtered by hydrophobic PTFE syringe filters of 0.22 µm pore size (BGB Analytik AG, Rheinfelden, Germany). Carbon isotope analysis was performed in triplicate immediately after sampling. Samples were further stored at 4°C until they were derivatized for nitrogen isotope analysis[115].

Carbon isotope analysis of biodegradation samples was modified compared to a recently developed method [1]. Since separation of glyphosate (sole phosphorus source) and glutamate (carbon source) was not possible on a Hypercarb (porous graphite carbon) column (see Figure 2 in Supporting Information), a mixed- phase Primesep 100 column 100 × 4.6 mm, 3 µm particle size (SIELC Technologies, ProspectHeights, IL, USA) was used instead. The column combines both hydrophobic and ion- exchange interactions as previously shown for separation of amino acids[119,120](see Figure S2 in the Appendix III). This enabled the separation of glyphosate and glutamate using a modified phosphate buffer as mobile phase at pH 3.1 (see Figure 2 supporting info). At pH 3.1 glyphosate (pKa = 2.6) was negatively charged while glutamate (pKa = 2.1) was neutral (see scheme 1 in supporting information). Glutamate was retained (more interaction) on the column while glyphosate eluted first because of charge repulsion. Base line separation of glyphosate and glutamate enabled accurate measurement of carbon isotope ratios. The mobile phase eluent was 2.5 mM NaH_2PO_4 adjusted to pH 3.1 with H_3PO_4. The flow rate was 300 µLmin^{-1} in isocratic mode. The injected sample volume was 25 µL. The reagents to convert the HPLC effluent to CO_2 were phosphoric acid (1.5 M) and sodium peroxodisulfate (0.84 M). For all experiments the flow rate of each reagent was 50 µLmin^{-1}. The wet chemical oxidation was performed at a reactor temperature of 99.9 °C. The helium (grade 5.0) flow rate of the separation unit to transfer CO_2 to the IRMS was set to 2.3 mL/min.

Nitrogen isotope analysis was adapted according to the recently developed method (for description see the Appendix III) [115]

The Rayleigh model for a closed system was used to quantify the isotopic fractionation (equation 3-1), where the enrichment factor (ε) describes the relationship between the change in carbon isotope ratios (R_t/R_o) and the change concentrations ($f = C_t/C_o$) [94] where R_t and R_o are the compound isotope ratios of heavy and light isotope of an element at given time and at beginning of reaction, respectively. δ^hE and δ^hE_o are the corresponding isotope ratios in per mil notation and *f* is fraction of remaining substrate (C_t/C_o)

$$\ln \frac{R_t}{R_0} = \ln\left(\frac{1+\delta^h E}{1+\delta^h E_0}\right) = \varepsilon \ln f \qquad (3\text{-}1)$$

3.3 Results and discussion

3.3.1 Isolation and biodegradation of glyphosate

The repeated subculturing of the sampled soil in the MS1 medium containing 3 mM glyphosate as sole P-source was able to isolate the strain with glyphosate-degrading activity. The bacteria were rod-shaped as observed on light microscope (see Figure 5 Supporting Info). Identification was confirmed with 16S RNA sequencing. Sequence alignment (BLAST) showed a 99 % homology with *Ochrobactrum anthropic, O. rhizosphaerae, O. pituitosum* and *O. intermedium* which all belong to the family of Brucellaceae of Alpha proteobacteria, and 70 % homology with *Ochrobactrum haematophilum.* The strain was identified as *Ochrobactrum sp.* FrEM. (see phylogenic tree AIII Figure S6 Supporting Information chapter 3).

Figure 3-1 shows the decrease in glyphosate concentrations and the simultaneous increase in optical density (OD 590 nm) when the strain was grown on glyphosate. Glyphosate degradation was induced after undergoing phosphorous starvation similar to other studies [121,34]. No evidence of AMPA was observed during the biodegradation of glyphosate. However, there was evidence of sarcosine formation (attributed by the retention time in LC/IRMS) which suggests that degradation involved C-P bond cleavage catalyzed by the C-P lyase enzyme.

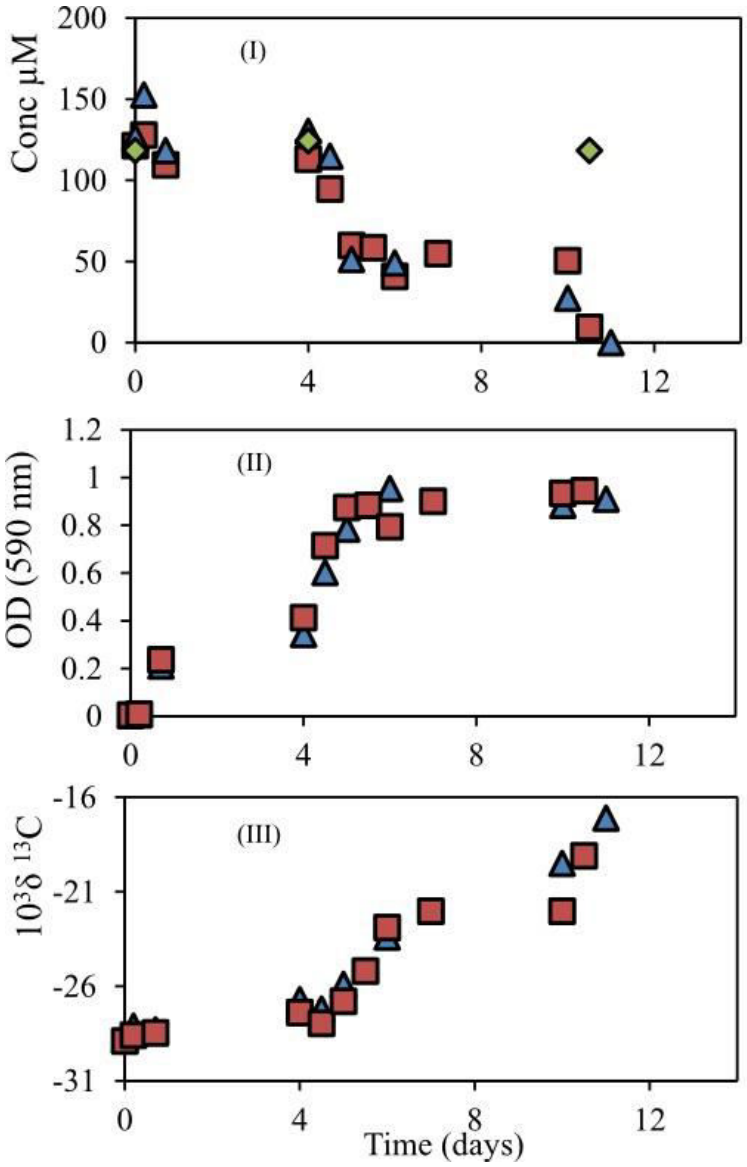

Figure 3-1: Panel (I) Degradation of glyphosate by *Ochrobactrum* sp. FrEM when grown in MS1 medium containing 120 µM glyphosate as the only phosphorous source (blue triangles and red rectangle represent replicates and green diamonds the control) . Panel (II) Measured bacterial growth (OD 590 nm) with time (blue triangles and red rectangle represent replicates). Panel (III) $\delta^{13}C$ values during glyphosate degradation by *Ochrobactrum sp* FrEM (blue triangles and red rectangle represent replicates)

3.3.2 Stable isotope fractionation of glyphosate during biodegradation

Figure 3-1 panel III further shows that biodegradation with *Ochrobactrum sp.* FrEM was associated with small, but significant carbon isotope fractionation. $\delta^{13}C$ values of glyphosate changed from -28 ‰ ± 0.5‰ to -19 ‰ ± 0.5‰ upon 90 % conversion reflecting an enrichment of $^{13}C/^{12}C$ as the reaction proceeded. From the corresponding enrichment factor of ε_C = -5.5‰ ± 0.5‰ (Figure 3-2, Panel A) a primary apparent kinetic isotope effect AKIE in the C-P bond cleavage may be calculated according to the equation 3-2:

$$AKIE = \left(\frac{1}{\frac{n}{x}\varepsilon + 1} \right) \qquad (3\text{-}2)$$

where n denotes the number of carbon atoms at the reactive positions, ε represents the enrichment factor and x the total number of carbon atoms[59].The calculated primary apparent kinetic isotope effect during glyphosate biodegradation was $AKIE_{carbon}$ 1.016.

In contrast, preliminary results obtained from a limited number nitrogen isotope measurements indicate only small nitrogen isotope fractionation (ε_N = -0.6‰ ± 0.7‰) (Figure 3-2, panel B). The isotope effect was within the confidence interval of the measurement which was ±1.7‰. The observed small nitrogen isotope effect suggests a secondary nitrogen isotope effect since the nitrogen atom is not at the reactive position.

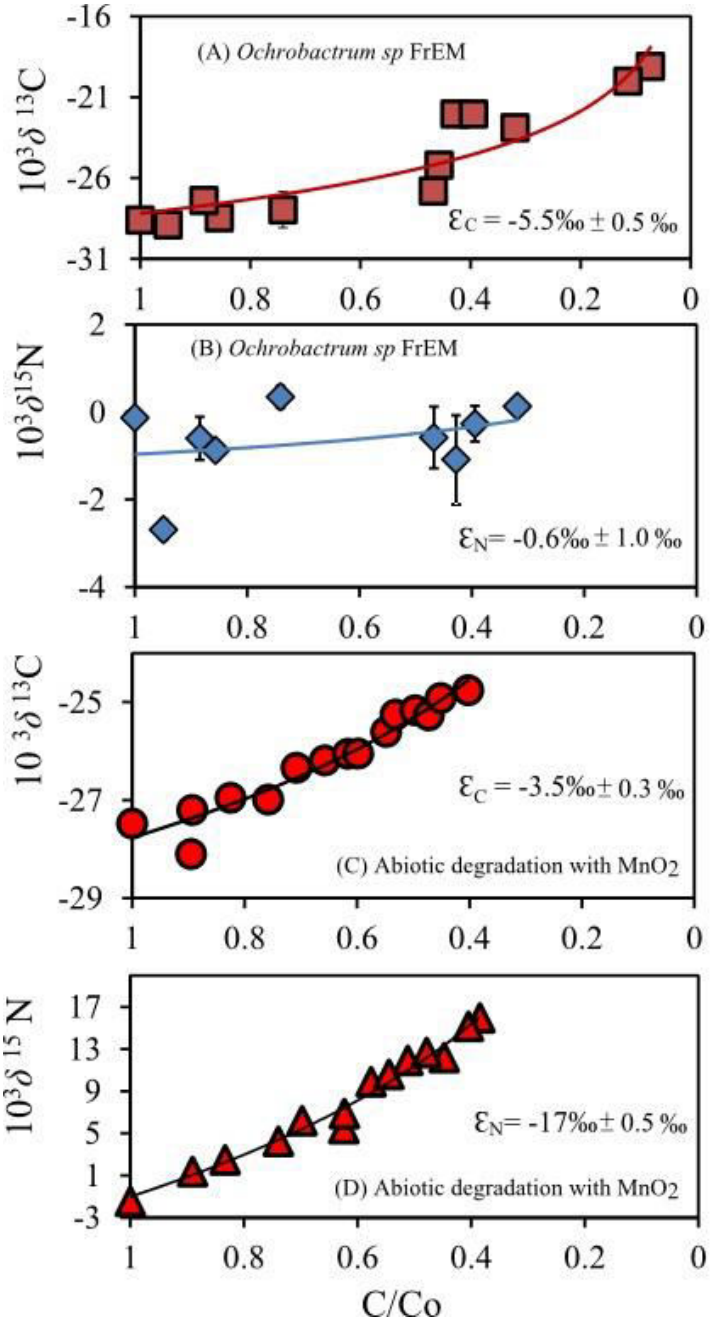

Figure 3-2: Panel (A) $\delta^{13}C$ values during glyphosate degradation by *Ochrobactrum sp* FrEM (red rectangles).Panel (B) $\delta^{15}N$ values during glyphosate degradation by *Ochrobactrum sp* FrEM (blue diamonds). Error bar of nitrogen isotope data represent standard deviation of GC/IRMS measurements. Panel (C) $\delta^{13}C$ values of glyphosate during abiotic degradation with Mn_2O (red circles), Panel (D) $\delta^{15}N$ values of glyphosate during abiotic degradation with Mn_2O (red triangles).

3.3.3 Stable isotope fractionation of glyphosate during abiotic degradation

In contrast to biotic degradation, abiotic transformation of glyphosate by MnO_2 formed two simultaneous transformation products: 1) AMPA as a result of C-N bond cleavage and 2) sarcosine as a result of C-P bond cleavage in the glyphosate molecule (Figure 3, Supporting Information). $\delta^{13}C$ values of glyphosate changed from -28 ‰ ± 0.3‰ to -24.7 ‰ ± 0.7‰ upon 60 % conversion reflecting an enrichment of $^{13}C/^{12}C$ as the reaction proceeded. From the corresponding enrichment factor of ε_C = -3.6‰ ± 0.3‰ (Figure 3-2, Panel C) a primary apparent kinetic isotope effect AKIE in the C-N bond cleavage can be calculated as $AKIE_{carbon}$ 1.011. This value is lower than the AKIE of the oxidation of aromatic amines by MnO_2 which is in the range 1.018 to 1.022[122]

In contrast, strong nitrogen isotope fractionation during abiotic degradation was observed. $\delta^{15}N$ values of glyphosate changed from -0.2 ‰ ± 0.5‰ to -17 ‰ ± 0.5‰ upon 60 % conversion reflecting an enrichment of $^{15}N/^{14}N$ as the reaction proceeded. The calculated nitrogen isotope enrichment factors from replicate experiments were as high as ε_N = -17.8‰ ± 1.0‰ corresponding to a kinetic isotope effect of $AKIE_{nitrogen}$ = 1.018. During glyphosate degradation, $\delta^{15}N$ isotope values of AMPA started from more negative values compared to initial glyphosate composition at -15‰ and AMPA become preferentially enriched in $^{15}N/^{14}N$ as the reaction proceeded and is expected to reach the initial isotope composition of glyphosate after glyphosate is completely degraded for reason of isotopic mass balance. Overall the strong nitrogen isotope fractionation is expected to leave a strong imprint to be used to identify transformation when occurring natural systems.

3.3.4 Dual isotope plot

Multi-element isotope analysis potentially offers the opportunity to distinguish different degradation pathways. The reason is that different transformation reactions typically involve different bonds and different elements leading to characteristically different trends in dual isotope plots[116,96,61]. Figure 3-3 shows a dual element isotope plot ($\delta^{15}N$ verses $\delta^{13}C$) combining carbon and nitrogen isotope ratios analysed during biodegradation of glyphosate (by *Ochrobactrum sp.* FrEM) and abiotic degradation (by MnO_2). The respective slopes of abiotic degradation ($\Delta = \delta^{15}N / \delta^{13}C = 4.6$) and the preliminary data on biodegradation ($\Delta = \delta^{15}N / \delta^{13}C = 0.1$) show different trends indicating the potential to distinguish between abiotic and biodegradation of glyphosate.

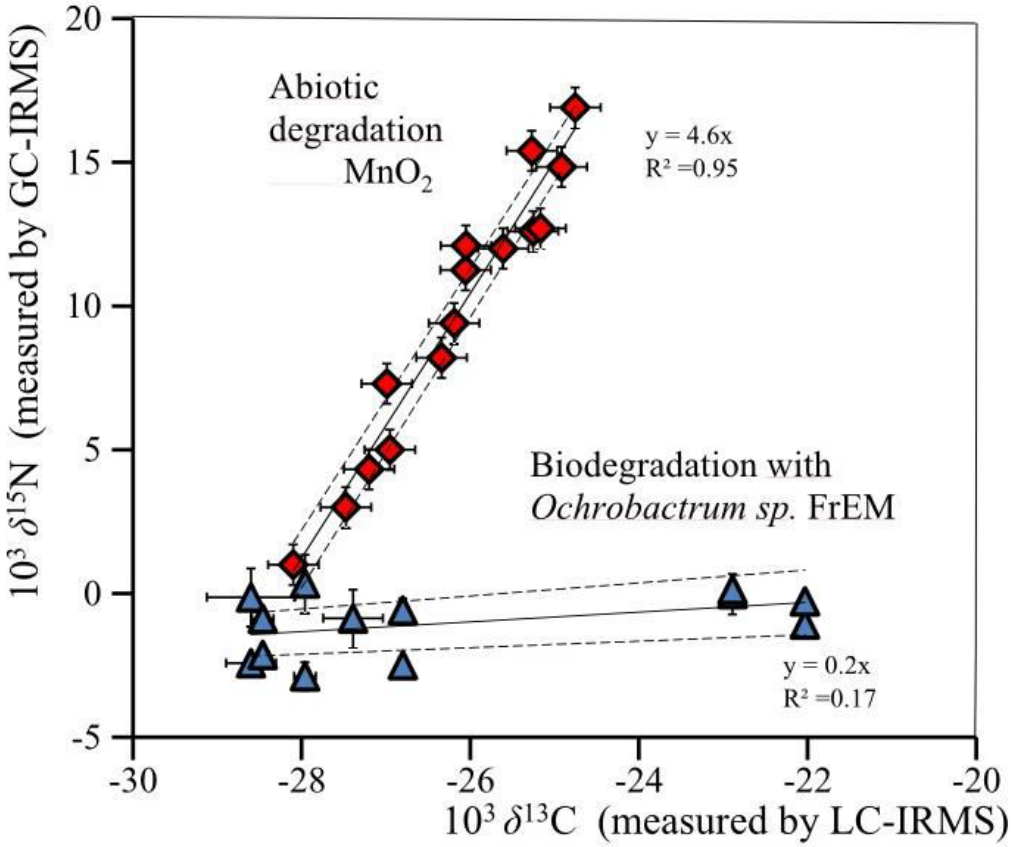

Figure 3-3: Dual element isotope plot for nitrogen versus carbon isotope ratios ($\delta^{13}C$ vs. $\delta^{15}N$) during glyphosate biodegradation with *Ochrobactrum sp*. FrEM (blue triangles) and the oxidative abiotic degradation of glyphosate with MnO_2 (red diamonds). The dashed lines indicate 95% confidence intervals (Cl)

3.4 Environmental significance

Glyphosate and AMPA are frequent surface and groundwater contaminants. There is great potential to use compound-specific isotope analysis to detect their degradation in natural systems. The $\delta^{13}C$ values of glyphosate changed from -28 ‰ to -19 ‰ during biodegradation with *Ochrobactrum sp.* FrEM. On the other hand, the $\delta^{13}C$ values of glyphosate herbicides measured from different manufactures were between -33‰ to -24‰[1]. An isotopic enrichment above the $\delta^{13}C$ values of glyphosate herbicides may leave a robust imprint of biodegradation imprint in natural systems and provide additional evidence of biodegradation. Abiotic degradation of glyphosate with MnO_2 (a ubiquitous transition metal oxide present in soil) caused the $\delta^{15}N$ values to change from 0 ‰ to -17 ‰. This was clearly outside the range of the measured $\delta^{15}N$ values of glyphosate herbicides products which were between -2 ‰ to 3 ‰. In case of glyphosate natural samples, the slope obtained from the dual isotope analysis may suggest the preferred degradation pathway. However, the assessment of the environmental fate of glyphosate and AMPA may only be feasible when sensitive enrichment methods for sensitive isotope analysis become available in the future. It may also allow the investigation of different sources of AMPA (pesticide metabolite vs transformation product of laundry products).

Chapter 4

Enrichment Method Development with Alumina

Extraction of Glyphosate from Water with Activated Alumina: Parameter Optimization and Preliminary Isotope Measurements

Emmanuel O. Mogusu and Martin Elsner

Abstract

Glyphosate (*N*-phosphomethylglycine) is a systemic, non-selective herbicide widely applied for weed control during cultivation of corn, sugar beet and cotton. The frequent detection of glyphosate and AMPA (amino methylphosphonic acid) in surface and groundwater motivates research into their environmental fate. While CSIA bears potential to distinguish sources and degradation of glyphosate and AMPA, the absence of a sensitive enrichment method currently makes such investigations challenging in natural systems. Here we tested alumina as adsorbent for the enrichment of glyphosate from water. Commercial activated alumina was found to have a high adsorption capacity of 85 mg/g corresponding to a sorption site density of 2 µmol/m^2. Adsorption of glyphosate on activated alumina was pH dependent. Adsorption occurred at pH 6-8 where glyphosate was negatively charged and the alumina surface was still positively charged because the pH was lower than the PZC (point of zero charge). Desorption of glyphosate, in contrast, was favored above pH 10 where glyphosate molecules and the alumina surface were both negatively charged. Preliminary isotope analysis ($^{13}C/^{12}C$ & $^{15}N/^{14}N$) of glyphosate suggested that no significant isotope discrimination is expected after enrichment on activated alumina highlighting the potential of activated alumina to enrich glyphosate and AMPA from water for subsequent compound-specific isotope analysis.

4.1 Introduction

Phosphorus-containing xenobiotics are of great economic importance and have found extensive applications as insecticides, herbicides, detergent additives and as flame retardants. Many contain a C-P bond, which is chemically and thermally very stable leaving biological degradation as main breakdown pathway in the environment [123]. Glyphosate (*N*-phosphomethylglycine) - an organophosphonate - is perhaps the single most frequently used herbicide today. It is a systemic, non-selective, broad-spectrum, post-emerging herbicide effective in weed control for cultivation of corn, soya and sugar beet [124,125,19]. On the other hand, the frequent detection of AMPA and glyphosate in groundwater [52,126,49] together with the recent classification of glyphosate as probable carcinogen motivates research into their environmental fate [26].

For example, AMPA is also a key metabolite of phosphonate chelating agents that have wide application in household washing detergents, corrosion inhibitors and oil drilling which then makes its assessment complex[53,127]. However, investigating the degradation and sources of glyphosate and AMPA using conventional methods (measuring the change in concentration) is challenging because metabolites are not always detected, establishing mass balance is difficult and requires extensive monitoring campaigns. Compound-specific isotopic analysis (CSIA) is a promising alternative to investigate sources and degradation of organic pollutants.

Recently, the potential of CSIA (compound-specific isotope analysis) of glyphosate and AMPA to distinguish sources and degradation of these compounds has been brought forward [115,1]. Until now, however, CSIA of glyphosate and AMPA is still challenging in natural systems because: (1) relatively large amounts of glyphosate and AMPA (150 ng and 250 ng, respectively) [115] are required for precise isotope analysis whereas (2) glyphosate and AMPA are typically present at trace concentrations (µg/l) in natural water so that extraction of 30-50 liters of water would be needed to reach the required amounts (150 ng and 250 ng, respectively) for isotope analysis.

However, the physical properties of glyphosate and AMPA (highly polar, zwitterionic, high solubility in water) make it challenging to apply traditional approaches such as liquid-liquid extraction since glyphosate does not partition into organic solvents. Solid phase extraction (SPE) is a well-known technique for pre-concentration and sample clean-up of numerous different classes of compounds [128,129]. In fact, SPE pre-concentration analysis of glyphosate and AMPA in different matrices (food, soil and water) was successfully

performed in combination with LC-MS/MS (liquid chromatography tandem mass spectrometry) after modifying the polar groups (by addition of a non-polar group, typically FMOC-Cl) [82,130]). Unfortunately, this approach is not suitable for stable isotope analysis because the introduction of additional carbon atoms during derivatization entails potential isotope fractionation during derivatization and the additional atoms "dilute" isotope changes in the target compound [98]. Other studies have used supported liquid membrane devices (SLM) for enrichment and purification of glyphosate and AMPA from fruit juices. SLM is a porous polymeric hydrophobic membrane with hydrophilic solvents immobilized in its pores. [131,132]. However, the optimization of the pH of the donor phase, donor flow rate/stirring rate, the non-selective character of Aliquot 336 (commercial extractant- quaternary ammonium chloride) that result in the competition with other anions (Cl^-, NO_3^-) and more importantly the insufficient capacity for CSIA are disadvantages of this method [133,134]. In another study, anion exchange resins were used for extraction and pre-concentration of glyphosate and AMPA. However, the large amount of resin that would be required and the competition with other anions present in water make this approach challenging and uneconomic for extraction of low concentrations from large amounts of water [135]. Finally, passive samplers were also used to monitor the flux- proportional concentration of glyphosate in soil and groundwater. The device was packed with γ alumina as the adsorbent together with integrated traces (i.e calcium citrate- the integrated traces store the information on the volume of water that has passed the sampler during the installation period). The device enabled flux-proportional monitoring of the concentration of glyphosate with a 3.3 % recovery. In a recent study, a passive sampler fitted with titanium dioxide (TiO_2) as binding phase was used as measure to estimate the concentration of glyphosate and AMPA in surface water. Glyphosate and AMPA were retained well with TiO_2 and eluted with 1 M NaOH with good recoveries (>65%) [136,137]. Also mechanistic studies show that glyphosate adsorbs strongly to soil organic matter, mineral surfaces and metal oxides [138-141]. It adsorbs to mineral surfaces by formation of surface complexes with the constituent metal ion at the surface [142,143]. The binding appears to be stronger at pH = 6 where the phosphono-group is deprotonated [144]. Sorption of glyphosate on different adsorbents is well established [13,139]. In a recent study, glyphosate was shown to adsorb to activated alumina and at the same time to form ternary complexes with Zn^{2+} ions [145]. In addition, competitive sorption of glyphosate and phosphate has extensively been studied [146,48,140,147,148]. Phosphate was shown to facilitate desorption of glyphosate. While these studies emphasize the promise of metal oxide-based solid phases as extractant for SPE of glyphosate and AMPA, the

available methods have not yet been tested and optimized to extract and enrich the amounts necessary for sensitive isotope analysis. To close this research gap, an enrichment method for sensitive isotope analysis is warranted.

This chapter presents our first preliminary work for the extraction of glyphosate from water as a prerequisite for glyphosate and AMPA isotope analysis in natural systems. The objectives of this work were: (1) to choose a convenient sorbent material for the enrichment of glyphosate from water, (2) to determine the best conditions for sorption and to characterize the number of sorption sites, (3) to characterize drivers behind desorption in dependence on pH and (4) to obtain the first data on the associated isotope fractionation during sorption and desorption on activated alumina

4.2 Experimental Methods

4.2.1 Materials

Glyphosate (99%, CAS No. 1071-83-6), AMPA (99%, CAS No. 1071-83-6), ammonium acetate (99%), ammonium carbonate (99%), potassium dihydrogenphosphate (99%), 1.0 M Iso-PCF (isopropyl chloroformate) in hexane, 2.0 M TMSD (trimethyl silyl diazomethane) in ethyl ether as well as diethyl ether, methanol, ethyl acetate and *tert*-butanol (with purities >99%), FMOC-Cl (9-Fluorenylmethyl chloroformate 97% purity were all purchased from Sigma-Aldrich (GmbH Steinheim, Germany). Sodium peroxodisulfate ($Na_2S_2O_8$), potassium hydroxide (KOH), phosphoric acid (H_3PO_4) and monosodium phosphate (KH_2PO_4) (all with purities >99% from Fluka; Steinheim; Germany) were used as LC eluents and oxidation reagents. Stock glyphosate and AMPA standards were prepared in MilliQ water (generated with a Millipore Advantage A10 system, Millipore, Molsheim, France).

The activated alumina was kindly provided in two particle sizes by the Albemarle, Mertinswerk, Germany. The BET specific surface area was 250 m^2/g and sodium oxide content of 0.3 %. Goethite (30-63% Fe) was purchased from Sigma-Aldrich (GmbH Steinheim, Germany). Quartz sand was supplied by Dorsilit Nr. 5F, Quarzsande GmbH, Germany.

4.2.2 Batch adsorption experiment

To select a suitable adsorbent for glyphosate extraction, three adsorbents (activated alumina, goethite and quartz) were tested because of their long history as adsorbents of charged pollutants [149,150]. Adsorption isotherms of glyphosate on the different adsorbents were

determined in batch experiments where the initial glyphosate concentration was varied from 20 mg/L to 500 mg/L (0.1 mM to 3 mM). No buffer was added so that in the case of activated alumina the corresponding pH value varied between 2.7 (high glyphosate concentration) to 6.2 (low glyphosate concentration) when measured immediately after glyphosate addition, and between 6.2 to 8.8 after equilibration for 24 hours. In the case goethite it varied between 5.2 and 2.8 with increasing glyphosate concentration (as shown in Figure 1 (a) and Figure S3 (c) in the Appendix). In each batch experiment 1 mg of the adsorbent (activated alumina, goethite and quartz) was loaded into a 50 ml plastic Falcon tube. Then, 45 ml of solution containing different concentrations of glyphosate were added to the tubes. The tubes were shaken on an orbit shaker at 100 rpm overnight at 25 °C. After the reaction period, all samples were centrifuged and the supernatant was sampled and glyphosate concentrations were analyzed by LC/MSMS as described previously [151,82]. The quantity of glyphosate that was adsorbed was calculated by the difference of the initial and residual amounts of glyphosate in solution divided by the weight of the adsorbent.

A Langmuir model was used to describe the experimental results of glyphosate adsorption on adsorbents according to equation 4.1 and 4.2

$$Q_e = q_m \frac{K_L C_e}{1 + K_L C_e} \qquad (4.1)$$

$$\frac{1}{Q_e} = \frac{1}{q_m K_L}\frac{1}{C_e} + \frac{1}{K_L} \qquad (4.2)$$

where Q_e represents the amount of glyphosate adsorbed on activated alumina (mg/g), q_m is the maximum amount of glyphosate per unit weight of activated alumina for complete monolayer coverage, K_L is the equilibrium adsorption constant related to the affinity to the adsorption sites (L/mg) and C_e is the equilibrium glyphosate concentration in solution (mg/L). The reciprocal form of the Langmuir model was used to perform the linear regression according to equation 4.2 (see also Figure S5 in the Appendix IV).

4.2.3 Desorption efficiency

To test the desorption efficiency, after adsorption the activated alumina pellets were collected into separate 50 ml falcon plastic tubes. Fourty milliliters of either ammonium hydroxide

(NH_4OH), ammonium carbonate ($(NH_4)_2CO_3$), or potassium dihydrogenphosphate (KH_2PO_4) were added at different concentrations (0.2 mM, 0.9 mM, 2.5 mM, 10 mM, 24 mM, 50 mM and 1 M). The pH of each of the eluents at each concentration was measured during desorption of the glyphosate. The solutions were agitated and samples were collected every hour for direct analysis of glyphosate concentrations by LC-MS/MS (see section 4.2.5 LC-MS/MS measurement).

4.2.4 Extraction of glyphosate on packed alumina column

To test the extraction of glyphosate from a large volume of water, modified packed alumina columns were used. The modified packed alumina columns were prepared by taking 1 ml plastic syringe tubes cleaned by flushing with MilliQ water. At the tip of each tube a prop of porous soft lab paper towel material (to prevent loss of alumina during packing) was inserted. Then, the column was packed with 0.5 g of activated alumina and rinsed with water until all air bubbles had disappeared. MilliQ water was allowed to run through the packed alumina column for 2 min to ensure it was not blocked. Figure 6 represents the schematic setup used for the enrichment of glyphosate with these modified packed alumina columns. The setup consisted of an 8 port vacuum manifold which was connected to a vacuum pump and a waste trap.

To test the extraction efficiency, glyphosate was spiked to either 0.25 L or 1 L water of different types (MilliQ water, surface and groundwater) to obtain concentrations of 100 µg/l. The surface and groundwater samples were sampled from Isar River and Mangfalltal groundwater - Munich, respectively. The extraction efficiencies were determined by calculating recoveries of the spiked samples.

4.2.5 LC-MS/MS measurements

For the analysis of glyphosate concentrations from desorption experiments, samples were analyzed by direct injection (20 µL volume) into the LC-MS/MS system (Applied Biosystems, Foster City, CA, USA). A C18, 5 µm, 30 mm×2 mm i.d., PEEK-lined Luna column purchased from Phenomenex (Germany) was used for analyte separation. The mobile phase was composed of water buffered with 1.5 mM ammonium carbonate at pH 9 (solvent A) and 50% (v/v) MeOH (solvent B). The LC gradient for the separation included a linear increase of B from 10% to 90% between 0 and 4 min. One minute was allowed to establish initial conditions and the column was re-equilibrated for 3 min after the run, resulting in a total run time of 7 min. The flow rate was 0.2 mL min^{-1} and the column temperature was 30

°C. The chromatogram and MS/MS parameters of glyphosate are given in Figure S2 and Table S1, respectively. For the adsorption isotherm experiment, glyphosate concentrations were measured according to the method by Zanini *et al* [151]. Briefly, glyphosate samples were first derivatized using FMOC-Cl at pH 9 and then the glyphosate derivative was analyzed by LC/MS-MS. A C18, 5 µm, 30 mm×2 mm i.d., PEEK-lined Luna column from Phenomenex (Germany) was used for separation. The mobile phase was composed of water buffered with 1.5 mM ammonium acetate at pH 9 (solvent A) adjusted with NH_3 and MeOH (solvent B). The LC gradient for the separation included a linear increase of B from 10% to 25% between 0 and 3 min. This was followed by an isocratic gradient of B between 3 to 6 min, followed by a linear increase of B from 25% to 90% between 6 and 15 min Three minutes were allowed to establish initial conditions and the column was re-equilibrated for 7 min after the run, resulting in a total run time of 25 min. The flow rate was 0.2 mL min^{-1} and the column temperature was 30 °C. (MS/MS parameters are shown in Table S2 in Appendix IV)

4.2.6 Nitrogen isotope analysis by GC/IRMS

The derivatization of glyphosate and AMPA followed the procedure described previously [115]. Nitrogen isotope analysis of the N-isopropyl carbonyl tri methyl ester derivative was conducted by GC/IRMS according to the method by Mogusu *et al*. [115]. The GC/IRMS system consisted of a Trace GC Ultra-gas chromatograph (Thermo Fisher Scientific, Milan, Italy) linked to a Finnigan MAT 253 (Thermo Fisher Scientific, Bremen, Germany) by a Finnigan GC combustion III interface (Thermo Fisher Scientific, Bremen, Germany). Helium (grade 5.0, supplied by Linde, Germany) was used as carrier gas at a flow rate of 1.4 mL min^{-1}. The analytes were injected by a GC CombiPal autosampler (CTCAnalytik, Zwingen, Switzerland) in splitless mode at a constant injector temperature of 250°C and after 1 min, the split ratio was switched to 1:10. Separation was achieved on a 30 m DB-5 column (Agilent Technologies, USA) with 0.25 mm i.d. and 1.0 µm film thickness. The oven temperature was programmed as follows: the initial temperature of 80°C was held for 1 min. Then the temperature was increased to 230°C at 10°C min^{-1}. The final temperature was held for 8 min [115].

4.2.7 Carbon isotope analysis by LC/IRMS

Carbon isotope analysis of glyphosate was conducted by LC/IRMS according to the method by Kujawinski *et al*. [1]. The LC/IRMS system consisted of a Finnigan Surveyor HPLC system including a Surveyor MS pump and a Surveyor autosampler coupled to a Finnigan MAT 253 IRMS via a Finnigan LC isolink interface (all instruments Thermo Fisher Scientific Bremen, Germany). For separation a Hypercarb column 100 × 4.6 mm, 3 µm particle size (Thermo Scientific, Langerwehe, Germany) was used. The eluent was a 2.5 mM NaH_2PO_4 solution adjusted to pH 1.9 with conc. H_3PO_4. The flow rate was 300 µL min^{-1} in isocratic mode. The injected sample volume was 25 µL..

4.2.8 Elemental analysis / isotope ratio mass spectrometry (EA/IRMS)

Carbon and nitrogen isotopic ratios of reference materials of glyphosate and AMPA ("laboratory working standards") were determined by EA/IRMS consisting of a EuroEA (EuroVector, Milano, Italy) coupled to a Finnigan MAT253 IRMS (Thermo Fisher Scientific, Bremen, Germany) by a Finnigan ConFlow III interface (Thermo Fisher Scientific, Bremen, Germany). The materials were calibrated against the reference materials USGS 40 (L-glutamic acid), USGS 41 (L-glutamic acid), IAEA 600 (caffeine) provided by the International Atomic Agency (IAEA, Vienna, Austria)

The isotope mass balance during adsorption of glyphosate on alumina was calculated from $\delta^{13}C$ values and from the fraction of glyphosate sorbed according to the following equation:

$$\delta\,{}^{13}C^{0} = \delta\,{}^{13}C^{A} \times F^{A} + \delta\,{}^{13}C^{NA} \times F^{NA} \qquad (4\text{-}3)$$

where, F^{A} represents the fraction of glyphosate adsorbed (superscript A – adsorbed), F^{NA} represents the fraction remaining in solution after adsorption (superscript NA- not-adsorbed)..

4.3 Results and Discussions

4.3.1 Adsorption isotherm

Adsorption isotherm studies were conducted to determine the adsorption capacity of glyphosate on activated alumina from aqueous solution. Figure 4-1 shows a plot of the uptake of glyphosate by the adsorbent (activated alumina) against the glyphosate equilibrium concentration in solution (see also adsorption isotherms for goethite and quartz in Figure S3 in supporting info). The Langmuir adsorption isotherm was used to describe the experimental data. The adsorption capacity (q_m) was calculated from the linear regression in Figure S5 (a).

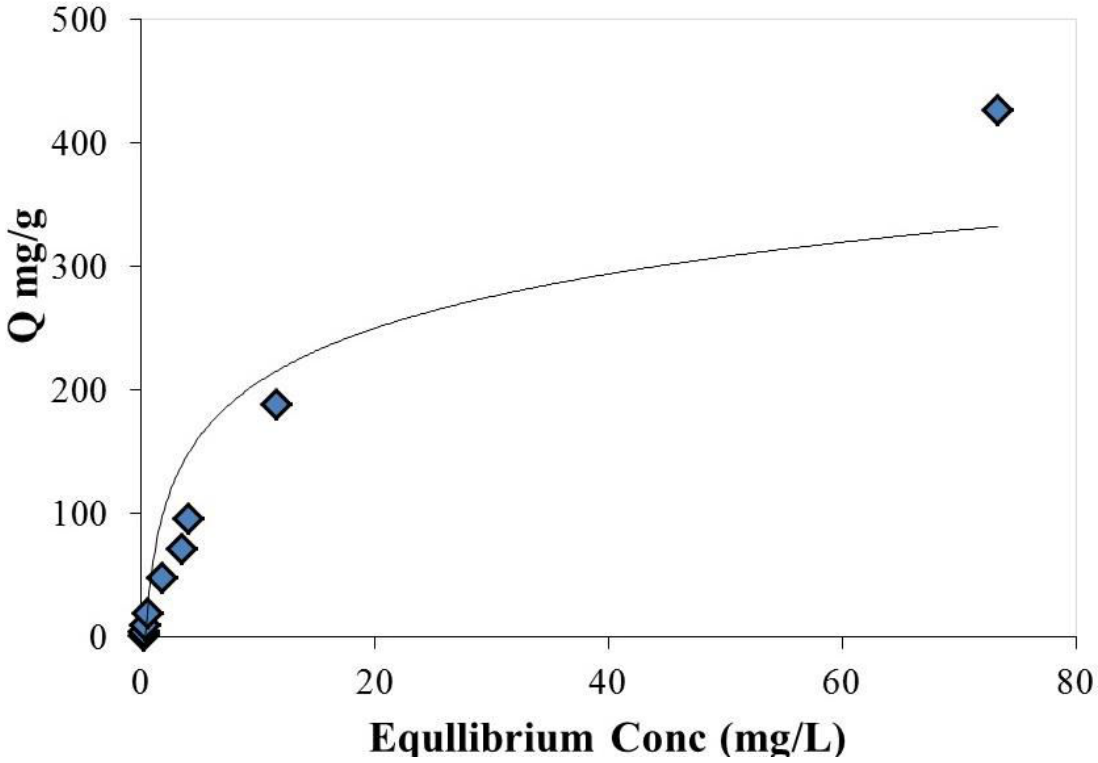

Figure 4-1: Adsorption isotherm of glyphosate on activated alumina. Solid line corresponds to the fit with the Langmuir equation.

It was observed that the Langmuir isotherm fitted the experimental data reasonably well. The correlation co-efficient (R^2= 0.99), which is a measure of the goodness of fit, confirms the good representation of the experimental data with this model. The Langmuir model assumes that the adsorption surface is homogenous and that the adsorption sites are equivalent with only mono-layer coverage. From the isotherm, the activated alumina had a relatively high adsorption capacity towards glyphosate of Q= 85 mg/g. This value is similar to those reported for phosphate adsorption [150,152]. With a BET surface area of 250 m^2/g this corresponds to a surface site density of 2 µmol/m^2 (1.2 site/nm^2). This surface adsorption site density for

glyphosate is in a similar range as that reported for phosphate adsorption (2.5 µmol/m^2) on alumina [153-155]., With such a high glyphosate adsorption capacity, an extraction efficiency of close to 100 % would be expected especially at concentrations between 0.1 mM and 0.3 mM of glyphosate at a 1:1 solid to solution ratio. This shows that the activated alumina can potentially be used as a suitable adsorbent for glyphosate extraction.

4.3.2 Expected effect of pH on adsorption

The schematic representation Figure 1 (a) shows the speciation of glyphosate during adsorption of glyphosate on an activated alumina surface. At the beginning of the experiment, glyphosate dissociated in water at concentrations between 500 ppm to 20 ppm (3 mM to 0.1 mM) giving rise to pH values between 3 and 6. This corresponds to a pH range in which the net charge of glyphosate in aqueous solution is -1 (see Figure 2). After equilibration in the presence of alumina for 24 h the pH increased to values between 6 and 8 (Figure 2). In this pH range the net charge of glyphosate in aqueous solution is -2. An even higher pH of 9.5 was observed when alumina was equilibrated in milliQ water in the absence of glyphosate for 24 hrs. This pH value was in the range of the PZC (point of zero charge) of alumina of 8 to 9.3 [156-158] – i.e. at the pH value at which the surface charges of alumina is zero. Hence, the alumina surface is positively charged at pH < pH_{PCZ} and negatively charged at pH > pH_{PCZ}, and the alumina surface acts as a buffer around its own PZC. These considerations suggest that glyphosate is best adsorbed at a pH that is lower than the PZC (point of zero charge) so that the alumina surface is positively charged, but still in a range where glyphosate is deprotonated and carries a negative charge. The decrease in adsorption at higher pH most probably results from changes in the electrostatic interaction between the adsorbed species, whose negative charge increases with pH [159]. These results show that in order to achieve optimum adsorption of glyphosate on alumina surface, the packed alumina column should be preconditioned with water for a few hours with water at a pH below the PZC.

(a)

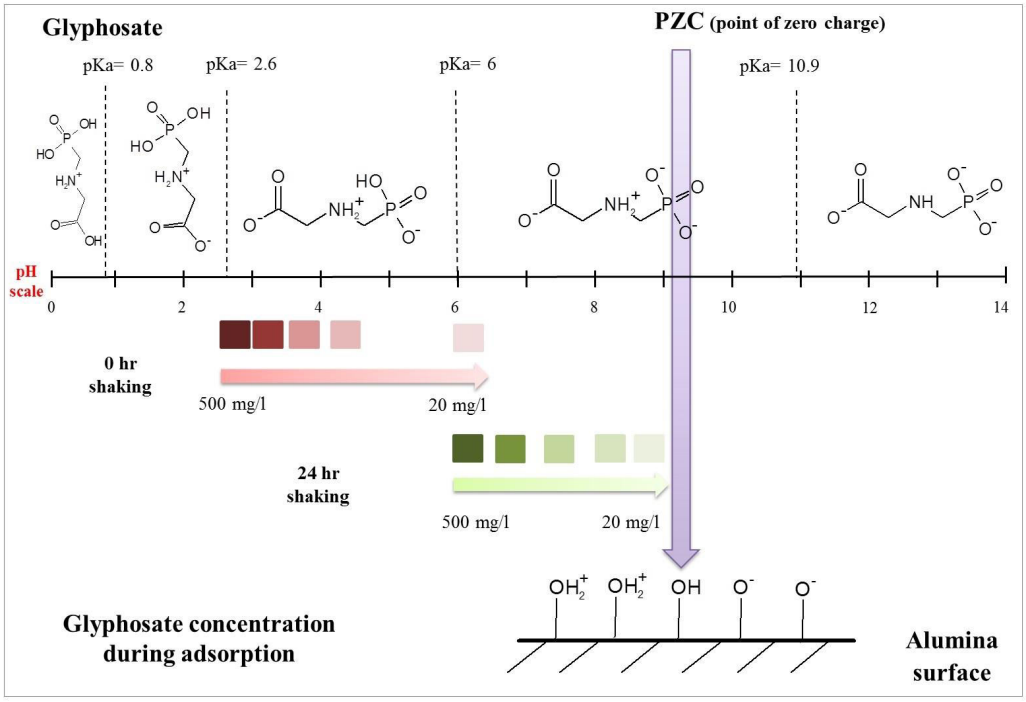

(b)

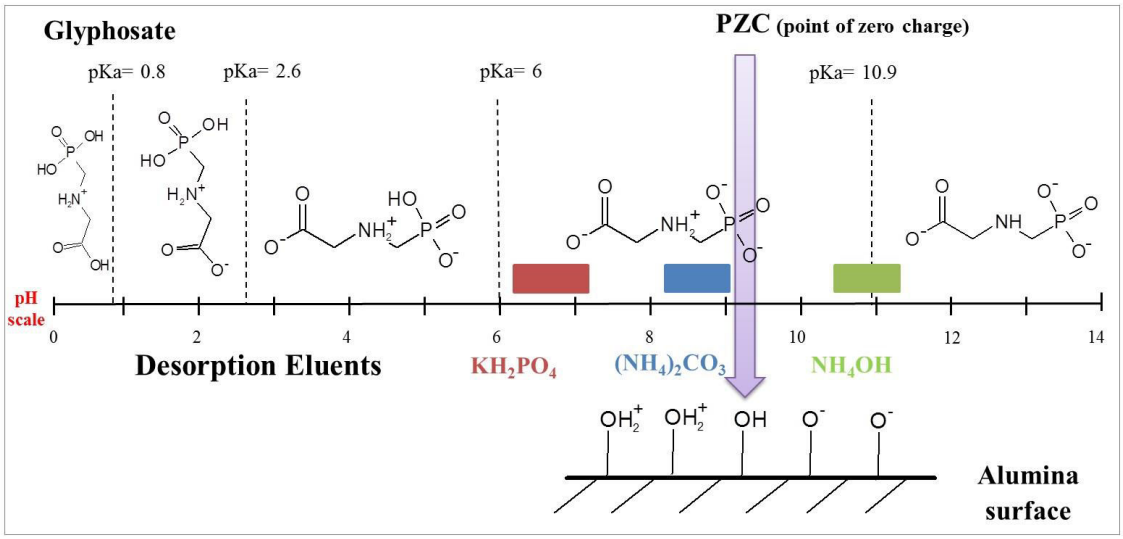

Figure 4-2: Panel (a) pH speciation of glyphosate during adsorption on activated alumina surfaces at different glyphosate concentrations. Brown squares represent the glyphosate speciation at different concentrations and Green squares represent the glyphosate speciation on alumina surface after 24 hours equilibration. Panel (b) pH speciation of glyphosate during desorption on activated alumina surfaces with different eluents solution. Brown rectangle represents potassium dihydrogen phosphate, blue rectangle represents ammonium carbonate and green rectangle represents ammonium hydroxide elution solution.

4.3.3 Desorption of glyphosate

Desorption experiments were conducted in order to investigate the efficiency of glyphosate desorption with the following selected eluents. (i) Potassium dihydrogen phosphate (KH_2PO_4) to investigate competitive desorption of phosphonate by phosphate at pH values below the PZC; (ii) ammonium carbonate ($(NH_4)_2CO_3$) to investigate desorption at pH values below the PZC and (iii) ammonium hydroxide (NH_4OH) to investigate desorption at pH values above the PZC. Figure 1 (b) shows the pH regime of the used eluent solution for desorption of glyphosate from the alumina surface. The pH of the elution solution at different concentrations is shown in Figure 2 (a). The pH values decreased with eluent concentration for KH_2PO_4 while they increased with concentration for both $(NH_4)_2CO_3$ and NH_4OH. Figure 2 (b) shows the recovery of glyphosate with the different eluent solutions. KH_2PO_4 had the lowest recovery (< 5 %) and the recovery even decreased with increasing eluent concentration. In contrast, addition of $(NH_4)_2CO_3$ and NH_4OH eluent solutions (with gave better recoveries of 20 % and 40 %, respectively, where recovery was largely concentration-independent for $(NH_4)_2CO_3$, but increased with increasing concentrations of NH_4OH. (see Figure S2 in the Appendix IV).

(a)

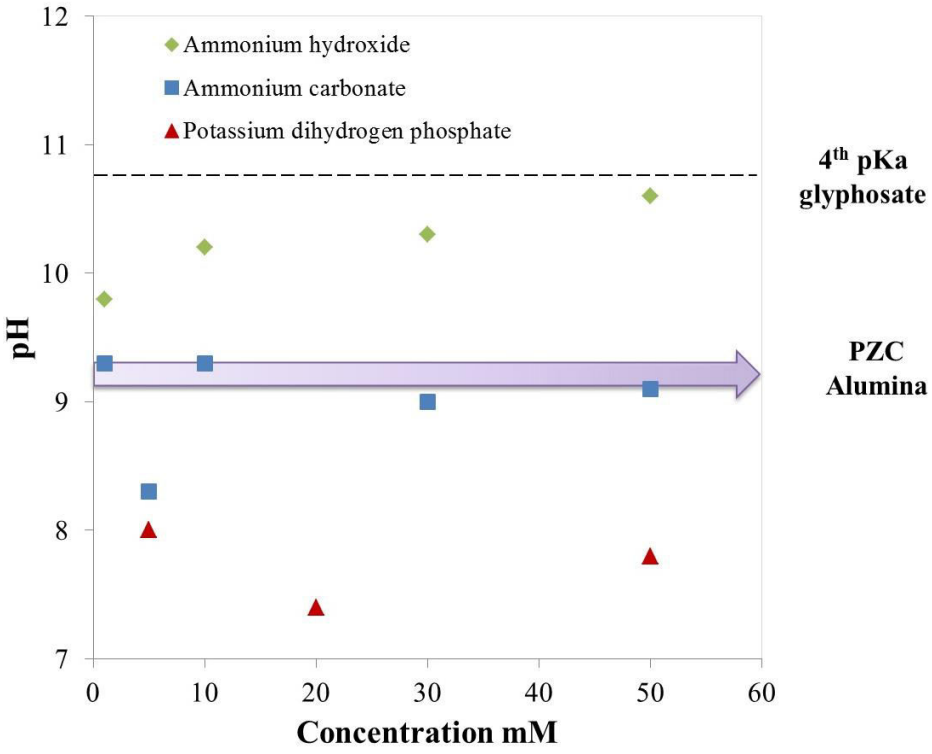

(b)

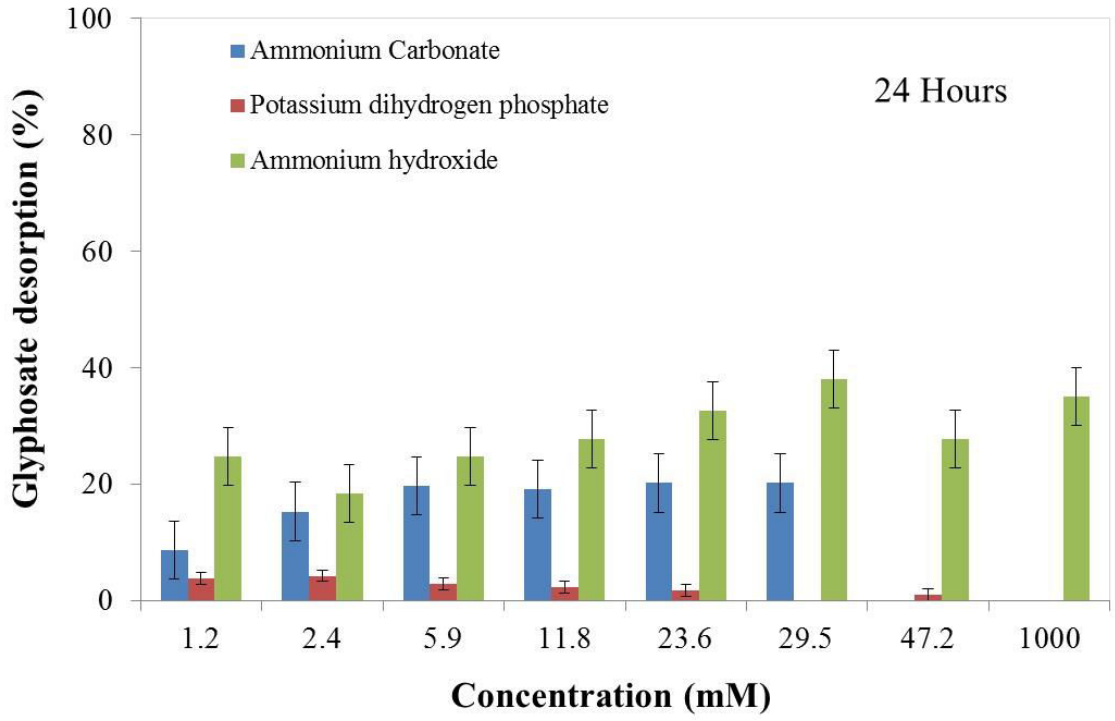

Figure 4-3: Panel (a) pH of the different elution solution used for desorption of glyphosate on activated alumina and Panel (b) Recovery percentage of adsorbed glyphosate on alumina using the three elution solutions at different concentrations.

Taken together, these results strongly suggest that pH was the dominating driver in the desorption of glyphosate where desorption increased with increasing pH. Further, the low recoveries upon addition of KH_2PO_4 imply that competitive desorption of glyphosate through adsorption of phosphate was negligible at low pH.

These observations are consistent with the picture of electrostatic interactions in outer sphere complexes as shown in Figure 4. Such a mechanism was already invoked in a previous study for phosphate adsorption[160]. On the other hand, numerous studies provide compelling insight for inner sphere complexation [155,161-164]. Therefore, this indicates the possibilities that (i) outer sphere complexes are formed initially and gradually become inner sphere complexation - in such a case it would be crucial that the desorption is performed quickly after adsorption; alternatively (ii) the adsorption of phosphonates occurs consistently through inner sphere complexes, which can be desorbed at high pH despite their inner-sphere character. In follow-up experiments, the possibility of desorbing glyphosate at high pH values

with phosphate solution can be explored in order to combine the effect of electrostatic repulsion at high pH and competitive desorption. However, this was not done in this study.

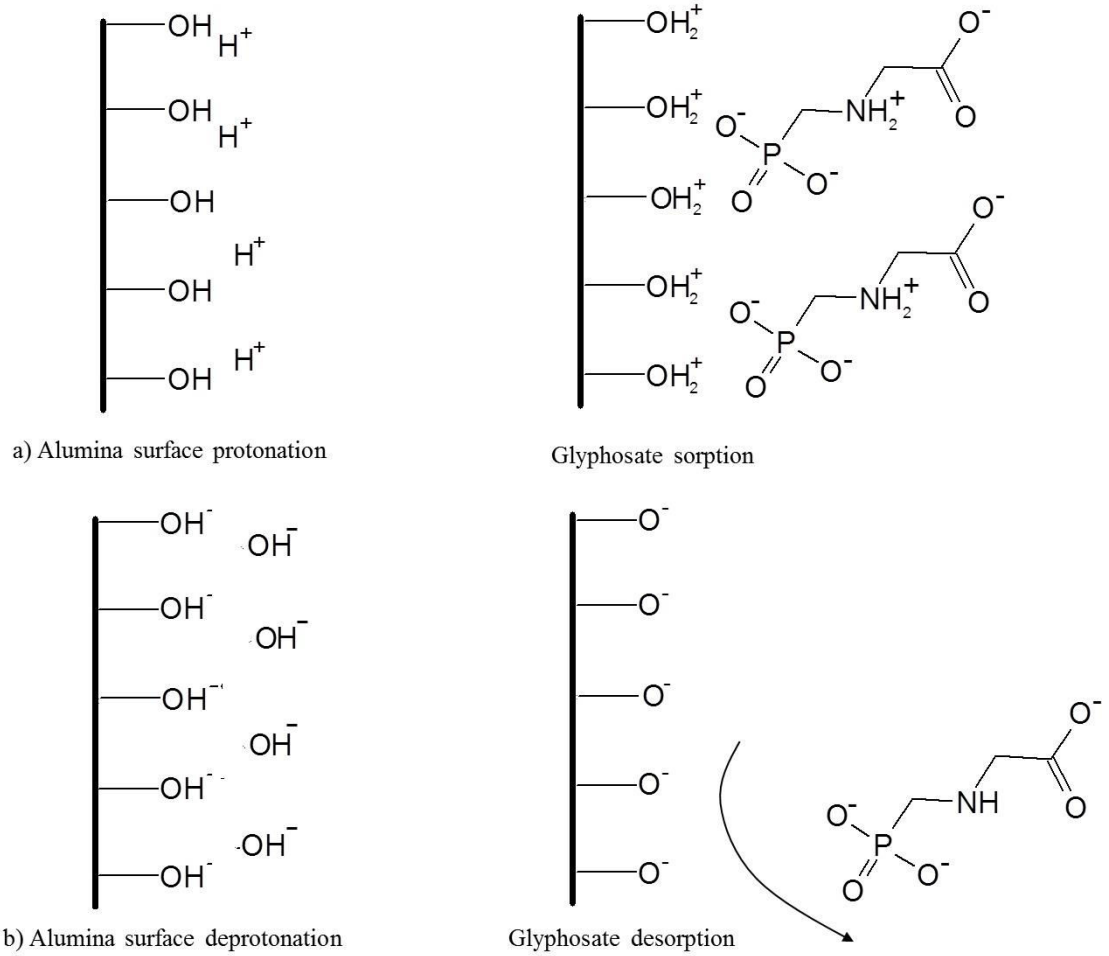

Figure 4-4: schematic representation of glyphosate adsorption on protonation alumina surface and desorption of glyphosate (deprotonation reaction at alumina surface).

4.3.4 Isotope effects of glyphosate during sorption on alumina

A common concern to all pre-concentration techniques is the possibility of systematic isotopic fractionation during sorption, desorption and phase transfer [98]. An evaluation of the associated isotope effects during glyphosate sorption on alumina was conducted. Figure 3 (a) shows the carbon and nitrogen isotope values against the fraction of adsorbed glyphosate. An increase of both $^{15}N/^{14}N$ and $^{13}C/^{12}C$ of glyphosate in the remaining solution was observed after 80 % adsorption. This means that light isotopes were adsorbed preferentially onto the alumina surface compared to heavy isotopes. For example, $\delta^{13}C$ values of glyphosate in solution increased to -27‰ ± 0.4‰ upon 80 % (0.8 fraction adsorbed) adsorption reflecting an enrichment of $^{13}C/^{12}C$ during adsorption. In a similar way, $\delta^{15}N$ values of glyphosate in

solution increased to 5‰ ± 0.7‰ upon 80 % (0.8 fraction adsorbed) adsorption reflecting an enrichment of $^{14}N/^{15}N$ during adsorption.

(a)

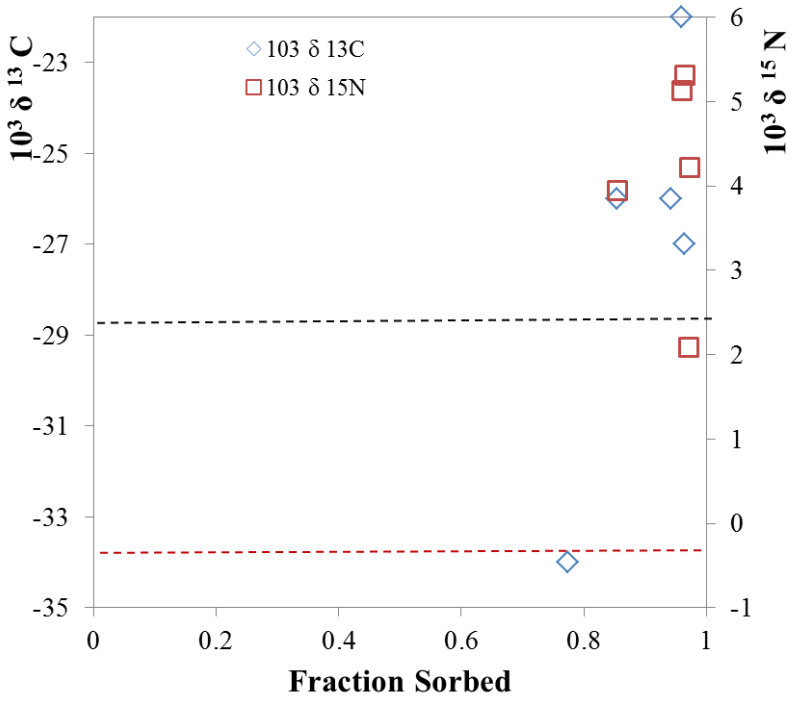

(b)

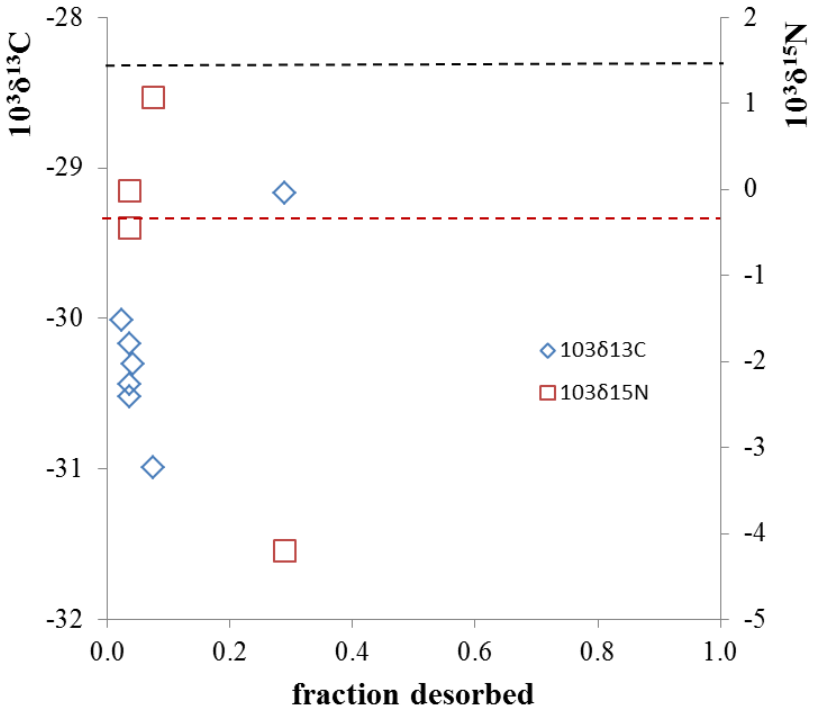

Figure 4-5: Panel (a) $\delta^{13}C$ and $\delta^{15}N$ values of glyphosate during adsorption on activated alumina. Panel (b) $\delta^{13}C$ and $\delta^{15}N$ values of glyphosate during desorption on activated alumina. The dashed lines represent the standard glyphosate nitrogen and carbon isotope values measure with EA-IRMS.

Despite this significant isotope fractionation in the remaining glyphosate in solution, nevertheless no significant isotope fractionation is expected in the rest of the mass balance: the adsorbed glyphosate on alumina. Taking account of the isotopic mass balance considerations according to equation 4.3, the $\delta^{13}C$ values would decrease by 0.4‰ while the $\delta^{15}N$ values by 0.8‰ in the adsorbed glyphosate, and this would fall within the uncertainty of the measurement.

Figure 3 (b) shows the associated carbon and nitrogen isotope values of glyphosate after desorption from the activated alumina surface with an eluent solution of 1M NH_4OH. With 30% the glyphosate recovery was similar to the previous batch experiment (see above). $\delta^{13}C$ values of glyphosate in solution decreased to -30.4 ‰ ± 0.4‰ at 30 % desorption (fraction desorbed: 0.3). However, these values were close to the input laboratory glyphosate standard carbon isotope values which were characterized by EA/IRMS (-28.9 ± 0.1 ‰). On the other hand, $\delta^{15}N$ values of glyphosate in solution increased to 1 ‰ ± 0.7‰ upon 30 % desorption (fraction desorbed: 0.3). Remarkably, these values were close to the input laboratory glyphosate nitrogen isotope values which were characterized by EA/IRMS (-0.3 ± 0.1 ‰). Further improvement of the enrichment strategy may result in even better recoveries. In this case, it is expected that the isotope values of glyphosate after enrichment will show even smaller differences in isotope values compared to the glyphosate laboratory working standard.

4.3.5 Glyphosate enrichment on modified column

Based on these promising results, a series of glyphosate extraction experiments were conducted with 1 ml modified packed alumina columns. The column setup was chosen to further optimize the recovery of glyphosate for large volume extraction of field samples (sampling water in the field followed by extraction and elution of the adsorbed glyphosate and AMPA in the laboratory). Figure 6 shows the schematic setup which was used for the enrichment of glyphosate and AMPA. About 0.5 g of alumina (due to the high adsorption capacity) was sufficient for the adsorption of glyphosate and AMPA. Table 1 shows the recoveries with the modified column approach. As compared to the batch experiment, better recoveries of glyphosate (70– 90 %), (60 – 70 %) from 1 L and 250 ml extraction volume respectively, were obtained. These results demonstrate the potential of the modified alumina column for enrichment of glyphosate out of aqueous samples. Further optimization may be

necessary for large volume extraction of glyphosate on alumina in the presence of other ions that might compete with glyphosate for adsorption.

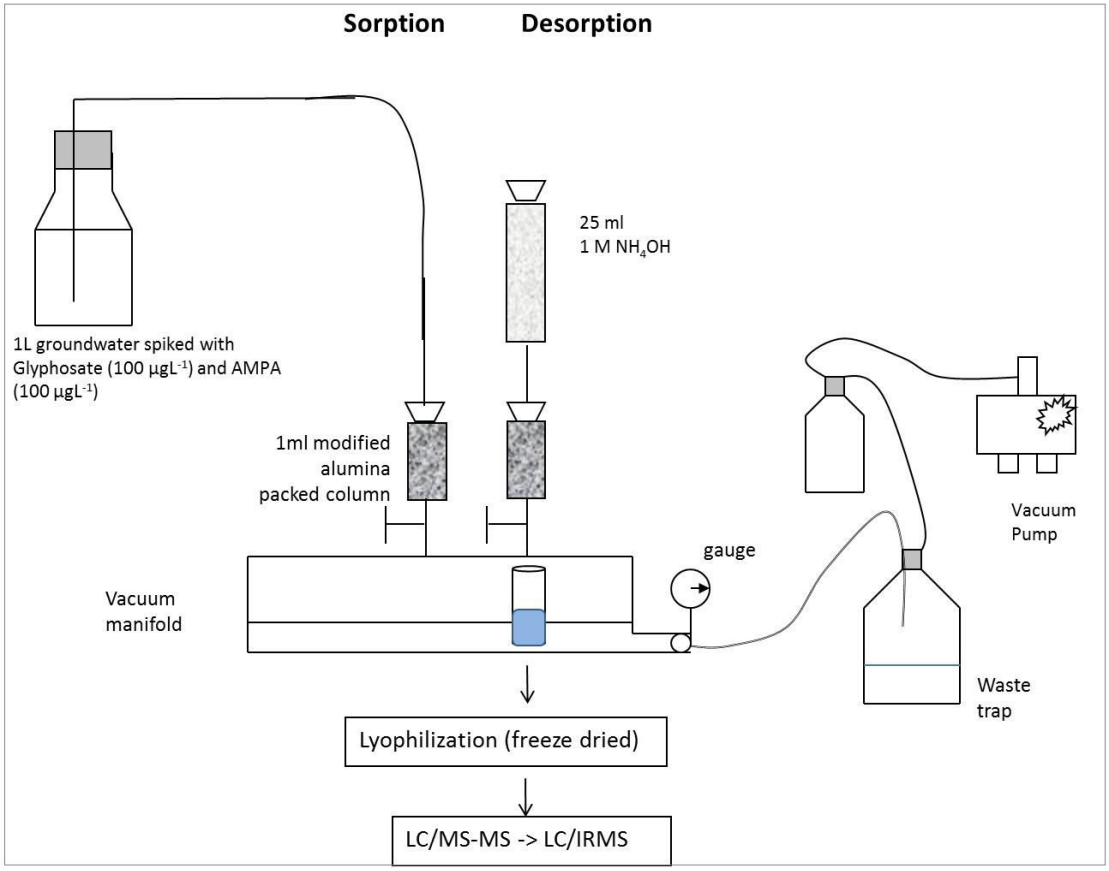

Figure 4-6: Schematic setup for the extraction of glyphosate and AMPA from water on packed modified 1ml activated alumina

Description	Recovery (%)	$10^3\,\delta^{13}C$	$10^3\delta^{13}C$ (EA-IRMS)
Batch adsorption			
Glyphosate (spiked)-Distilled water, surface water, groundwater			
Extraction from 500 mL (500 µg/L spiked concentration)	50-60 ± 8 (n=4)	-29.2	-28.99
Extraction from 250 mL (500 µg/L spiked concentration)	55-60 ± 8 (n=3)	-26.5	-28.99
Modified column			
Glyphosate (spiked)-Distilled water, surface water, groundwater			
Extraction from 1 L (500 µg/L spiked concentration)	70-90 ± 8 (n=4)	-27.2	-28.99
Extraction from 250 mL (100 µg/L spiked concentration)	60-70 ± 8 (n=5)	n.d	

n.d = not determined

Table 4-1: Overview of recovery and carbon isotope values of activated alumina extracted glyphosate and AMPA

4.4 Conclusion

In chapter 2 of this thesis, compound-specific isotope analysis was brought forward to distinguish sources and degradation of glyphosate and AMPA. However, the current lack of sensitive enrichment methods makes it challenging to apply CSIA to detect degradation of glyphosate and formation of AMPA in natural systems. To this end, we developed an enrichment approach that uses activated alumina packed in modified columns to extract glyphosate from water. The activated alumina showed a high adsorption capacity and sorption density for glyphosate of 85 mg/g and 2 µmol/m^2, respectively. Glyphosate was adsorbed at pH values lower than the PZC (point of zero charge) of the alumina surface. In contrast, desorption was most efficient at pH values above the PZC (point of zero charge). Very small shifts in stable carbon and nitrogen isotope values showed that only little fractionation was involved during the enrichment with activated alumina. Therefore, there is promising potential to employ the extraction method with activated alumina to enrich glyphosate and AMPA from natural water.

Conclusion and Outlook

5.0 Conclusion and Outlook

Compound specific isotope analysis (CSIA) is now a well-established routine approach to monitor the natural attenuation of traditional groundwater organic contaminants (e.g BTEX, TCE). Assessing the degradation of chemical micro-pollutant (e.g pesticides, pharmaceuticals and commercial care products) using CSIA has a promising potential. However, it still remains a challenge because majority of the micro-pollutants are highly polar, have high solubility in water and are present at low (sub-mg/l) concentration. To this end, to advance the application of CSIA to investigate pesticide degradation, this thesis focused on glyphosate (*N*-phosphomethylglycine) herbicide which has become the number one single herbicide (Roundup) applied today in corn, soybeans and sugar beet cultivation. The recent classification of glyphosate as probably carcinogenic to humans by the World Health Organization's cancer research unit and the frequent detection of AMPA and Glyphosate in surface, groundwater motivates the research to understand their environmental fate. In addition, the source of AMPA is still unresolved, because phosphonates chelating agents (used as detergents, corrosion inhibitors) also form AMPA as the key metabolite.

Before this work started, stable isotope analysis methods to measure the stable isotope ratios of glyphosate and AMPA had yet to be developed. This was because of the physical properties of glyphosate and AMPA (high water solubility and polar nature) that makes analytics a challenge. Even though Kujawinski *et al* 2013 had brought forward the first LC/IRMS method to measure carbon isotope ratios of glyphosate and AMPA, and though the method's promise for product authentication was demonstrated, the approach was still limited in its ability to distinguish different sources of glyphosate products. To this end, to exploit the full potential of multiple element ("two-dimensional") compound-specific isotope analysis for source discrimination, an additional element was developed as demonstrated in chapter 2 of this thesis.

We, therefore, developed the first compound-specific $^{15}N/^{14}N$ analysis of glyphosate and AMPA by a two-step derivatization in combination with GC/IRMS. We demonstrated that buffering solutions at pH 10 was critical for obtaining accurate nitrogen isotope ratios. A combination of $\delta^{15}N$ and $\delta^{13}C$ analysis (i) enabled an improved distinction of commercial glyphosate products and (ii) showed that glyphosate isotope values during degradation by MnO_2 clearly fell outside the commercial product range (for $\delta^{15}N$ of the commercial samples

was from +3.3 ‰ to -1.5 ‰ while $\delta^{13}C$ values ranged from -24.6 ‰ to -33.7 ‰) . These results highlighted the potential of combined carbon and nitrogen isotopes analysis to trace sources and degradation of glyphosate.

Though, the first results on dual element (C, N) isotope analysis of glyphosate look promising to distinguish sources and degradation pathways, additional research was still necessary before the next step can be taken to investigate glyphosate and AMPA degradation in natural systems. In particular, two questions were of central focus:

1. Can laboratory degradation studies demonstrate significant isotope fractionation associated with biodegradation of glyphosate, the main degradation pathway in nature?

2. Can suitable enrichment methods be validated for sensitive isotope analysis of glyphosate at low concentrations?

In order to close the first knowledge gap above, we conducted a reference laboratory experiment. To this end, a bacterial strain (*Ochrobactrum* sp. FrEM) was isolated from a vineyard in northern France which showed the ability to grow on glyphosate as the sole phosphorus source. The evidence of transformation metabolite - sarcosine confirmed an alternative degradation route - (C-P cleavage) sarcosine pathway. For the first time the associated ($^{13}C/^{12}C$ & $^{15}N/^{14}N$) isotope fractionation during biodegradation of glyphosate have been reported. Only a small but significant carbon isotope fractionation was observed ε_C = -6‰ ± 0.5‰ which suggested that the intrinsic isotope fractionation may have been masked due to mass transfer limitation. The carbon isotope shift was significant to leave an imprint of degradation. On the other hand, small nitrogen isotope fractionation of ε_N = -0. 6‰ ± 1.0‰ indicated a secondary nitrogen isotope effect. Additional experiments with bacteria strains that degrade glyphosate to AMPA should be conducted. An alternative carbon source for cultivation of the bacteria (we used high glutamate concentration 10 g/L) should be tested. This is because glutamate interfered with the analysis of glyphosate. This would reduce its interference during the analysis of glyphosate and transformation products. The best alternative would be when glyphosate is used both as C-source and P-source. It is worth noting here, that buffering the pH during derivatization of biodegradation samples is critical otherwise precise nitrogen isotope ratios would be difficult to achieve.

In the case of abiotic degradation of glyphosate with manganese dioxide (MnO_2), the first nitrogen enrichment factors were also reported. The nitrogen isotope fractionations were as high as ε_N = -17‰ ±0.5‰. Certainly, the strong nitrogen fractionation during abiotic

degradation of glyphosate would leave a robust imprint of degradation in natural systems. MnO_2 are ubiquitous in the environment and would contribute to the degradation of glyphosate in the environment. It was however, surprising that glyphosate abiotic degradation formed both AMPA and sarcosine. The exact mechanism involved during the abiotic degradation of glyphosate is still unclear. Further experiments should be conducted to understand the mechanism of glyphosate degradation on MnO_2 surface.

The amounts needed for precise nitrogen isotope analysis of glyphosate and AMPA (150 and 250 ng respectively) require a pre-enrichment method. Our first preliminary results on glyphosate and AMPA enrichment with activated alumina offer promising potential. The high adsorption capacity and surface density of the activated alumina means that a small amount of alumina would be needed to pack on the modified column (0.5 g of alumina on the 1 ml modified alumina column). The adsorption of glyphosate was pH dependent. Glyphosate was better adsorbed at pH value that was lower than the PZC (point of zero charge) of alumina surface because of its own charge and surface charge of alumina. On the other hand, desorption of glyphosate was favored when the alumina surface charge was negatively charged (desorption was most efficient at pH values above the PZC (point of zero charge)). The small shift in carbon and nitrogen isotope ratios means that the extraction process causes no fractionation. To improve glyphosate recoveries further optimizations (for example, the adsorption and desorption flow rate, competing ions present in water) are required and this would in theory lower the shift in the isotope ratios that was observed.

Overall, this research thesis has contributed towards the assessment of glyphosate and AMPA degradation and first step to determine the source of AMPA (a frequent groundwater contaminant which is also a key metabolite for phosphonates that are used in laundry detergents). These are:

i) Nitrogen isotope analysis method was developed, optimized and validated for glyphosate and AMPA analysis. The dual element plot (δ^{13} C verses δ^{15} N isotope) was capable of distinguishing the different commercial glyphosate products and abiotic degradation of glyphosate. Chapter 2 of this thesis was published in Analytical Bioanalytical Chemistry Journal

ii) The first carbon and nitrogen enrichment factors were determined during glyphosate biodegradation (with *Ochrobactrum sp* strain FrEM 15651) and glyphosate abiotic degradation with MnO_2. This will be important in future studies for characterization of

degradation processes and extent of degradation in natural systems when sensitive extraction methods become available. Chapter 3 will be submitted to Environmental Science & Technology Letters

iii) A promising first extraction approach to enrich glyphosate and AMPA from water using activated alumina packed columns for CSIA. Chapter 4 is in preparation as a Technical Note

The source of AMPA and its fate in groundwater will be made possible when sensitive enrichment becomes available in the future.

To this end, future studies are still needed to investigate (bio) degradation of glyphosate which leads to the formation of AMPA (main degradation pathway). The associated isotopic fractionation during AMPA formation during biodegradation could also be explored. Evaluation of the changes of the isotopic ratios would give insights into the fate of AMPA in groundwater as shown in Figure 5-2. AMPA is formed as a result of the cleavage of the C-N bond which would show no changes in the $^{13}C/^{12}C$ isotope ratio. This is because AMPA stems from the N atom at the non-reacting position of the substrate (glyphosate). On the other hand, the other metabolite glyoxylate is expected to be preferentially enriched and possess more ^{13}C isotope value during the reaction. However, two probable isotopic patterns are expected: (1) a lighter ^{13}C isotope signature for AMPA compared to initial substrate isotope ratio or (2) a heavy ^{13}C isotope signature for AMPA compared to initial substrate isotope ratio. In the event, AMPA is further degraded the ^{13}C isotope signature of AMPA is expected to be preferentially enriched. The enrichment of AMPA in heavy isotope directly provides a plausible line of evidence of biodegradation. On the other hand, nitrogen isotope analysis would show a significant nitrogen enrichment factor of the remaining substrate (glyphosate) when rate limiting step involves the C-N bond cleavage. AMPA is expected to be depleted in ^{15}N isotope value at the beginning of the reaction which becomes preferentially enriched in ^{15}N isotope values as the reaction progresses. However, it would be difficult to distinguish AMPA further degradation using nitrogen isotope analysis (Figure 5-2 (b))

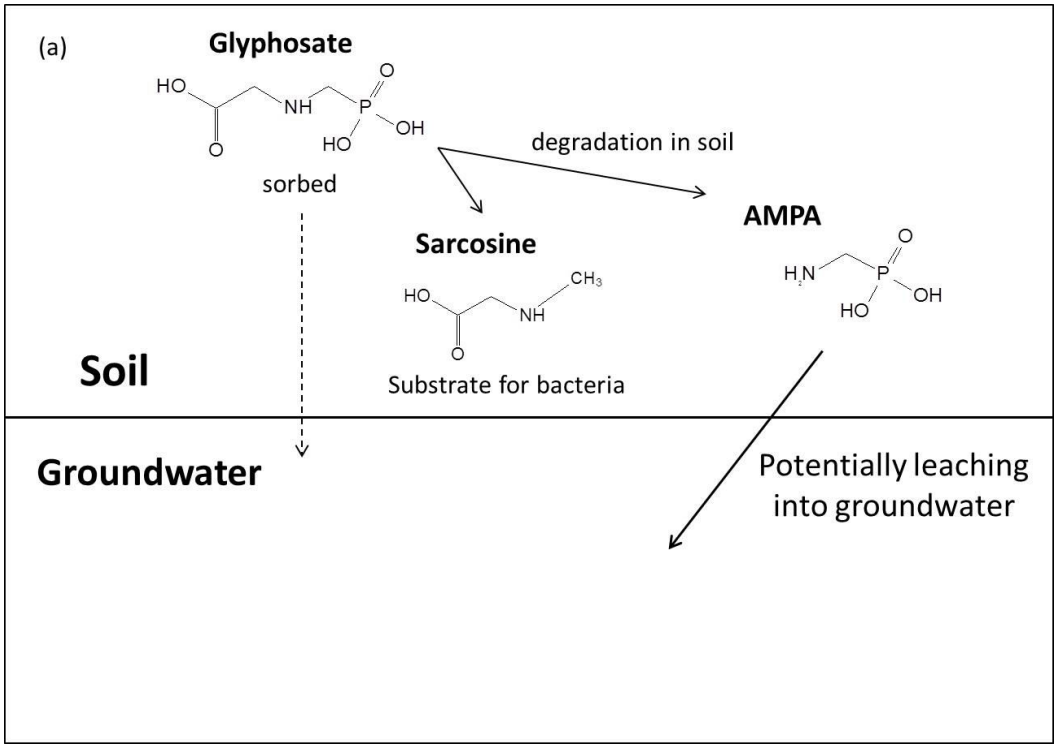
(a)
Glyphosate
degradation in soil
sorbed
Sarcosine
AMPA
Substrate for bacteria
Soil
Groundwater
Potentially leaching
into groundwater

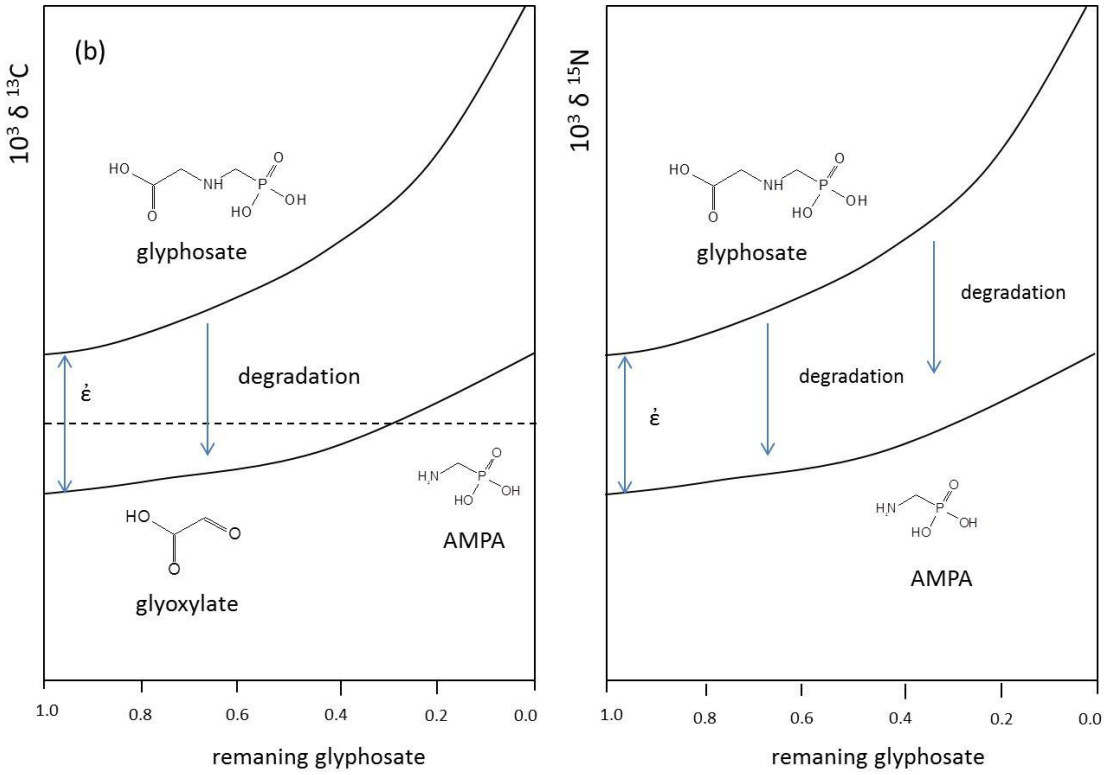
(b)
$10^3\ \delta\ ^{13}C$
glyphosate
degradation
ε̇
glyoxylate
AMPA
1.0
0.8
0.6
0.4
0.2
0.0
remaning glyphosate
$10^3\ \delta\ ^{15}N$
glyphosate
degradation
degradation
ε̇
AMPA
1.0
0.8
0.6
0.4
0.2
0.0
remaning glyphosate

Figure 5-2: (a) Environmental fate of glyphosate and AMPA. Glyphosate is strongly sorbed to soil matter. (b) Expected isotope fractionation during glyphosate degradation and resulting isotope signature of AMPA during its formation. (in this case AMPA degradation is not considered)

Our first preliminary results show the potential of activated alumina to enrich glyphosate from water. Further optimization test experiments on the influence of pH conditions are needed. The possibility of desorbing glyphosate at high pH values with phosphate solution can be explored in order to combine the effect of pH and competitive desorption. Lastly, the low glyphosate environmental concentration (< 0.1 µg/L) requires the extraction of large volume (several liters- 50L) of water. Therefore, the further optimization of the large volume extraction of glyphosate using packed modified alumina columns should be conducted.

References

1. Kujawinski DM, Wolbert JB, Zhang L, Jochmann MA, Widory D, Baran N, Schmidt TC (2013) Carbon isotope ratio measurements of glyphosate and AMPA by liquid chromatography coupled to isotope ratio mass spectrometry. Analytical and Bioanalytical Chemistry 405 (9):2869-2878. doi:10.1007/s00216-012-6669-0

2. Arias-Estévez M, López-Periago E, Martínez-Carballo E, Simal-Gándara J, Mejuto J-C, García-Río L (2008) The mobility and degradation of pesticides in soils and the pollution of groundwater resources. Agriculture, Ecosystems & Environment 123 (4):247-260

3. Beale DJ, Kaserzon SL, Porter NA, Roddick FA, Carpenter PD (2010) Detection of s-triazine pesticides in natural waters by modified large-volume direct injection HPLC. Talanta 82 (2):668-674. doi:http://dx.doi.org/10.1016/j.talanta.2010.05.030

4. GoK (2010- 2020) Agricultural sector development strategy

5. PCPB (2010) Annual report.

6. Hanke I, Wittmer I, Bischofberger S, Stamm C, Singer H (2010) Relevance of urban glyphosate use for surface water quality. Chemosphere 81 (3):422-429. doi:http://dx.doi.org/10.1016/j.chemosphere.2010.06.067

7. Albers CN, Feld L, Ellegaard-Jensen L, Aamand J (2015) Degradation of trace concentrations of the persistent groundwater pollutant 2, 6-dichlorobenzamide (BAM) in bioaugmented rapid sand filters. Water Research

8. Schwarzenbach RP, Gschwend PM, Imboden DM (2003) Environmental organic chemistry. second edition edn. John Wiley & Sons, Inc., New Jersey

9. Meckenstock RU, Morasch B, Griebler C, Richnow HH (2004) Stable isotope fractionation analysis as a tool to monitor biodegradation in contaminated acquifers. JContamHydrol 75 (3-4):215-255

10. Hornsby AG (1996) Pesticide properties in the environment, vol 1. Springer Science & Business Media,

11. Kerle E, Jenkins J, Vogue P (1994) pesticide persistence and mobility for groundwater and surface water protection.

12. Tiryaki O, Temur C (2010) The fate of pesticide in the environment. J Biol Environ Sci 4 (10):29-38

13. Borggaard OK, Gimsing AL (2008) Fate of glyphosate in soil and the possibility of leaching to ground and surface waters: a review. Pest Management Science 64 (4):441-456

14. Woodburn AT (2000) Glyphosate: production, pricing and use worldwide. Pest Management Science 56 (4):309-312

15. Kjær J, Ernstsen V, Jacobsen OH, Hansen N, de Jonge LW, Olsen P (2011) Transport modes and pathways of the strongly sorbing pesticides glyphosate and pendimethalin through structured drained soils. Chemosphere 84 (4):471-479. doi:http://dx.doi.org/10.1016/j.chemosphere.2011.03.029

16. Coupe RH, Kalkhoff SJ, Capel PD, Gregoire C (2012) Fate and transport of glyphosate and aminomethylphosphonic acid in surface waters of agricultural basins. Pest Management Science 68 (1):16-30. doi:10.1002/ps.2212

17. Shehata A, Schrödl W, Aldin AA, Hafez H, Krüger M (2013) The Effect of Glyphosate on Potential Pathogens and Beneficial Members of Poultry Microbiota In Vitro. Curr Microbiol 66 (4):350-358. doi:10.1007/s00284-012-0277-2

18. Baylis AD (2000) Why glyphosate is a global herbicide: strengths, weaknesses and prospects. Pest Management Science 56 (4):299-308. doi:10.1002/(SICI)1526-4998(200004)56:4<299::AID-PS144>3.0.CO;2-K

19. Dill GM, Sammons RD, Feng PCC, Kohn F, Kretzmer K, Mehrsheikh A, Bleeke M, Honegger JL, Farmer D, Wright D, Haupfear EA (2010) Glyphosate: Discovery, Development, Applications, and Properties. In: Glyphosate Resistance in Crops and Weeds. John Wiley & Sons, Inc., pp 1-33. doi:10.1002/9780470634394.ch1

20. Dill GM (2005) Glyphosate-resistant crops: history, status and future. Pest Management Science 61 (3):219-224. doi:10.1002/ps.1008

21. Duke SO (2014) Perspectives on Transgenic, Herbicide-Resistant Crops in the USA Almost 20 Years after Introduction. Pest management science

22. Carman JA, Vlieger HR, Ver Steeg LJ, Sneller VE, Robinson GW, Clinch-Jones CA, Haynes JI, Edwards JW (2013) A long-term toxicology study on pigs fed a combined genetically modified (GM) soy and GM maize diet. J Org Syst 8:38-54

23. Krüger M, Schrödl W, Neuhaus J, Shehata AA (2013) Field investigations of glyphosate in urine of Danish dairy cows.

24. Samsel A, Seneff S (2013) Glyphosate, pathways to modern diseases II: Celiac sprue and gluten intolerance. Interdisciplinary Toxicology 6 (4):159-184. doi:10.2478/intox-2013-0026

25. Samsel A, Seneff S (2013) Glyphosate's Suppression of Cytochrome P450 Enzymes and Amino Acid Biosynthesis by the Gut Microbiome: Pathways to Modern Diseases. Entropy 15 (4):1416-1463

26. WHO (2015) IARC Monographs: evaluation of five organophosphate insecticides and herbicides. WHO 112

27. Schuette J (1998) Environmetal fate of glyphosate. Environmental Monitoriing and pesticide management. doi:http://www.cdpr.ca.gov/docs/emon/pubs/fatememo/glyphos.pdf

28. Piriyapittaya M, Jayanta S, Mitra S, Leepipatpiboon N (2008) Micro-scale membrane extraction of glyphosate and aminomethylphosphonic acid in water followed by high-performance liquid chromatography and post-column derivatization with fluorescence detector. Journal of chromatography A 1189 (1-2):483-492. doi:10.1016/j.chroma.2008.01.074

29. Pesticide Database (2011). doi:http://sitem.herts.ac.uk/aeru/ppdb/en/Reports/2395.htm

30. E.J. Franz MKM, J.A. Sikoroski (1997) Glyphosate- a Unique Global herbicide. American Chemical society, Washington

31. Franz JE, Mao MK, Sikorski JA (1997) Glyphosate: a unique global herbicide. American Chemical Society,

32. Pipke R, Amrhein N (1988) Degradation of the Phosphonate Herbicide Glyphosate by Arthrobacter atrocyaneus ATCC 13752. Applied and Environmental Microbiology 54 (5):1293-1296

33. Dick RE, Quinn JP (1995) Glyphosate-degrading isolates from environmental samples: occurrence and pathways of degradation. Applied Microbiology and Biotechnology 43 (3):545-550. doi:10.1007/BF00218464

34. Sviridov AV, Shushkova TV, Zelenkova NF, Vinokurova NG, Morgunov IG, Ermakova IT, Leontievsky AA (2012) Distribution of glyphosate and methylphosphonate catabolism systems in soil bacteria Ochrobactrum anthropi and Achromobacter sp. Applied Microbiology and Biotechnology 93 (2):787-796

35. Shushkova TV, Ermakova IT, Sviridov AV, Leontievsky AA (2012) Biodegradation of glyphosate by soil bacteria: Optimization of cultivation and the method for active biomass storage. Microbiology 81 (1):44-50. doi:10.1134/S0026261712010134

36. Ermakova I, Kiseleva N, Shushkova T, Zharikov M, Zharikov G, Leontievsky A (2010) Bioremediation of glyphosate-contaminated soils. Applied Microbiology and Biotechnology 88 (2):585-594. doi:10.1007/s00253-010-2775-0

37. Barrett KA, McBride MB (2005) Oxidative Degradation of Glyphosate and Aminomethylphosphonate by Manganese Oxide. Environmental Science & Technology 39 (23):9223-9228. doi:10.1021/es051342d

38. Ndjeri M, Pensel A, Peulon S, Haldys V, Desmazières B, Chaussé A (2013) Degradation of glyphosate and AMPA (amino methylphosphonic acid) solutions by thin films of birnessite electrodeposited: A new design of material for remediation processes? Colloids and Surfaces A: Physicochemical and Engineering Aspects 435 (0):154-169. doi:http://dx.doi.org/10.1016/j.colsurfa.2013.01.022

39. Stone AT (1987) Reductive Dissolution of Manganese(III/Iv) Oxides by Substituted Phenols. Environmental Science & Technology 21 (10):979-988. doi:10.1021/es50001a011

40. Forrez I, Carballa M, Verbeken K, Vanhaecke L, SchluÌˆsener M, Ternes T, Boon N, Verstraete W (2010) Diclofenac Oxidation by Biogenic Manganese Oxides. Environmental Science & Technology 44 (9):3449-3454. doi:10.1021/es9027327

41. He Y, Xu J, Zhang Y, Guo C, Li L, Wang Y (2012) Oxidative transformation of carbamazepine by manganese oxides. Environmental Science and Pollution Research 19 (9):4206-4213. doi:10.1007/s11356-012-0949-2

42. Wang D, Shin JY, Cheney MA, Sposito G, Spiro TG (1999) Manganese dioxide as a catalyst for oxygen-independent atrazine dealkylation. Environmental science & technology 33 (18):3160-3165

43. Carlisle SM, Trevors JT (1988) Glyphosate in the environment. Water Air Soil Pollut 39 (3-4):409-420. doi:10.1007/BF00279485

44. Lund-HØie K, Friestad HO (1986) Photodegradation of the herbicide glyphosate in water. Bulletin of environmental contamination and toxicology 36 (1):723-729

45. Manassero A, Passalia C, Negro AC, Cassano AE, Zalazar CS (2010) Glyphosate degradation in water employing the H2O2/UVC process. Water Research 44 (13):3875-3882. doi:10.1016/j.watres.2010.05.004

46. Chen JQ, Hu ZJ, Wang NX (2012) Photocatalytic mineralization of glyphosate in a small-scale plug flow simulation reactor by UV/TiO2. Journal of Environmental Science and Health, Part B 47 (6):579-588

47. Aslam S, Iqbal A, Deschamps M, Recous S, Garnier P, Benoit P (2015) Effect of rainfall regimes and mulch decomposition on the dissipation and leaching of S-metolachlor and glyphosate: a soil column experiment. Pest Management Science 71 (2):278-291. doi:10.1002/ps.3803

48. Gimsing AL, Borggaard OK, Bang M (2004) Influence of soil composition on adsorption of glyphosate and phosphate by contrasting Danish surface soils. European Journal of Soil Science 55 (1):183-191. doi:10.1046/j.1365-2389.2003.00585.x

49. Battaglin WA, Meyer MT, Kuivila KM, Dietze JE (2014) Glyphosate and Its Degradation Product AMPA Occur Frequently and Widely in U.S. Soils, Surface Water, Groundwater, and Precipitation. JAWRA Journal of the American Water Resources Association 50 (2):275-290. doi:10.1111/jawr.12159

50. IFEN (2009) Les pesticides dans les Eaux. Données 2006. doi:http://www.ifen.fr/donnees-essentielles/eau/

51. Mamy L, Barriuso E, Gabrielle B (2005) Environmental fate of herbicides trifluralin, metazachlor, metamitron and sulcotrione compared with that of glyphosate, a substitute broad spectrum herbicide for different glyphosate-resistant crops. Pest management science 61 (9):905-916

52. Battaglin WA, Kolpin DW, Scribner EA, Kuivila KM, Sandstrom MW (2005) Glyphosate, other herbicides, and transformation products in midwestern streams, 20021. Wiley Online Library,

53. Nowack B (2003) Environmental chemistry of phosphonates. Water Research 37 (11):2533-2546

54. Nowack B, Stone AT (2000) Degradation of Nitrilotris(methylenephosphonic Acid) and Related (Amino)Phosphonate Chelating Agents in the Presence of Manganese and Molecular Oxygen. Environmental Science & Technology 34 (22):4759-4765. doi:10.1021/es0000908

55. Cretnik S, Thoreson KA, Bernstein A, Ebert K, Buchner D, Laskov C, Haderlein S, Shouakar-Stash O, Kliegman S, McNeill K, Elsner M (2013) Reductive Dechlorination of TCE by Chemical Model Systems in Comparison to Dehalogenating Bacteria: Insights from Dual Element Isotope Analysis (13C/12C, 37Cl/35Cl). Environmental Science & Technology 47 (13):6855-6863. doi:10.1021/es400107n

56. Schmidt TC, Zwank L, Elsner M, Berg M, Meckenstock RU, Haderlein SB (2004) Compound-specific stable isotope analysis of organic contaminants in natural environments: a critical review of the state of the art, prospects, and future challenges. Anal Bioanal Chem 378 (2):283-300

57. Kopinke FD, Georgi A, Voskamp M, Richnow HH (2005) Carbon isotope fractionation of organic contaminants due to retardation on humic substances: Implications for natural attenuation studies in aquifers. Environ Sci Technol 39 (16):6052-6062

58. Elsner M (2010) Stable isotope fractionation to investigate natural transformation mechanisms of organic contaminants: principles, prospects and limitations. J Environ Monit 12 (11):2005-2031

59. Elsner M, Zwank L, Hunkeler D, Schwarzenbach RP (2005) A new concept linking observable stable isotope fractionation to transformation pathways of organic pollutants. Environ Sci Technol 39 (18):6896-6916

60. Aelion CM, Hohener P, Hunkeler D, Aravena R (eds) (2009) Environmental Isotopes in Bioremediation and Biodegradation. CRC Press,

61. Meyer AH, Penning H, Elsner M (2009) C and N isotope fractionation suggests similar mechanisms of microbial atrazine transformation despite involvement of different Enzymes (AtzA and TrzN). Environ Sci Technol 43 (21):8079-8085. doi:10.1021/es9013618

62. Penning H, Sorensen SR, Meyer AH, Aamand J, Elsner M (2010) C, N, and H Isotope Fractionation of the Herbicide Isoproturon Reflects Different Microbial Transformation Pathways. Environ Sci Technol 44 (7):2372-2378. doi:10.1021/es9031858

63. Hartenbach AE, Hofstetter TB, Tentscher PR, Canonica S, Berg M, Schwarzenbach RP (2008) Carbon, hydrogen, and nitrogen isotope fractionation during light-Induced transformations of atrazine. Environ Sci Technol 42 (21):7751-7756

64. Reinnicke S (2011) Compound specific istotope analysis of the pesticides bentazone, MCPA, dichlobenil and its main metabolite BAM: Method validation and degradation studies. Ph.D. Thesis, Technical University of Munich, München

65. Jochmann MA, Blessing M, Haderlein SB, Schmidt TC (2006) A new approach to determine method detection limits for compound-specific isotope analysis of volatile organic compounds. Rapid Communications in Mass Spectrometry 20 (24):3639-3648

66. Blessing M, Jochmann M, Schmidt T (2008) Pitfalls in compound-specific isotope analysis of environmental samples. Analytical and Bioanalytical Chemistry 390 (2):591-603

67. Meckenstock RU, Morasch B, Warthmann R, Schink B, Annweiler E, Michaelis W, Richnow HH (1999) $^{13}C/^{12}C$ isotope fractionation of aromatic hydrocarbons during microbial degradation. Environmental Microbiology 1 (5):409-414

68. Audí-Miró C, Cretnik S, Otero N, Palau J, Shouakar-Stash O, Soler A, Elsner M (2013) Cl and C isotope analysis to assess the effectiveness of chlorinated ethene degradation by zero-valent iron: Evidence from dual element and product isotope values. Applied Geochemistry 32 (0):175-183. doi:http://dx.doi.org/10.1016/j.apgeochem.2012.08.025

69. Reinnicke S, Simonsen A, Sørensen SR, Aamand J, Elsner M (2012) C and N Isotope Fractionation during Biodegradation of the Pesticide Metabolite 2,6-Dichlorobenzamide (BAM): Potential for Environmental Assessments. Environ Sci Technol 46 (3):1447-1454. doi:10.1021/es203660g

70. Maier MP, De Corte S, Nitsche S, Spaett T, Boon N, Elsner M (2014) C & N Isotope Analysis of Diclofenac to Distinguish Oxidative and Reductive Transformation and to Track Commercial Products. Environmental Science & Technology 48 (4):2312-2320. doi:10.1021/es403214z

71. Qiu S, Gözdereliler E, Weyrauch P, Lopez ECM, Kohler H-PE, Sørensen SR, Meckenstock RU, Elsner M (2014) Small 13C/12C Fractionation Contrasts with Large Enantiomer Fractionation in Aerobic Biodegradation of Phenoxy Acids. Environmental Science & Technology 48 (10):5501-5511. doi:10.1021/es405103g

72. Spahr S, Huntscha S, Bolotin J, Maier MP, Elsner M, Hollender J, Hofstetter TB (2013) Compound-specific isotope analysis of benzotriazole and its derivatives. Analytical and Bioanalytical Chemistry 405 (9):2843-2856. doi:10.1007/s00216-012-6526-1

73. Helander M, Saloniemi I, Saikkonen K (2012) Glyphosate in northern ecosystems. Trends in Plant Science 17 (10):569-574. doi:http://dx.doi.org/10.1016/j.tplants.2012.05.008

74. Landry D, Dousset S, Fournier J-C, Andreux F (2005) Leaching of glyphosate and AMPA under two soil management practices in Burgundy vineyards (Vosne-Romanée, 21-France). Environmental Pollution 138 (2):191-200. doi:http://dx.doi.org/10.1016/j.envpol.2005.04.007

75. Struger J, Thompson D, Staznik B, Martin P, McDaniel T, Marvin C (2008) Occurrence of Glyphosate in Surface Waters of Southern Ontario. Bulletin of Environmental Contamination and Toxicology 80 (4):378-384. doi:10.1007/s00128-008-9373-1

76. Jaworska J, Van Genderen-Takken H, Hanstveit A, van de Plassche E, Feijtel T (2002) Environmental risk assessment of phosphonates, used in domestic laundry and cleaning agents in the Netherlands. Chemosphere 47 (6):655-665. doi:http://dx.doi.org/10.1016/S0045-6535(01)00328-9

77. Ghanem A, Bados P, Kerhoas L, Dubroca J, Einhorn J (2007) Glyphosate and AMPA analysis in sewage sludge by LC-ESI-MS/MS after FMOC derivatization on strong anion-exchange resin as solid support. Analytical Chemistry 79 (10):3794-3801. doi:10.1021/ac062195k

78. Ghanem A, Bados P, Estaun AR, de Alencastro LF, Taibi S, Einhorn J, Mougin C (2007) Concentrations and specific loads of glyphosate, diuron, atrazine, nonylphenol and metabolites thereof in French urban sewage sludge. Chemosphere 69 (9):1368-1373

79. Patsias J, Papadopoulou A, Papadopoulou-Mourkidou E (2001) Automated trace level determination of glyphosate and aminomethyl phosphonic acid in water by on-line anion-exchange solid-phase extraction followed by cation-exchange liquid chromatography and

post-column derivatization. Journal of Chromatography A 932 (1–2):83-90. doi:http://dx.doi.org/10.1016/S0021-9673(01)01253-5

80. Bijlsma L, Beltrán E, Boix C, Sancho J, Hernández F (2014) Improvements in analytical methodology for the determination of frequently consumed illicit drugs in urban wastewater. Analytical and Bioanalytical Chemistry 406 (17):4261-4272. doi:10.1007/s00216-014-7818-4

81. See HH, Hausert PC (2011) Electric Field-Driven Extraction of Lipophilic Anions across a Carrier-Mediated Polymer Inclusion Membrane. Analytical Chemistry 83 (19):7507-7513. doi:10.1021/ac201772g

82. Hanke I, Singer H, Hollender J (2008) Ultratrace-level determination of glyphosate, aminomethylphosphonic acid and glufosinate in natural waters by solid-phase extraction followed by liquid chromatography–tandem mass spectrometry: performance tuning of derivatization, enrichment and detection. Analytical and Bioanalytical Chemistry 391 (6):2265-2276. doi:10.1007/s00216-008-2134-5

83. Kataoka H, Ryu S, Sakiyama N, Makita M (1996) Simple and rapid determination of the herbicides glyphosate and glufosinate in river water, soil and carrot samples by gas chromatography with flame photometric detection. Journal of Chromatography A 726 (1–2):253-258. doi:http://dx.doi.org/10.1016/0021-9673(95)01071-8

84. Tseng S-H, Lo Y-W, Chang P-C, Chou S-S, Chang H-M (2004) Simultaneous Quantification of Glyphosate, Glufosinate, and Their Major Metabolites in Rice and Soybean Sprouts by Gas Chromatography with Pulsed Flame Photometric Detector. Journal of Agricultural and Food Chemistry 52 (13):4057-4063. doi:10.1021/jf049973z

85. Lee EA, Zimmerman LR, Bhullar BS, Thurman EM (2002) Linker-Assisted Immunoassay and Liquid Chromatography/Mass Spectrometry for the Analysis of Glyphosate. Analytical Chemistry 74 (19):4937-4943. doi:10.1021/ac020208y

86. Petersen J, Grant R, Larsen SE, Blicher-Mathiesen G (2012) Sampling of herbicides in streams during flood events. J Environ Monit 14 (12):3284-3294. doi:10.1039/C2EM30771E

87. Maillard E, Imfeld G (2014) Pesticide Mass Budget in a Stormwater Wetland. Environmental Science & Technology. doi:10.1021/es500586x

88. Braeckevelt M, Fischer A, KÃ¤stner M (2012) Field applicability of Compound-Specific Isotope Analysis (CSIA) for characterization and quantification of in situ contaminant degradation in aquifers. Applied Microbiology and Biotechnology 94 (6):1401-1421. doi:10.1007/s00253-012-4077-1

89. Schmidt TC, Jochmann MA (2012) Origin and Fate of Organic Compounds in Water: Characterization by Compound-Specific Stable Isotope Analysis. In: Cooks RG, Yeung ES

(eds) Annual Review of Analytical Chemistry, Vol 5, vol 5. Annual Review of Analytical Chemistry. pp 133-155. doi:10.1146/annurev-anchem-062011-143143

90. Weller P, Boner M, Foerstel H, Becker H, Peikert B, Dreher W (2011) Isotopic Fingerprinting for the Authenticity Control of Crop Protection Active Compounds using the Representative Insecticide Fipronil. Journal of Agricultural and Food Chemistry 59 (9):4365-4370. doi:10.1021/jf104766e

91. NicDaéid N, Meier-Augenstein W, Kemp HF, Sutcliffe OB (2012) Using Isotopic Fractionation to Link Precursor to Product in the Synthesis of (±)-Mephedrone: A New Tool for Combating "Legal High" Drugs. Analytical Chemistry 84 (20):8691-8696. doi:10.1021/ac3019069

92. Aeppli C, Bastviken D, Andersson P, Gustafsson Ö (2013) Chlorine Isotope Effects and Composition of Naturally Produced Organochlorines from Chloroperoxidases, Flavin-Dependent Halogenases, and in Forest Soil. Environmental Science & Technology 47 (13):6864-6871. doi:10.1021/es3037669

93. Meyer AH, Elsner M (2012) $^{13}C/^{12}C$ and $^{15}N/^{14}N$ Isotope Analysis to Characterize Natural Degradation of Atrazine: Evidence from Parent and Daughter Compound Values. Environ Sci Technol submitted

94. Hofstetter TB, Berg M (2011) Assessing transformation processes of organic contaminants by compound-specific stable isotope analysis. TrAC Trends in Analytical Chemistry 30 (4):618-627

95. Fischer A, Theuerkorn K, Stelzer N, Gehre M, Thullner M, Richnow HH (2007) Applicability of Stable Isotope Fractionation Analysis for the Characterization of Benzene Biodegradation in a BTEX-contaminated Aquifer. Environ Sci Technol 41 (10):3689-3696

96. Zwank L, Berg M, Elsner M, Schmidt TC, Schwarzenbach RP, Haderlein SB (2005) New evaluation scheme for two-dimensional isotope analysis to decipher biodegradation processes: application to groundwater contamination by MTBE. Environ Sci Technol 39 (4):1018-1029

97. Lutz SR, Van Breukelen BM (2014) Combined Source Apportionment and Degradation Quantification of Organic Pollutants with CSIA: 1. Model Derivation. Environmental Science & Technology 48 (11):6220-6228. doi:10.1021/es405400w

98. Elsner M, Jochmann MA, Hofstetter TB, Hunkeler D, Bernstein A, Schmidt TC, Schimmelmann A (2012) Current challenges in compound-specific stable isotope analysis of environmental organic contaminants. Anal Bioanal Chem 403 (9):2471-2491. doi:10.1007/s00216-011-5683-y

99. Barja BC, dos Santos Afonso M (1998) An ATR−FTIR Study of Glyphosate and Its Fe(III) Complex in Aqueous Solution. Environmental Science & Technology 32 (21):3331-3335. doi:10.1021/es9800380

100. Ramstedt M, Norgren C, Sheals J, Shchukarev A, Sjöberg S (2004) Chemical speciation of N-(phosphonomethyl)glycine in solution and at mineral interfaces. Surface and Interface Analysis 36 (8):1074-1077. doi:10.1002/sia.1844

101. Reinnicke S, Bernstein A, Elsner M (2010) Small and Reproducible Isotope Effects during Methylation with Trimethylsulfonium Hydroxide (TMSH): A Convenient Derivatization Method for Isotope Analysis of Negatively Charged Molecules. Analytical Chemistry 82 (5):2013-2019. doi:10.1021/ac902750s

102. McKenzie RM (1971) The synthesis of birnessite, cryptomelane, and some other oxides and hydroxides of manganese. Mineralogical Magazine 38:493-502

103. Marlier JF (2001) Multiple isotope effects on the acyl group transfer reactions of amides and esters. Accounts of Chemical Research 34 (4):283-290

104. Skarpeli-Liati M, Turgeon A, Garr AN, Arnold WA, Cramer CJ, Hofstetter TB (2011) pH-Dependent Equilibrium Isotope Fractionation Associated with the Compound Specific Nitrogen and Carbon Isotope Analysis of Substituted Anilines by SPME-GC/IRMS. Analytical Chemistry 83 (5):1641-1648. doi:10.1021/ac102667y

105. Rishavy MA, Cleland WW (1999) C-13, N-15, and O-18 equilibrium isotope effects and fractionation factors. Can J Chem-Rev Can Chim 77 (5-6):967-977

106. Diefenbach M, Brönstrup M, Aschi M, Schröder D, Schwarz H (1999) HCN Synthesis from Methane and Ammonia: Mechanisms of Pt+-Mediated C−N Coupling. Journal of the American Chemical Society 121 (45):10614-10625. doi:10.1021/ja992642w

107. Tian J, Shi H, Li X, Yin Y, Chen L (2012) Coupling mass balance analysis and multi-criteria ranking to assess the commercial-scale synthetic alternatives: a case study on glyphosate. Green Chemistry 14 (7):1990-2000. doi:10.1039/C2GC35349K

108. Mamy L, Gabrielle B, Barriuso E (2010) Comparative environmental impacts of glyphosate and conventional herbicides when used with glyphosate-tolerant and non-tolerant crops. Environmental Pollution 158 (10):3172-3178

109. Bøhn T, Cuhra M, Traavik T, Sanden M, Fagan J, Primicerio R (2014) Compositional differences in soybeans on the market: Glyphosate accumulates in Roundup Ready GM soybeans. Food Chemistry 153:207-215

110. Struger J, Van Stempvoort D, Brown S (2015) Sources of aminomethylphosphonic acid (AMPA) in urban and rural catchments in Ontario, Canada: Glyphosate or phosphonates in wastewater? Environmental Pollution 204:289-297

111. Horth H, Blackmore K (2009) Survey of glyphosate and AMPA in groundwaters and surface waters in Europe. Report by WRc plc, Swindon, Swindon, Wiltshire, United Kingdom No: UC8073 2

112. Fenner K, Canonica S, Wackett LP, Elsner M (2013) Evaluating Pesticide Degradation in the Environment: Blind Spots and Emerging Opportunities. Science 341 (6147):752-758. doi:10.1126/science.1236281

113. Duke SO (2010) Glyphosate degradation in glyphosate-resistant and-susceptible crops and weeds. Journal of agricultural and food chemistry 59 (11):5835-5841

114. Sviridov A, Shushkova T, Ermakova I, Ivanova E, Epiktetov D, Leontievsky A (2015) Microbial degradation of glyphosate herbicides (Review). Applied Biochemistry and Microbiology 51 (2):188-195

115. Mogusu EO, Wolbert JB, Kujawinski DM, Jochmann MA, Elsner M (2015) Dual element (15N/14N, 13C/12C) isotope analysis of glyphosate and AMPA by derivatization-gas chromatography isotope ratio mass spectrometry (GC/IRMS) combined with LC/IRMS. Analytical and Bioanalytical Chemistry:1-12

116. Hofstetter TB, Schwarzenbach RP, Bernasconi SM (2008) Assessing Transformation Processes of Organic Compounds Using Stable Isotope Fractionation. Environ Sci Technol 42 (21):7737-7743

117. Pangallo KC, Reddy CM, Poyton M, Bolotin J, Hofstetter TB (2012) d^{15}N Enrichment Suggests Possible Source for Halogenated 1'-Methyl-1,2'-bipyrroles (MBPs). Environmental Science & Technology 46 (4):2064-2070. doi:10.1021/es203143c

118. Gregoire C, Payraudeau S, Domange N (2010) Use and fate of 17 pesticides applied on a vineyard catchment. International Journal of Environmental and Analytical Chemistry 90 (3-6):406-420

119. Godin JP, Hau J, Fay LB, Hopfgartner G (2005) Isotope ratio monitoring of small molecules and macromolecules by liquid chromatography coupled to isotope ratio mass spectrometry. Rapid Communications in Mass Spectrometry 19 (18):2689-2698

120. Godin J-P, Fay L-B, Hopfgartner G (2007) Liquid chromatography combined with mass spectrometry for ^{13}C isotopic analysis in life science research. Mass Spectrometry Reviews 26 (6):751-774

121. Hadi F, Mousavi A, Noghabi KA, Tabar HG, Salmanian AH (2013) New bacterial strain of the genus Ochrobactrum with glyphosate-degrading activity. Journal of Environmental Science and Health, Part B 48 (3):208-213. doi:10.1080/03601234.2013.730319

122. Skarpeli-Liati M, Pati SG, Bolotin J, Eustis SN, Hofstetter TB (2012) Carbon, Hydrogen, and Nitrogen Isotope Fractionation Associated with Oxidative Transformation of Substituted Aromatic N-Alkyl Amines. Environ Sci Technol 46 (13):7189-7198. doi:10.1021/es300819v

123. Kertesz MA, Cook AM, Leisinger T (1994) Microbial metabolism of sulfurand phosphorus-containing xenobiotics. FEMS Microbiology Reviews 15 (2–3):195-215. doi:http://dx.doi.org/

124. Aparicio VC, De Gerónimo E, Marino D, Primost J, Carriquiriborde P, Costa JL (2013) Environmental fate of glyphosate and aminomethylphosphonic acid in surface waters and soil of agricultural basins. Chemosphere 93 (9):1866-1873. doi:http://dx.doi.org/10.1016/j.chemosphere.2013.06.041

125. Duke SO, Lydon J, Koskinen WC, Moorman TB, Chaney RL, Hammerschmidt R (2012) Glyphosate Effects on Plant Mineral Nutrition, Crop Rhizosphere Microbiota, and Plant Disease in Glyphosate-Resistant Crops. Journal of Agricultural and Food Chemistry 60 (42):10375-10397. doi:10.1021/jf302436u

126. Tang T, Boënne W, Desmet N, Seuntjens P, Bronders J, van Griensven A (2015) Quantification and characterization of glyphosate use and loss in a residential area. Science of The Total Environment 517:207-214

127. Nowack B, VanBriesen JM (2005) Chelating agents in the environment. Biogeochemistry of chelating agents:1-18

128. Rodrigues AM, Ferreira V, Cardoso VV, Ferreira E, Benoliel MJ (2007) Determination of several pesticides in water by solid-phase extraction, liquid chromatography and electrospray tandem mass spectrometry. Journal of Chromatography A 1150 (1):267-278

129. Dujaković N, Grujić S, Radišić M, Vasiljević T, Laušević M (2010) Determination of pesticides in surface and ground waters by liquid chromatography–electrospray–tandem mass spectrometry. Analytica chimica acta 678 (1):63-72

130. Hernández F, Ibáñez M, Pozo ÓJ, Sancho JV (2008) Investigating the presence of pesticide transformation products in water by using liquid chromatography-mass spectrometry with different mass analyzers. J Mass Spec 43 (2):173-184

131. Khrolenko MV, Wieczorek PP (2005) Determination of glyphosate and its metabolite aminomethylphosponic acid in fruit juices using supported-liquid membrane preconcentration

method with high-performance liquid chromatography and UV detection after derivatization with p-toluenesulphonyl chloride. Journal of Chromatography A 1093 (1-2):111-117. doi:10.1016/j.chroma.2005.07.062

132. Chimuka L, Nemutandani T, Cukrowska E, Tutu H (2008) Performance optimization of a membrane assisted passive sampler for monitoring of ionizable organic compounds in water. J Environ Monit 10 (1):129-135. doi:10.1039/b713072d

133. Chimuka L, Cukrowska E, Jonsson JA (2004) Why liquid membrane extraction is an attractive alternative in sample preparation. Pure Appl Chem 76 (4):707-722. doi:10.1351/pac200476040707

134. Rios C, Salvadó V, Hidalgo M (2002) Facilitated transport and preconcentration of the herbicide glyphosate and its metabolite AMPA through a solid supported liquid-membrane. Journal of membrane science 203 (1):201-208

135. Salvado (2006) Extraction and preconcentration of the Herbicide glyphosate andits metabolite AMPA using Anion-Exchange solid phases. Microchimica Acta 153:203-209

136. Fauvelle V, Nhu-Trang T-T, Feret T, Madarassou K, Randon J, Mazzella N (2015) Evaluation of Titanium Dioxide as a Binding Phase for the Passive Sampling of Glyphosate and Aminomethyl Phosphonic Acid in an Aquatic Environment. Analytical Chemistry 87 (12):6004-6009. doi:10.1021/acs.analchem.5b00194

137. De Jonge H, Rothenberg G (2005) New device and method for flux-proportional sampling of mobile solutes in soil and groundwater. Environmental Science & Technology 39 (1):274-282. doi:10.1021/es049698x

138. Candela L, Caballero J, Ronen D (2010) Glyphosate transport through weathered granite soils under irrigated and non-irrigated conditions—Barcelona, Spain. Science of the total environment 408 (12):2509-2516

139. Gimsing AL, Borggaard OK (2007) PHOSPHATE AND GLYPHOSATE ADSORPTION BY HEMATITE AND FERRIHYDRITE AND COMPARISON WITH OTHER VARIABLE-CHARGE MINERALS. Clays and Clay Minerals 55 (1):108-114. doi:10.1346/ccmn.2007.0550109

140. de Jonge H, de Jonge LW, Jacobsen OH, Yamaguchi T, Moldrup P (2001) Glyphosate sorption in soils of different pH and phosphorus content. Soil Science 166 (4):230-238

141. Sprankle P, Meggitt W, Penner D (1975) Adsorption, mobility, and microbial degradation of glyphosate in the soil. Weed Science:229-234

142. Pessagno RC, Torres Sánchez RM, dos Santos Afonso M (2008) Glyphosate behavior at soil and mineral–water interfaces. Environmental Pollution 153 (1):53-59. doi:http://dx.doi.org/10.1016/j.envpol.2007.12.025

143. Ayoob S, Gupta AK, Bhat VT (2008) A Conceptual Overview on Sustainable Technologies for the Defluoridation of Drinking Water. Critical Reviews in Environmental Science and Technology 38 (6):401-470. doi:10.1080/10643380701413310

144. Albers CN, Banta GT, Hansen PE, Jacobsen OS (2009) The influence of organic matter on sorption and fate of glyphosate in soil – Comparing different soils and humic substances. Environmental Pollution 157 (10):2865-2870. doi:http://dx.doi.org/10.1016/j.envpol.2009.04.004

145. Li W, Wang Y-J, Zhu M, Fan T-T, Zhou D-M, Phillips BL, Sparks DL (2013) Inhibition Mechanisms of Zn Precipitation on Aluminum Oxide by Glyphosate: A 31P NMR and Zn EXAFS Study. Environmental science & technology 47 (9):4211-4219

146. GIMSING AL, BORGGAARD OK (2002) Competitive adsorption and desorption of glyphosate and phosphate on clay silicates and oxides. Clay Minerals 37 (3):509-515. doi:10.1180/0009855023730049

147. Laitinen P, Rämö S, Nikunen U, Jauhiainen L, Siimes K, Turtola E (2009) Glyphosate and phosphorus leaching and residues in boreal sandy soil. Plant and soil 323 (1-2):267-283

148. Zhao B, Zhang J, Gong J, Zhang H, Zhang C (2009) Glyphosate mobility in soils by phosphate application: Laboratory column experiments. Geoderma 149 (3):290-297

149. Waiman CV, Avena MJ, Regazzoni AE, Zanini GP (2013) A real time in situ ATR-FTIR spectroscopic study of glyphosate desorption from goethite as induced by phosphate adsorption: Effect of surface coverage. Journal of Colloid and Interface Science 394 (0):485-489. doi:http://dx.doi.org/10.1016/j.jcis.2012.12.063

150. Camacho LM, Torres A, Saha D, Deng S (2010) Adsorption equilibrium and kinetics of fluoride on sol–gel-derived activated alumina adsorbents. Journal of colloid and interface science 349 (1):307-313

151. Waiman CV, Avena MJ, Garrido M, Fernandez Band B, Zanini GP (2012) A simple and rapid spectrophotometric method to quantify the herbicide glyphosate in aqueous media. Application to adsorption isotherms on soils and goethite. Geoderma 170:154-158. doi:10.1016/j.geoderma.2011.11.027

152. Choi J-W, Lee S-Y, Lee S-H, Kim J-E, Park K-Y, Kim D-J, Hong S-W (2012) Comparison of surface-modified adsorbents for phosphate removal in water. Water, Air, & Soil Pollution 223 (6):2881-2890

153. Stumm W, Morgan JJ (1995) Aquatic Chemistry. Wiley-Interscience,

154. Özacar M (2003) Adsorption of phosphate from aqueous solution onto alunite. Chemosphere 51 (4):321-327

155. Li W, Feng X, Yan Y, Sparks DL, Phillips BL (2013) Solid-state NMR spectroscopic study of phosphate sorption mechanisms on aluminum (Hydr) oxides. Environmental science & technology 47 (15):8308-8315

156. Ntalikwa JW (2007) Determination of surface charge density of α-alumina by acid-base titration. Bulletin of the Chemical Society of Ethiopia 21 (1)

157. Tombácz E (2007) pH-dependent surface charging of metal oxides. Chemical Engineering 53 (2):77-86

158. Tombácz E, Szekeres M, Kertész I, Turi L (1995) pH-dependent aggregation state of highly dispersed alumina, titania and silica particles in aqueous medium. In: Trends in Colloid and Interface Science IX. Springer, pp 160-168

159. Johnson BB, Quill E, Angove MJ (2012) An investigation of the mode of sorption of inositol hexaphosphate to goethite. Journal of colloid and interface science 367 (1):436-442

160. Javid M, Mustafa S, Gul R, Zaman M, Haider S (2004) Sorption/desorption properties of gamma-Al2O3 towards phosphate anions. Journal of the Chemical Society of Pakistan 26 (2):116-119

161. Zheng T-T, Sun Z-X, Yang X-F, Holmgren A (2012) Sorption of phosphate onto mesoporous γ-alumina studied with in-situ ATR-FTIR spectroscopy. Chem Cent J 6:26

162. Feuillie C, Sverjensky DA, Hazen RM (2014) Attachment of Ribonucleotides on α-Alumina as a Function of pH, Ionic Strength, and Surface Loading. Langmuir 31 (1):240-248

163. Sheals J, Sjöberg S, Persson P (2002) Adsorption of glyphosate on goethite: molecular characterization of surface complexes. Environmental science & technology 36 (14):3090-3095

164. Barja BC, dos Santos Afonso M (2004) Aminomethylphosphonic Acid and Glyphosate Adsorption onto Goethite: A Comparative Study. Environmental Science & Technology 39 (2):585-592. doi:10.1021/es035055q

Appendices

Appendix I: List of Tables and Figures

TABLE 1-1 COMMON NAME, MOLAR MASS HALF-LIFE, GUS VALUE (GROUNDWATER UBIQUITY SCORE), SORPTION COEFFICIENT (K_{OC}), WATER SOLUBILTY, VAPOUR PRESSURE INDEX, HENRY'S CONSTANT INDEX AND PKA FOR GLYPHOSATE AND METABOLITE AMPA 6

FIGURE 1-1: POSTULATED GLYPHOSATE DEGRADATION (BIOTIC & ABIOTIC) PATHWAYS LEADING TO ITS METABOLITES AMPA AND SARCOSINE. STRAINS ISOLATED FROM SOIL, WASTE WATER AND SEDIMENT WITH GLYPHOSATE DEGRADATION ACTIVITY. OXIDATIVE ABIOTIC DEGRADATION WITH MnO_2 AND ADVANCED OXIDATION BY H_2O_2/UV 7

FIGURE 2-1. DERIVATIZATION REACTION OF GLYPHOSATE AND AMPA WITH ISOPROPYL CHLOROFORMATE (ISO-PCF) AND TRIMETHYL SILYL DIAZOMETHANE (TMSD). 18

FIGURE 2-2: AN ILLUSTRATION OF THE SPECIATION OF GLYPHOSATE AND AMPA DEPENDENCE TO PH SHOWING THE DIFFERENT PKA VALUES FOR GLYPHOSATE AND AMPA (PKA = 0.8, 2.6, 6, 10.9; 0.9, 5.6,10.2) [58] RESPECTIVELY. THE BLUE AND RED ARROWS REPRESENT THE PH VALUES AT WHICH DERIVATIZATION WITH ISO-PCF WERE TESTED. 19

FIGURE 2-3: GC/IRMS CHROMATOGRAM OF DERIVATIZED IN-HOUSE LABORATORY STANDARDS (AMPLITUDES REPRESENT *M/Z* 28): AMPA N-ISOPROPYL METHYL ESTER (720 S) AND GLYPHOSATE N-ISOPROPYL METHYL ESTER (920 S) AT CONCENTRATIONS OF 20 MM AND 13 MM, RESPECTIVELY. THE THREE PEAKS AT THE BEGINNING AND THE END OF THE CHROMATOGRAM ARE FROM N_2 MONITORING GAS. 25

FIGURE 2-4 (A) AMPLITUDES OF GLYPHOSATE AND AMPA DERIVATIVES (M/Z 28) VS. PH. (B) $\Delta^{15}N$ ISOTOPE RATIOS OF THE DERIVATIVES DEPENDING ON PH. BLUE AND RED CROSSES "×" INDICATE THE EXCESS RATIO OF THE ISOPROPYL CHLOROFORMATE DERIVATIZATION AGENT TO GLYPHOSATE AND AMPA OF 7. (ISO-PCF: ANALYTE = 7). BLUE AND RED "+" INDICATE THE EXCESS RATIO OF ISO-PCF TO GLYPHOSATE AND AMPA OF 4. (ISO-PCF: ANALYTE = 4). THE SOLID LINE AND RED DASHED LINES REPRESENT THE $\Delta^{15}N$ RATIOS MEASURED BY EA-IRMS OF GLYPHOSATE AND AMPA STANDARD (-0.3 ‰, -3.7 ‰, RESPECTIVELY). 27

FIGURE 2-5: $\Delta^{15}N$ VALUES OF GLYPHOSATE WITH INCREASED VORTEX TIME (MINUTES). BLUE DIAMONDS AND RED RECTANGLES REPRESENT AN EXCESS OF ISO-PCF TO GLUTAMATE OF 3 AND 4, RESPECTIVELY. THE DASHED LINE REPRESENTS THE EA-IRMS $\Delta^{15}N$ VALUE OF THE GLYPHOSATE STANDARD (-0.3‰). ERROR BARS REPRESENT THE STANDARD DEVIATION OF DUPLICATE MEASUREMENTS 29

FIGURE 2-6 (A) GC CHROMATOGRAM FOR NITROGEN ISOTOPE ANALYSIS OF GLYPHOSATE DERIVATIVE (1820 SEC) AND GLUTAMATE DERIVATIVE (1696 SEC) SEPARATION ON RTX-5 AMINE COLUMN. THREE REFERENCE N_2 GAS PULSE AT THE BEGINNING AND END OF CHROMATOGRAM. BLUE LINE (M/Z 30), GREEN LINE (M/Z 29), BROWN LINE (M/Z 28). (B) GC CHROMATOGRAM AFTER BACKFLASH MODE AND STRAIGHT MODE -GLYPHOSATE 30

FIGURE 2-7 (A) $\Delta^{15}N$ VALUES OF GLYPHOSATE (BLUE CROSSES) IN DEPENDENCE ON ISO-PCF: GLYPHOSATE RATIOS. EA-IRMS DETERMINED $\Delta^{15}N$ VALUE OF GLYPHOSATE STANDARD (-0.3 ‰) IS REPRESENTED BY THE BLACK DASHED LINE. (B) $\Delta^{15}N$ VALUES OF AMPA (RED CROSSES) IN DEPENDENCE ON ISO-PCF: AMPA RATIOS. EA-IRMS DETERMINED $\Delta^{15}N$ VALUE OF GLYPHOSATE STANDARD (-3.7 ‰) IS REPRESENTED BY THE RED DASHED LINE. (C) $\Delta^{15}N$ VALUES OF GLYPHOSATE (BLUE RECTANGLE) AND AMPA (RED DIAMONDS) VS. PEAK AMPLITUDES (M/Z 28) FROM MEASUREMENTS OF IN-HOUSE LABORATORY STANDARDS IN CONCENTRATIONS BETWEEN 0.6 MM TO 13 MM AND 0.9 MM TO 20 MM, RESPECTIVELY. THE BLUE RECTANGLE AND RED TRIANGLE REPRESENT THE N-ISOPROPYL METHYL ESTER DERIVATIVE OF GLYPHOSATE AND AMPA, RESPECTIVELY. THE DASHED LINES REPRESENT THE RESPECTIVE STANDARD DEVIATIONS

(SD) (BOTH ±0.8 ‰). THE BOLD LINES INDICATE THE 95% CONFIDENCE INTERVAL. THE VERTICAL DASHED LINES (BLUE AND BLACK) INDICATE THE LIMIT OF PRECISE $\Delta^{15}N$ ISOTOPE ANALYSIS OF GLYPHOSATE AND AMPA (100 MV, 133MV) RESPECTIVELY. 32

FIGURE 2-8 (A) DUAL ISOTOPE PLOT ($\Delta^{13}C$ VS. $\Delta^{15}N$) OF GLYPHOSATE FOR DIFFERENT COMMERCIAL HERBICIDE SAMPLES. THE LETTERS A-M REPRESENT COMMERCIAL HERBICIDES PRODUCTS WITH GLYPHOSATE AS ACTIVE INGREDIENT (SEE APPENDIX A2 TABLE SII SHOWS THE TRADE NAMES). (B) DUAL ISOTOPE PLOT ($\Delta^{13}C$ VS. $\Delta^{15}N$) OF THE SAME PRODUCTS FROM DIFFERENT MANUFACTURES TOGETHER WITH VALUES MEASURED DURING OXIDATIVE ABIOTIC DEGRADATION OF GLYPHOSATE WITH MnO_2 (RED AND BLUE CROSSES REPRESENTING REPLICATE EXPERIMENTS). ERROR BARS GIVEN CORRESPOND TO STANDARD DEVIATIONS OF THE METHODS (± 0.8‰ FOR $\Delta^{15}N$ ANALYSIS, ± 0.3‰ FOR $\Delta^{13}C$ ANALYSIS). 35

FIGURE 3-1: PANEL (I) DEGRADATION OF GLYPHOSATE BY *OCHROBACTRUM* SP. FREM WHEN GROWN IN MS1 MEDIUM CONTAINING 120 µM GLYPHOSATE AS THE ONLY PHOSPHOROUS SOURCE (BLUE TRIANGLES AND RED RECTANGLE REPRESENT REPLICATES AND GREEN DIAMONDS THE CONTROL) . PANEL (II) MEASURED BACTERIAL GROWTH (OD 590 NM) WITH TIME (BLUE TRIANGLES AND RED RECTANGLE REPRESENT REPLICATES). PANEL (III) $\Delta^{13}C$ VALUES DURING GLYPHOSATE DEGRADATION BY *OCHROBACTRUM SP* FREM (BLUE TRIANGLES AND RED RECTANGLE REPRESENT REPLICATES) 45

FIGURE 3-2: PANEL (A) $\Delta^{13}C$ VALUES DURING GLYPHOSATE DEGRADATION BY *OCHROBACTRUM SP* FREM (RED RECTANGLES).PANEL (B) $\Delta^{15}N$ VALUES DURING GLYPHOSATE DEGRADATION BY *OCHROBACTRUM SP* FREM (BLUE DIAMONDS). ERROR BAR OF NITROGEN ISOTOPE DATA REPRESENT STANDARD DEVIATION OF GC/IRMS MEASUREMENTS. PANEL (C) $\Delta^{13}C$ VALUES OF GLYPHOSATE DURING ABIOTIC DEGRADATION WITH Mn_2O (RED CIRCLES), PANEL (D) $\Delta^{15}N$ VALUES OF GLYPHOSATE DURING ABIOTIC DEGRADATION WITH Mn_2O (RED TRIANGLES). 47

FIGURE 3-3: DUAL ELEMENT ISOTOPE PLOT FOR NITROGEN VERSUS CARBON ISOTOPE RATIOS ($\Delta^{13}C$ VS. $\Delta^{15}N$) DURING GLYPHOSATE BIODEGRADATION WITH *OCHROBACTRUM SP*. FREM (BLUE TRIANGLES) AND THE OXIDATIVE ABIOTIC DEGRADATION OF GLYPHOSATE WITH MnO_2 (RED DIAMONDS). THE DASHED LINES INDICATE 95% CONFIDENCE INTERVALS (CL) 49

FIGURE 4-1: ADSORPTION ISOTHERM OF GLYPHOSATE ON ACTIVATED ALUMINA. SOLID LINE CORRESPONDS TO THE FIT WITH THE LANGMUIR EQUATION. 61

FIGURE 4-2: PANEL (A) PH SPECIATION OF GLYPHOSATE DURING ADSORPTION ON ACTIVATED ALUMINA SURFACES AT DIFFERENT GLYPHOSATE CONCENTRATIONS. BROWN SQUARES REPRESENT THE GLYPHOSATE SPECIATION AT DIFFERENT CONCENTRATIONS AND GREEN SQUARES REPRESENT THE GLYPHOSATE SPECIATION ON ALUMINA SURFACE AFTER 24 HOURS EQUILIBRATION. PANEL (B) PH SPECIATION OF GLYPHOSATE DURING DESORPTION ON ACTIVATED ALUMINA SURFACES WITH DIFFERENT ELUENTS SOLUTION. BROWN RECTANGLE REPRESENTS POTASSIUM DIHYDROGEN PHOSPHATE, BLUE RECTANGLE REPRESENTS AMMONIUM CARBONATE AND GREEN RECTANGLE REPRESENTS AMMONIUM HYDROXIDE ELUTION SOLUTION. 63

FIGURE 4-3: PANEL (A) PH OF THE DIFFERENT ELUTION SOLUTION USED FOR DESORPTION OF GLYPHOSATE ON ACTIVATED ALUMINA AND PANEL (B) RECOVERY PERCENTAGE OF ADSORBED GLYPHOSATE ON ALUMINA USING THE THREE ELUTION SOLUTIONS AT DIFFERENT CONCENTRATIONS. 65

FIGURE 4-4: SCHEMATIC REPRESENTATION OF GLYPHOSATE ADSORPTION ON PROTONATION ALUMINA SURFACE AND DESORPTION OF GLYPHOSATE (DEPROTONATION REACTION AT ALUMINA SURFACE). 66

FIGURE 4-5: PANEL (A) $\Delta^{13}C$ AND $\Delta^{15}N$ VALUES OF GLYPHOSATE DURING ADSORPTION ON ACTIVATED ALUMINA. PANEL (B) $\Delta^{13}C$ AND $\Delta^{15}N$ VALUES OF GLYPHOSATE DURING DESORPTION ON

ACTIVATED ALUMINA. THE DASHED LINES REPRESENT THE STANDARD GLYPHOSATE NITROGEN AND CARBON ISOTOPE VALUES MEASURE WITH EA-IRMS. 68
FIGURE 4-6: SCHEMATIC SETUP FOR THE EXTRACTION OF GLYPHOSATE AND AMPA FROM WATER ON PACKED MODIFIED 1ML ACTIVATED ALUMINA 69
TABLE 4-1: OVERVIEW OF RECOVERY AND CARBON ISOTOPE VALUES OF ACTIVATED ALUMINA EXTRACTED GLYPHOSATE AND AMPA..... 70
FIGURE 5-2: (A) ENVIRONMENTAL FATE OF GLYPHOSATE AND AMPA. GLYPHOSATE IS STRONGLY SORBED TO SOIL MATTER. (B) EXPECTED ISOTOPE FRACTIONATION DURING GLYPHOSATE DEGRADATION AND RESULTING ISOTOPE SIGNATURE OF AMPA DURING ITS FORMATION. (IN THIS CASE AMPA DEGRADATION IS NOT CONSIDERED) 75
AII: TABLE SI. THE $\Delta^{15}N$ & $\Delta^{13}C$ VALUES OF GLYPHOSATE FROM COMMERCIAL HERBICIDES SAMPLES. THE STANDARD DEVIATIONS GIVEN IN THE TABLE ARE THE ESTIMATE OF REPLICATE SAMPLE MEASUREMENTS, WHILE THOSE IN FIGURES 2-7 AND 2-8 IN CHAPTER 2 CORRESPOND TO THE STANDARD DEVIATION OF THE METHODS DETERMINED INDEPENDENTLY (IN FIGURE 2-6 IN CHAPTER 2) IX
AII: TABLE SII. THE TRADE NAMES OF MEASURED COMMERCIAL GLYPHOSATE PRODUCTS. X
AII: FIGURE S1. THE VARIATION IN $\Delta^{15}N$ ISOTOPE VALUES OF COMMERCIAL HERBICIDE (BLUE DIAMONDS) WITH INCREASING ISO-PCF: COMMERCIAL HERBICIDE RATIOS. THE DASHED PINK LINE REPRESENTS THE EA/IRMS $\Delta^{15}N$ VALUE OF GLYPHOSATE STANDARD (-0.28 ‰ ± 0.06 ‰). . X
AII: FIGURE S2. THE REPRODUCIBILITY OF $\Delta^{13}C$ VALUES OF GLYPHOSATE STANDARDS (SQUARES) AND AMPA STANDARDS (DIAMONDS) MEASURED WITH LC/IRMS. TRIANGLES ARE MEASUREMENTS OF COMMERCIAL GLYPHOSATE PRODUCTS ANALYZED BETWEEN THE STANDARD MEASUREMENTS. THE SOLID LINES REPRESENT THE STANDARD DEVIATION (SD) OF GLYPHOSATE AND AMPA (±0.34 ‰,) RESPECTIVELY. THE DASHED BLACK LINES REPRESENT THE EA/IRMS $\Delta^{15}N$ VALUE OF GLYPHOSATE AND AMPA STANDARD (-28.99 ‰ ± 0.06 ‰, -39.84 ‰ ± 0.10 ‰) RESPECTIVELY. XI
AII: FIGURE S3 CHROMATOGRAM OF GLYPHOSATE AND AMPA STANDARDS (300 mgL^{-1}, 345 mgL^{-1}) MEASURED WITH LC/IRMS. THE THREE FIRST PEAKS REPRESENT CO_2 MONITORING GAS. XII
AIII FIGURE S2: SPECIATION OF GLYPHOSATE, GLUTAMATE AND AMPA DEPENDING ON PH XIV
TABLE SI. TRANSITIONS PARAMETERS FOR GLYPHOSATE QUANTIFICATION AND CONFORMATION .. XVI
FIGURE S1: SPECIATION AND PKA VALUES OF GLYPHOSATE, GLUTAMATE, AMPA AND SARCOSINE. THE VERTICAL ARROW SHOWS THE OPTIMUM PH (3.1) FOR THE SEPARATION OF THE COMPOUNDS (GLYPHOSATE, GLUTAMATE, AMPA AND SARCOSINE) USING A PHOSPHATE BUFFER (2.5 MM NaH_2PO_4 BUFFER ADJUSTED AT PH 3.1)..... XVIII
FIGURE S3: $\Delta^{13}C$ ISOTOPE VALUES OF GLYPHOSATE (BLUE RECTANGLE), AMPA (RED TRIANGLE), SARCOSINE (GREEN DIAMOND) AND GLUTAMATE (BLACK CIRCLES) VERSUS PEAK AMPLITUDES (M/Z = 44) FROM MEASUREMENTS OF IN-HOUSE LABORATORY STANDARDS BY LC/IRMS ON A PRIMESEP 100 COLUMN IN CONCENTRATIONS BETWEEN 0.35 MM TO 6 MM , 0.5 MM TO 9 MM, 0.6MM TO 6 MM AND 0.35 MM TO 6 MM RESPECTIVELY. THE DASHED LINES REPRESENT THE RESPECTIVE STANDARD DEVIATIONS (SD) (± 0.3‰, ± 0.4‰, ± 0.5‰ AND ± 0.7‰ RESPECTIVELY). THE BOLD LINES INDICATE MEASURED EA-IRMS VALUES. XXI
TABLE S2: EVALUATION OF THE AKIE CARBON AND NITROGEN FOR ABIOTIC AND (BIO) DEGRADATION OF GLYPHOSATE..... XXII
FIGURE S5: PHYLOGENETIC POSITION OF THE STRAIN FREM WITHIN *OCHROBACTRUM* SPECIES. NEIGHBOUR-JOINING TREE BASED ON PARTIAL 16S RRNA SEQUENCE. THE BAR INDICATES 0.005 SUBSTITUTIONS PER NUCLEOTIDE. XXIII
FIGURE S7: PANEL A DEGRADATION OF GLYPHOSATE BY *OCHROBACTRUM ANTROPIA* GPK 3 WHEN GROWN IN MS1 MEDIUM CONTAINING 3 MM GLYPHOSATE AS THE ONLY PHOSPHOROUS SOURCE.

PANEL B MEASURED BACTERIAL GROWTH (OD 560 NM) OVER TIME. PANEL C DEGRADATION OF GLYPHOSATE BY *ACHROMOBACTER SP* WHEN GROWN IN MS1 MEDIUM CONTAINING 1.5 MM GLYPHOSATE AS THE ONLY PHOSPHOROUS SOURCE. PANEL D MEASURED BACTERIAL GROWTH (OD 560 NM) OVER TIME. XXV

AIII FIGURE S8: SCHEMATIC REPRESENTATION OF PESTICIDES RELEASED INTO THE ENVIRONMENT SUBJECTED TO VARIOUS PHYSICAL, CHEMICAL AND BIOLOGICAL PROCESSES. PROCESSES THAT DETERMINE THE FATE OF PESTICIDES IN THE ENVIRONMENT. XXVI

AIV: TABLE S1. TRANSITIONS PARAMETERS MEASURED FOR GLYPHOSATE QUANTIFICATION AND CONFORMATION XXVII

AIV: FIGURE S3. CHROMATOGRAM OF DIRECT GLYPHOSATE STANDARD (AT 100 μgL^{-1}) MEASURED BY LC/MS-MS XXVII

AIV: TABLE SII. TRANSITIONS PARAMETERS MEASURED FOR GLYPHOSATE QUANTIFICATION AND CONFORMATION XXVII

AIV: FIGURE S5. LANGMUIR ADSORPTION ISOTHERM MODEL FOR ACTIVATED ALUMINA AND GOETHITE XXVII

AIV: FIGURE S6. PICTURE OF THE GLYPHOSATE EXTRACTION SETUP WITH PACKED ACTIVATED ALUMINA XXVII

AIV: FIGURE S1: PANEL (A) CARBON ISOTOPE EFFECT AT EQUILIBRIUM CONCENTRATION DURING THE SORPTION GLYPHOSATE ON ACTIVATED ALUMINA PANEL (B) CARBON ISOTOPE EFFECT DURING THE SORPTION GLYPHOSATE ON GOETHITE AND PANEL (C) CARBON ISOTOPE EFFECT DURING THE SORPTION GLYPHOSATE ON QUARTZ. THE DASHED LINES REPRESENT THE STANDARD GLYPHOSATE CARBON ISOTOPE VALUES MEASURE WITH EA-IRMS. XXVIII

AIV: FIGURE S2: PANEL (A) ELUTION OF ADSORBED GLYPHOSATE ON ALUMINA WITH POTASSIUM DIHYDROGEN PHOSPHATE. PANEL (B) ELUTION OF ADSORBED GLYPHOSATE ON ALUMINA WITH AMMONIUM CARBONATE AND PANEL (C) ELUTION OF ADSORBED GLYPHOSATE ON ALUMINA WITH AMMONIUM HYDROXIDE. XXIX

AIV: TABLE S1. TRANSITIONS PARAMETERS MEASURED FOR GLYPHOSATE QUANTIFICATION AND CONFORMATION XXX

AIV: TABLE SII. TRANSITIONS PARAMETERS MEASURED FOR GLYPHOSATE QUANTIFICATION AND CONFORMATION XXXI

AIV: FIGURE S5. PANEL (A) LANGMUIR ADSORPTION ISOTHERM MODEL FOR ACTIVATED ALUMINA PANEL (B) LANGMUIR ADSORPTION ISOTHERM MODEL FOR GOETHITE XXXIII

AIV: FIGURE S6. PICTURE OF THE GLYPHOSATE EXTRACTION SETUP WITH PACKED ACTIVATED ALUMINA XXXIII

Appendix II: Chapter 2- SI
Supporting Information

Dual Element ($^{15}N/^{14}N$, $^{13}C/^{12}C$) Isotope Analysis of Glyphosate and AMPA: Derivatization-Gas Chromatography Isotope Ratio Mass Spectrometry (GC/IRMS) Combined with LC/IRMS

Emmanuel O. Mogusu[1], J. Benjamin Wolbert[2], Dorothea M. Kujawinski[2], Maik A. Jochmann[2] and Martin Elsner[1]

[1]Helmholtz Zentrum München, Institute of Groundwater Ecology, Ingolstädter Landstrasse 1, 85764 Neuherberg, Germany.

[2] University of Duisburg-Essen, Instrumental Analytical Chemistry, Universitätstraße 5, 45141 Essen, Germany

Contents

AII Table SI. The ^{15}N & $\delta^{13}C$ values of glyphosate from commercial herbicides samples.

AII Table SII. The trade names of measured commercial glyphosate products.

AII Figure S1. The variation in $\delta^{15}N$ isotope values of commercial herbicide (Blue diamonds) with increasing excess of iso-PCF derivatization agent

AII Figure S2. The reproducibility of glyphosate and AMPA laboratory standard measured with LC-IRMS.

AII Figure S3. The chromatogram of glyphosate and AMPA laboratory standard (1.7 mM, 3.1 mM) measured with LC-IRMS.

Producers	$10^3\delta^{13}C$	SD (n=3)	$10^3\delta^{15}N$	SD (n=4)
A	-29.8	0.2	-0.1	0.1
A	-26.3	0.2	-0.4	0.1
B	-31.3	0.1	0.2	0.4
B	-31.5	0.3	-0.2	0.2
C	-29.8	0.3	3. 3	0.1
D	-30.2	0.5	0.2	0.3
D	-28.2	0.1	-0.2	0.2
E	-30.0	0.5	2.5	0.1
F	-33.7	0.2	-0.6	0.2
G	-29.4	0.1	-1.5	0.2
H	-31.2	0.1	0.4	0.2
H	-28.1	0.4	2.2	0.1
I	-25.8	0.1	0.3	0.2
I	-24.6	0.1	-0.3	0.1
I	-26.4	0.1	0.1	0.9
J	-30.2	0.1	0.3	0.9
J	-30.6	0.1	0.5	0.3
J	-31.4	0,3	-0.7	0.1
K	-27.2	0.1	-1.5	0.2
K	-27.0	0.2	-1.3	0.3
L	-32.0	0.1	-0.9	0.2
L	-31.8	0.1	-0.5	0.1
L	-31.8	0.2	0.5	0.1
L	-31.6	0.2	-1.8	0.4
L	-31.9	0.2	-0.3	0.6
M	-25.6	0.9	1.0	0.6
M	-25.5	0.1	0.2	0.2
M	-26.1	0.5	-0.1	0.3

AII: Table SI. The $\delta^{15}N$ & $\delta^{13}C$ values of glyphosate from commercial herbicides samples. The standard deviations given in the Table are the estimate of replicate sample measurements, while those in Figures 2-7 and 2-8 in Chapter 2 correspond to the standard deviation of the methods determined independently (in Figure 2-6 in Chapter 2)

Producer	Trade name
A	R U Flash UP Plus
B	Clinic
C	Super UT 360
D	Freelancer
E	Gibson
F	Pratiko
G	Amegemax
H	Prologue 2
I	Round UP GT
J	Round UP
K	Round UP Gran
L	Vovox Direct
M	Bayer Garten

AII: Table SII. The trade names of measured commercial glyphosate products.

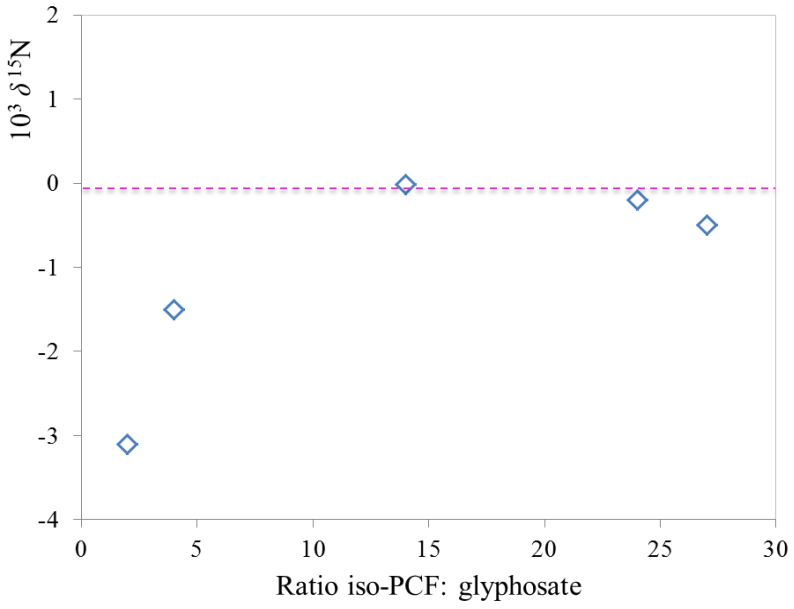

AII: Figure S1. The variation in $\delta^{15}N$ isotope values of commercial herbicide (blue diamonds) with increasing iso-PCF: commercial herbicide ratios. The dashed pink line represents the EA/IRMS $\delta^{15}N$ value of glyphosate standard (-0.28 ‰ ± 0.06 ‰).

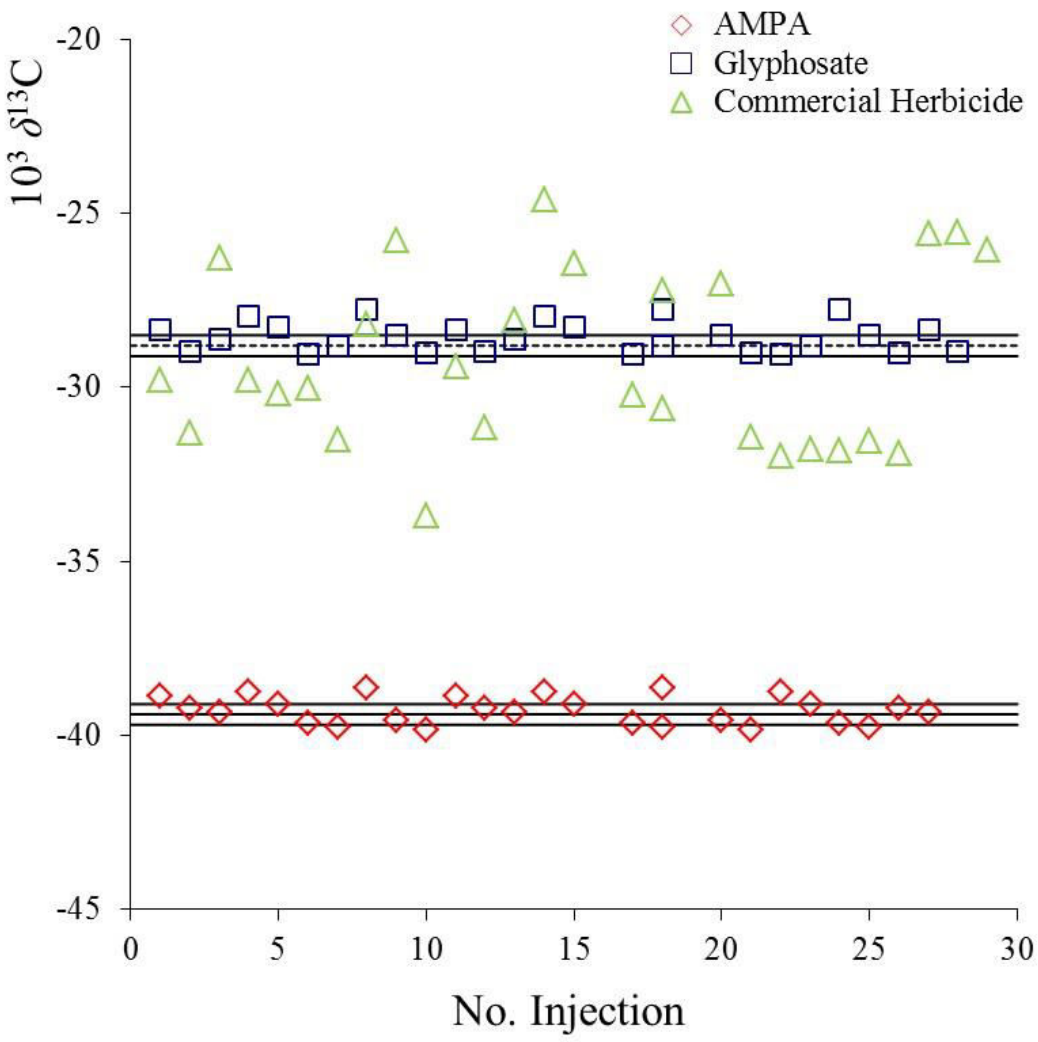

AII: Figure S2. The reproducibility of $\delta^{13}C$ values of glyphosate standards (squares) and AMPA standards (diamonds) measured with LC/IRMS. Triangles are measurements of commercial glyphosate products analyzed between the standard measurements. The solid lines represent the standard deviation (SD) of glyphosate and AMPA (±0.34 ‰,) respectively. The dashed black lines represent the EA/IRMS $\delta^{15}N$ value of glyphosate and AMPA standard (-28.99 ‰ ± 0.06 ‰, -39.84 ‰ ± 0.10 ‰) respectively.

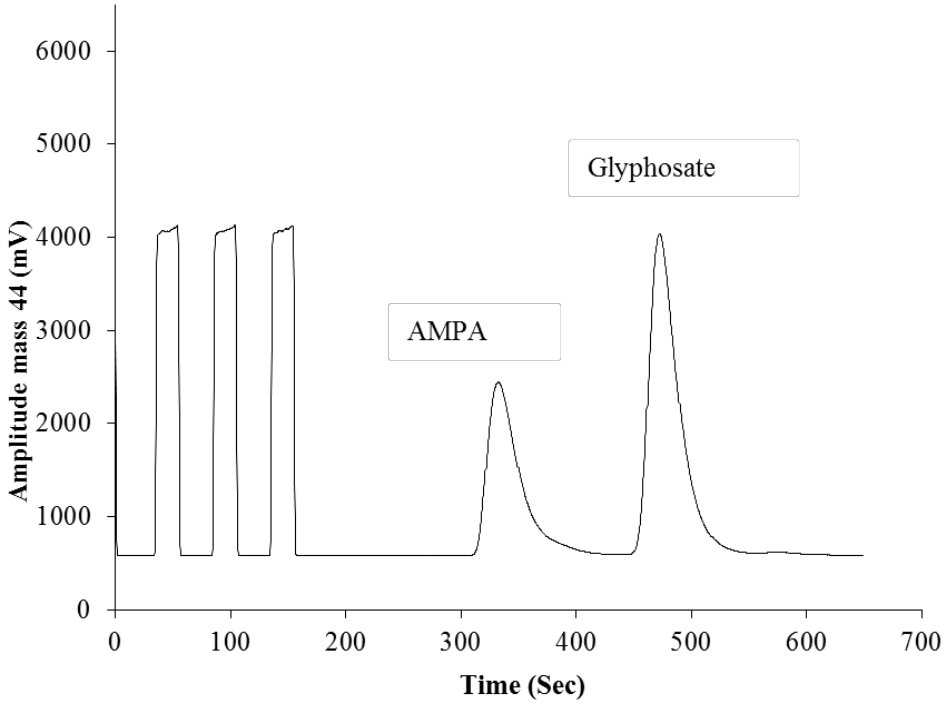

AII: Figure S3 Chromatogram of glyphosate and AMPA standards (300 mgL^{-1}, 345 mgL^{-1}) measured with LC/IRMS. The three first peaks represent CO_2 monitoring gas.

AII: Information on routine quality controls for IRMS measurements

Daily controls during the nitrogen and carbon analysis (GC/IRMS and LC/IRMS) included monitoring of background masses (Argon m/z 40, carbon dioxide m/z 44, nitrogen m/z 28 and water m/z 18) to exclude any leaks, repeated measurements of monitoring gas ("standard on-offs") and checks that monitoring gas measurements did not depend on the amount of sample introduced within the measurement range ("linearity test") (linearity better than 0.03 $‰V^{-1}$ over a range from 0.2 to 14.3 V; SD of standard on-offs better than 0.04 ‰) These tests were performed before each sequence to check the daily instrument performance. Before and after each run three monitoring gas pulses were introduced as an anchor to "calibrate" the analyte isotope value between measurements. Sample measurements were bracketed with glyphosate and AMPA laboratory reference standards.

AII: Graphic Art

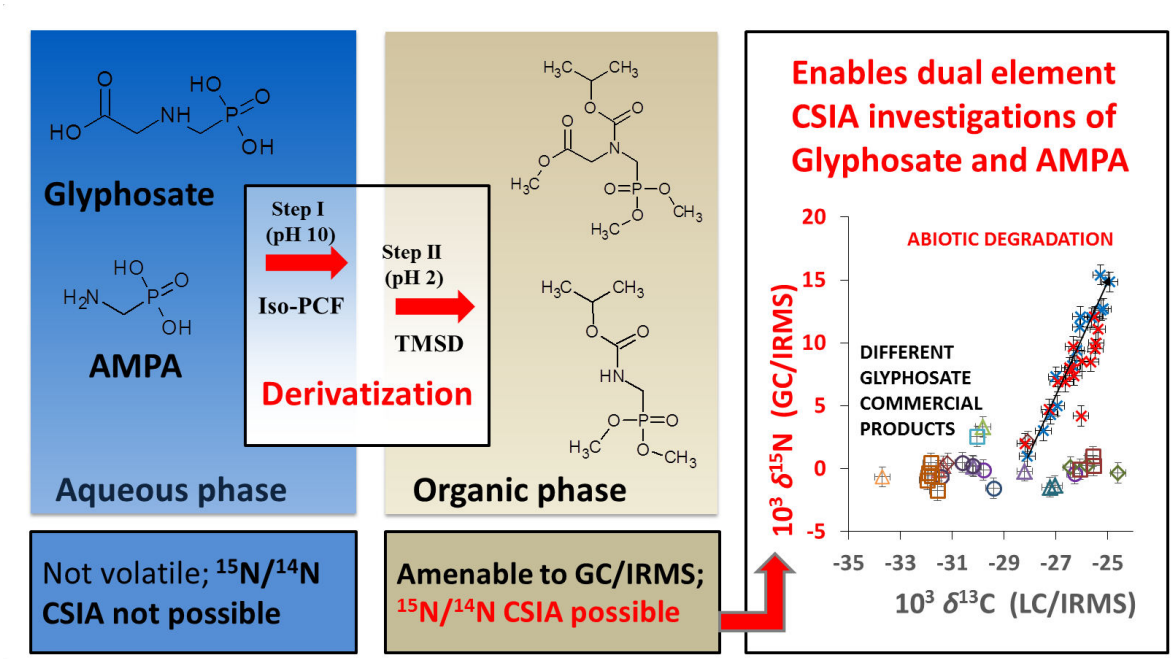

Appendix III: Chapter 3- SI
Supporting Information

Compound-specific Isotope Fractionation during Biodegradation of Glyphosate with *Ochrobactrum sp.* FrEM

Emmanuel O. Mogusu[1], J. Benjamin Wolbert[2], Maik A. Jochmann[2] Torsten Schmidt[2] and Martin Elsner[1*]

[1]Helmholtz Zentrum München, Institute of Groundwater Ecology, Ingolstädter Landstrasse 1, 85764 Neuherberg, Germany.

[2] University of Duisburg-Essen, Instrumental Analytical Chemistry, Universitätstraße 5, 45141 Essen, Germany

Contents

Materials, procedures and analytical methods

AIII: Figure S1: LC/IRMS (liquid chromatography- isotope ratio mass spectrometer) schematic setup

AIII: Table SI. Transitions parameters for glyphosate quantification and conformation

AIII Figure S2: Speciation of glyphosate, glutamate and AMPA depending on pH

AIII Figure S3: LC/IRMS chromatogram of glyphosate, AMPA and glutamate on a Primesep 100 column.

Challenges during glyphosate isotope analysis with LC/IRMS

AIII Figure S4: $\delta^{13}C$ isotope values of glyphosate, AMPA, sarcosine and glutamate versus peak amplitudes (m/z = **44**) in LC/IRMS analysis

AIII Figure S5: $\delta^{13}C$ & $\delta^{15}N$ isotope values of glyphosate, AMPA and sarcosine during abiotic degradation with MnO_2

AIII Table S2:Evaluation of the AKIE carbon and nitrogen for abiotic and (bio) degradation of glyphosate

AIII Figure S6: Phylogenetic position of strain *Ochrobactrum* FrEM within *Ochrobactrum* species

AIII Figure S7: Micrograph of *Ochrobactrum sp FrEM* cells by light microscopy

AIII: Figure S8: Degradation of glyphosate by *Ochrobactrum antropia* GPK 3

AIII Figure S9: Processes that determine the fate of pesticide in the environment.

Materials

Glyphosate (99%, CAS No. 1071-83-6), ammonium acetate (99%), 1.0 M Iso-PCF (isopropyl chloroformate) in hexane, 2.0 M TMSD (trimethyl silyl diazomethane) in ethyl ether, FMOC-Cl (9-Fluorenylmethyl chloroformate 97% purity) as well as diethyl ether, methanol, ethyl acetate, *tert*-butanol (with purities >99%) and sodium glutamate (with purities <99%) were all purchased from Sigma-Aldrich (GmbH Steinheim, Germany). Sodium peroxodisulfate ($Na_2S_2O_8$), potassium hydroxide (KOH), phosphoric acid (H_3PO_4) and monosodium phosphate (KH_2PO_4) (all with purities >99% from Fluka; Steinheim; Germany) were used as LC eluents and oxidation reagents. Glyphosate-FMOC (98.5%), AMPA-FMOC (97%) standards were obtained from Dr. Ehrenstorfer (Augsburg, Germany). Stock glyphosate and AMPA standards were prepared in MilliQ water (generated with a Millipore Advantage A10 system, Millipore, Molsheim, France).

The MS1 medium contained (in gL^{-1}): NH_4Cl, 2.0; $MgSO_4 \times 7H_2O$, 0.2; K_2SO_4, 0.5; as well as trace elements (in mgL^{-1}): $FeSO_4 \times 7H_2O$, 2.5; $CaCl_2 \times 6H_2O$,10.0; $CuSO_4 \times 5H_2O$, 2.0; H_3BO_3, 0.06; $ZnSO_4 \times 7H_2O$,20.0; $MnSO_4 \times H_2O$, 1.0; $NiCl_2 \times 6H_2O$, 0.05; $Na_2MoO_4 \times 2H_2O$, 0.3.

Derivatization reaction with FMOC-Cl

The quantification of glyphosate was performed on a LC/MS-MS (liquid chromatograph coupled to a tandem mass spectrometer) after a derivatization step with FMOC-Cl in alkaline medium [151,82]. Briefly, 0.5 ml of 4 mM borate buffer were mixed with 3 ml of glyphosate solution in 15 ml polypropylene centrifuge tubes. After that, 0.5 ml of 6.5 µM FMOC-Cl solution were added and the mixture was shaken on an overhead shaker. After 2 hrs of reaction, 4 ml of dichloromethane (DCM) were added and the mixture was centrifuged at 3000 g for 10 minutes to separate DCM from water (immiscible). DCM is used to extract excess FMOC-Cl which interferes with mass spectrometric measurements. A similar treatment was done for glyphosate and AMPA laboratory standards which were used for calibration.

LC/MS-MS measurements

The injection volume for LC/MS-MS was 20 µL. A Luna C18 column (5 µm, 30 mm×2 mm i.d., PEEK-lined, Phenomenex, Germany) was used for analyte separation. The mobile phase was composed of water buffered with 5 mM ammonium acetate at pH 9 (adjusted with ammonia) (solvent A) and MeOH (solvent B). The LC gradient for the separation consisted of

a linear increase of B from 10% to 25% between 0 and 3 min, an isocratic plateau from 3 to 6 min (75% A: 25% B); again a linear increase 25% to 90% between 6 to 15 min and a final isocratic plateau at 90% B from 15 to 18 min. Lastly, the column was re-equilibrated for 7 min, resulting in a total run time of 25 min. The flow rate was 0.2 mL min^{-1} and the column temperature was 30 °C.

The target substances were detected with a triple quadrupole mass spectrometer, an API 2000 (Applied Biosystems, Foster City, CA, USA), which was operated with a HPLC system consisting of a quaternary pump, a degasser and an autosampler (all Agilent 1100, Agilent Technologies, Waldbronn, Germany). The instrument was equipped with electrospray ionization and was calibrated using a 1,3,6-polytyrosine solution. Details of the substance-specific ionization parameters for detection of FMOC-derivatized analytes and isotopically labelled standards are shown in Table SI.

Table SI. Transitions parameters for glyphosate quantification and conformation

Analyte	Precusur ion (m/z)	Product ion *(m/z)*	Time (sec)	DP	EP	CE	CXP	CEP	RO_2
Glyphosate-FMOC	389.9	Q: 168	150	-21	-3.7	-14	-4	-22	10
Glyphosate-FMOC	389.9	q: 150	150	-41	-3	-34	0	-22	10
Glyphosate-FMOC	167.8	q:150	150	-46	-9	-8	0	-12	11
Glyphosate-FMOC	167.8	q: 80.9	150	-46	-9	-20	0	-12	9
AMPA-FMOC	332.5	Q: 109.9	150	-6	-5.5	-10	-2	-	-
AMPA-FMOC	109.8	q: 81.1	150	-21	-8	-16	0	-	-
1,2 ^{13}C ^{15}N Glyphosate-FMOC	389.9	Q: 171	150	-21	-3.7	-14	-4	-22	10

Q: transition used for quantification q: transition used for confirmation
DP:Declustering potential EP:Entrance potential CE:Collission energy CXP:Collission cell exit potential rod offset
CEP:Collission cell entrance potential RO_2:collision cell

Derivatization of glyphosate and AMPA for nitrogen isotope analysis

The derivatization reaction of glyphosate involved a three-step procedure as described in (Mogusu et al 2015). Briefly, the pH of 500 µL glyphosate sample was adjusted to 10 with a borate/NaOH buffer system. Immediately after, 300 µL of 1.0 M isopropyl chloroformate (iso-PCF) in hexane were added, and then vortexed for 10 minutes. Subsequently, the pH was adjusted to 1-2 with 50 µL 2 M HCl. The excess of derivatization agent was extracted with 3 ml ethyl ether and the organic layer was discarded. The aqueous solution was saturated with sodium chloride and extracted twice with 20% *tert*-butanol in ethyl ether. Subsequently, 200 µL of methanol were added to the ethereal extract together with 50 µL of 2.0 M TMSD in ether and the mixture was allowed to react at room temperature.

Nitrogen isotope analysis by GC/IRMS

The GC/IRMS system consisted of a Trace GC ultra-gas chromatograph (Thermo Fisher Scientific, Milan, Italy) linked to a Finnigan MAT 253 (Thermo Fisher Scientific, Bremen, Germany) by a Finnigan GC combustion III interface (Thermo Fisher Scientific, Bremen, Germany). The emission was set to 2 mA for nitrogen analysis. Helium (grade 5.0, supplied by Linde, Germany) was used as carrier gas at a flow rate of 1.4 mL min^{-1}. The samples (1 µL of N-isopropyl carbonyl methyl ester derivative) were injected by a GC CombiPal autosampler (CTCAnalytik, Zwingen, Switzerland) in splitless mode at a constant injector temperature of 250°C. After 1 min, the split ratio was switched to 1:10. To enable separation of glyphosate- and AMPA-derivatives from the interfering glutamate-derivative, an Rtx-5 Amine column (supplied by Restek, Germany) (30 m; 0.32 µm inner diameter; 1µm film thickness) was used with the following temperature program. The initial temperature of 80°C was held for 1 min. Then the temperature was increased to 150°C at 10°C min^{-1}, held for 1 min and then ramped to 230°C at 3°C min^{-1}. The final temperature was held for 2 min (Mogusu et al 2015).

EA/IRMS

Carbon and nitrogen isotope ratios of reference materials of glyphosate and AMPA ("working standards") were characterized by an elemental analyzer - isotope ratio mass spectrometer (EA-IRMS) consisting of a EuroEA (EuroVector, Milano, Italy) coupled to a FinniganTM MAT253 IRMS (Thermo Fisher Scientific, Bremen, Germany) by a FinniganTM ConFlow III interface (Thermo Fisher Scientific, Bremen, Germany). The materials were calibrated against the reference materials USGS 40, USGS 41 and IAEA 600 provided by the International Atomic Agency (IAEA, Vienna, Austria). The $\delta^{13}C$ and $\delta^{15}N$ isotope values were reported in per mille relative to PeeDee Belemnite (V-PDB) and air, respectively, according to equations S1-S2

$$\delta^{13}C_{sample,VPBD} = \frac{R\left(^{13}C/^{12}C\right)_{sample} - R\left(^{13}C/^{12}C\right)_{VPBD}}{R(^{13}C/^{12}C)_{VPBD}} \quad \text{(S1)}$$

$$\delta^{15}N_{sample,N_2-AIR} = \frac{R\left(^{15}N/^{14}N\right)_{sample} - R\left(^{15}N/^{14}N\right)_{N_2-AIR}}{R(^{15}N/^{14}N)_{N_2-AIR}} \quad \text{(S2)}$$

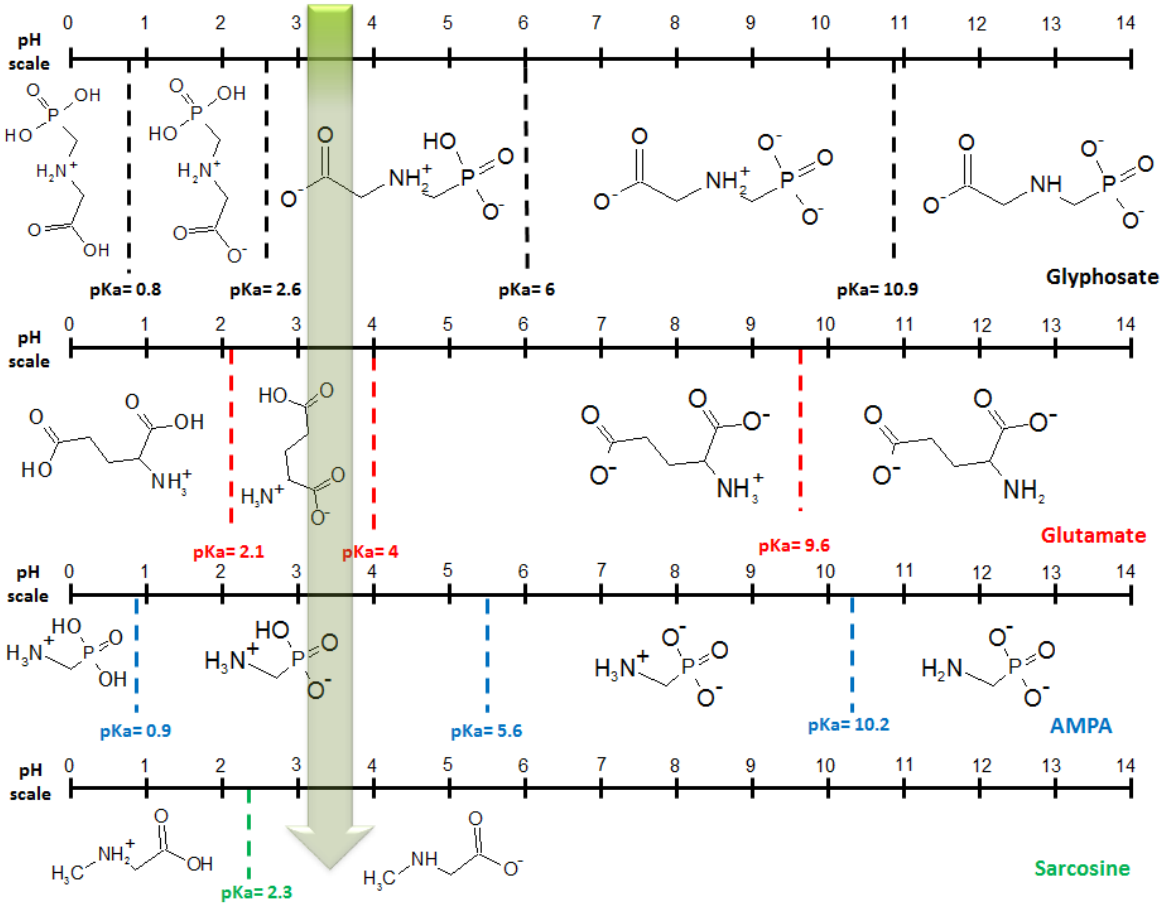

Figure S1: Speciation and pKa values of glyphosate, glutamate, AMPA and sarcosine. The vertical arrow shows the optimum pH (3.1) for the separation of the compounds (glyphosate, glutamate, AMPA and sarcosine) using a phosphate buffer (2.5 mM NaH_2PO_4 buffer adjusted at pH 3.1).

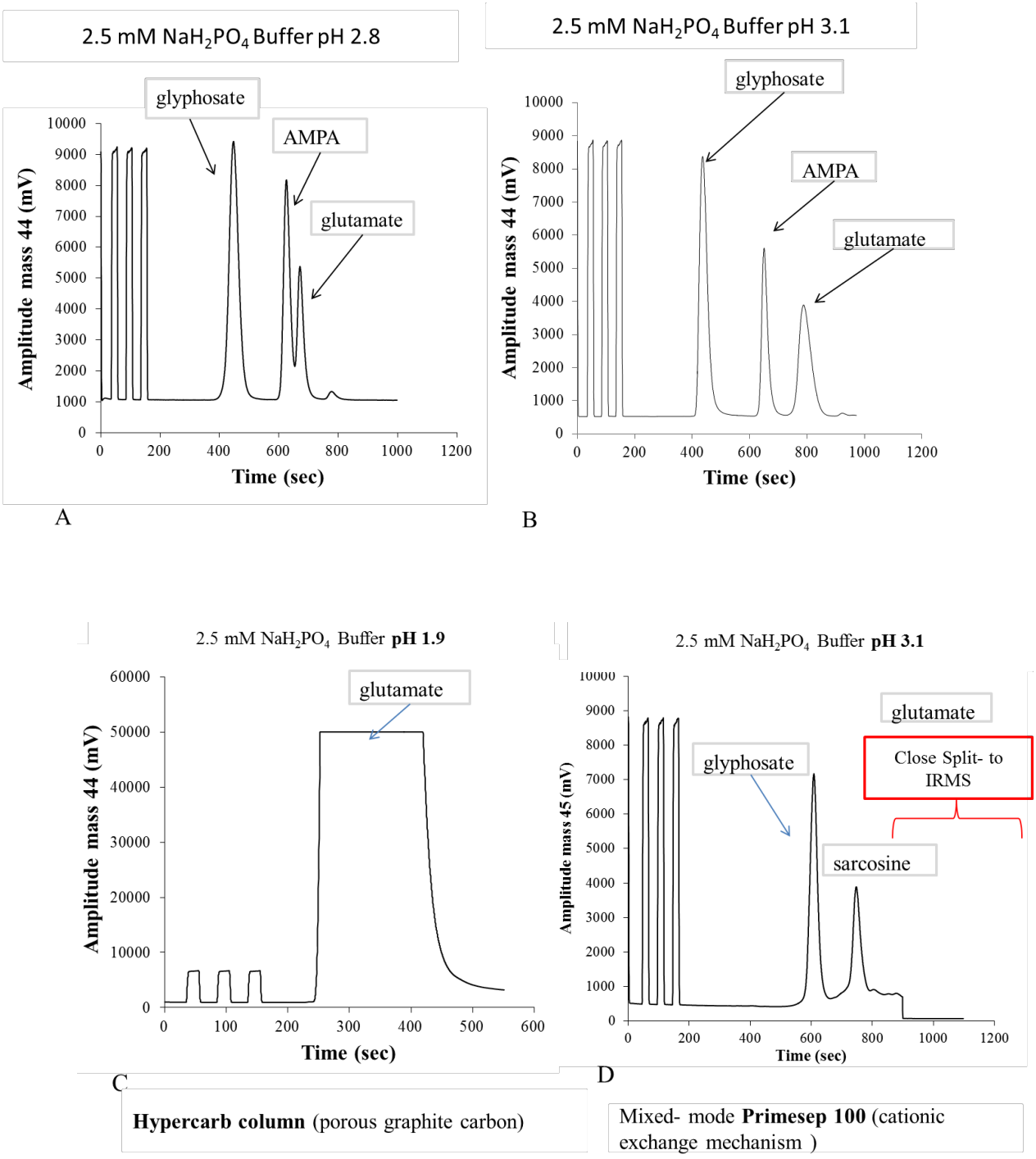

Figure S2: LC-IRMS chromatogram of glyphosate, AMPA and glutamate on a **Primesep 100** column. **Panels A and B** show the separation of glyphosate, AMPA and glutamate using

2.5 mM NaH_2PO_4 buffer at pH 3.1 and pH 2.8, respectively. **Panel C** shows the separation of glyphosate and glutamate biodegradation samples on a Hypercarb column according to the method of Kujawinski et al 2013). **Panel D** shows the chromatographic separation according to our modified method with a mixed- mode **Primesep 100** column with 2.5 mM NaH_2PO_4 buffer at pH 3.1

Practical challenges during separation on LC/IRMS

Even though the modified method with a Primsep 100 column achieved a good separation of glyphosate and glutamate at high concentrations (10 gL^{-1}) we caution that the following practical challenges may be encountered when analyzing high concentrations of carbon-containing compounds with sodium peroxodisulfate in large excess (0.84 M). 1) The high concentration of glutamate created a high CO_2 background after wet oxidation (compound conversion to CO_2) with sodium peroxodisulfate (0.84 M). This created a constant high CO_2 background, and in one run oversaturated the solution with CO_2 to such an extent that the overpressure damaged the separation unit (see Figure S1 panel C). In addition, the high background of oxygen also damaged the IRMS ion source, which had to be changed. 2) At the interface, capillaries were often clogged because of the high concentration (0.84 M) of sodium peroxodisulfate. To avoid these problems, introducing a fraction collection (separation) step to remove the high glutamate background before LC/IRMS measurements and using a lower concentration of (0.42 M) of sodium peroxodisulfate is recommendable.

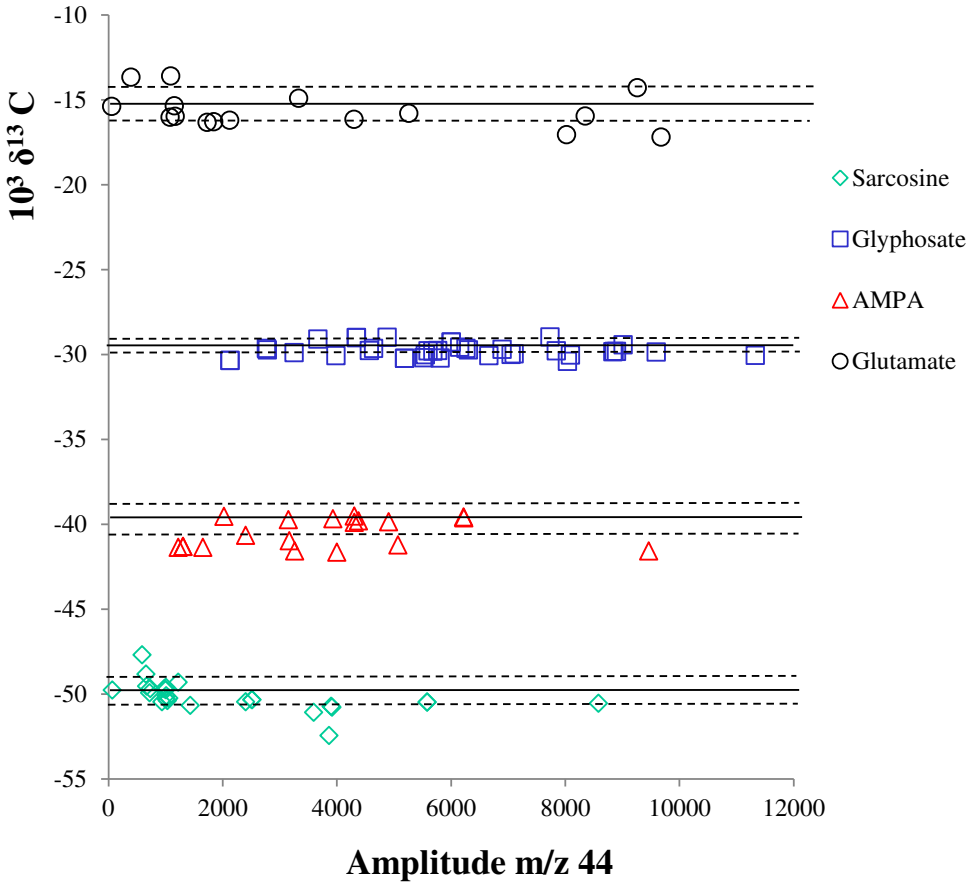

Figure S3: $\delta^{13}C$ isotope values of glyphosate (blue rectangle), AMPA (red triangle), sarcosine (green diamond) and glutamate (black circles) versus peak amplitudes (m/z = 44) from measurements of in-house laboratory standards by LC/IRMS on a Primesep 100 column in concentrations between 0.35 mM to 6 mM , 0.5 mM to 9 mM, 0.6mM to 6 mM and 0.35 mM to 6 mM respectively. The dashed lines represent the respective standard deviations (SD) (± 0.3‰, ± 0.4‰, ± 0.5‰ and ± 0.7‰ respectively). The bold lines indicate measured EA-IRMS values.

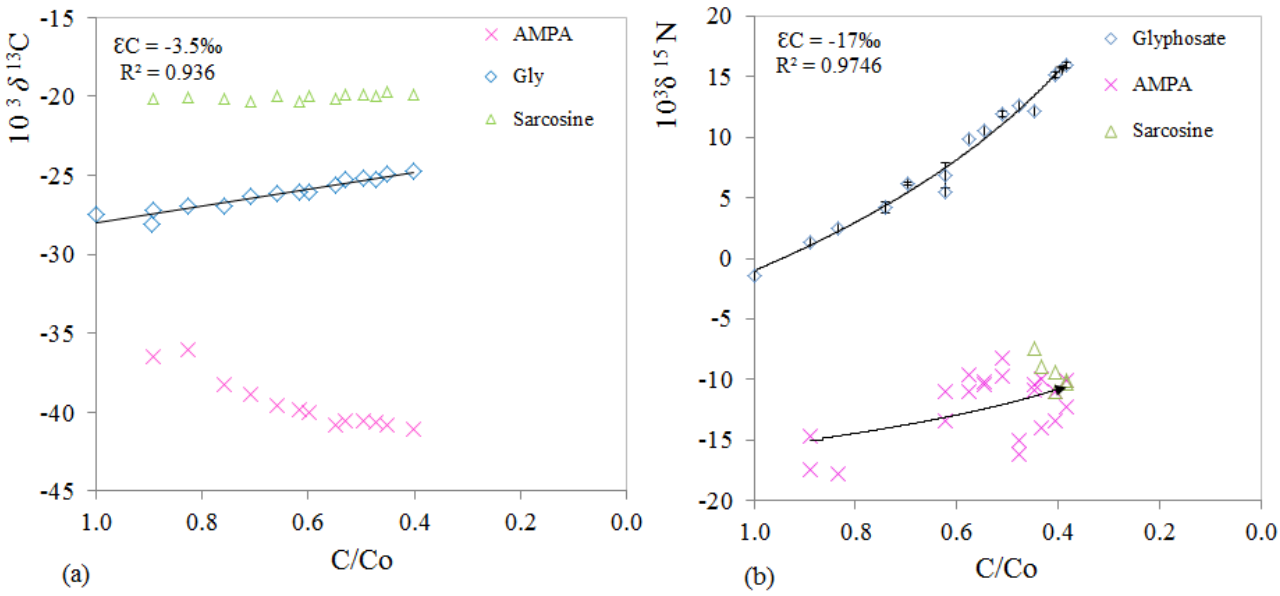

Figure S4: **Panel (a)** $\delta^{13}C$ isotope values of glyphosate (blue rectangle), AMPA (red crosses) and sarcosine (green trangles) during abiotic degradation with MnO_2. **Panel (b)** $\delta^{15}N$ isotope values of glyphosate (blue rectangle), AMPA (red crosses) and sarcosine (green trangles) during abiotic degradation with MnO_2.

	enzyme	ε_{carbon} [‰]	$\varepsilon_{nitrogen}$ [‰]	$\Delta=\delta^{15}N/\delta^{13}C = \varepsilon_{nitrogen}/\varepsilon_{carbon}$	$AKIE_{carbon}$	$AKIE_{nitrogen}$
Abiotic degradation (MnO_2)	-	-3.7 ± 0.3	-17.2 ± 0.3	4.6 ± 0.03	1.011	1.017
Ochrobactrum sp. FrEM	C-P Lyase	-5.5 ± 0.3	-0.6 ± 0.7	0.1 ± 0.06	1.016	1.000

Table S2: Evaluation of the AKIE carbon and nitrogen for abiotic and (bio) degradation of glyphosate

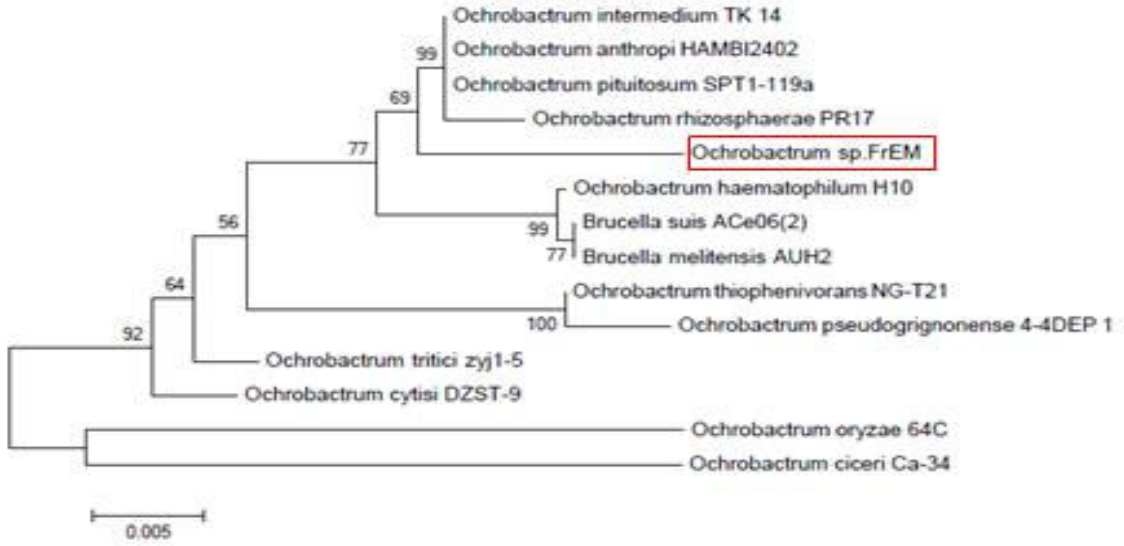

Figure S5: Phylogenetic position of the strain FrEM within *Ochrobactrum* species. Neighbour-joining tree based on partial 16S rRNA sequence. The bar indicates 0.005 substitutions per nucleotide.

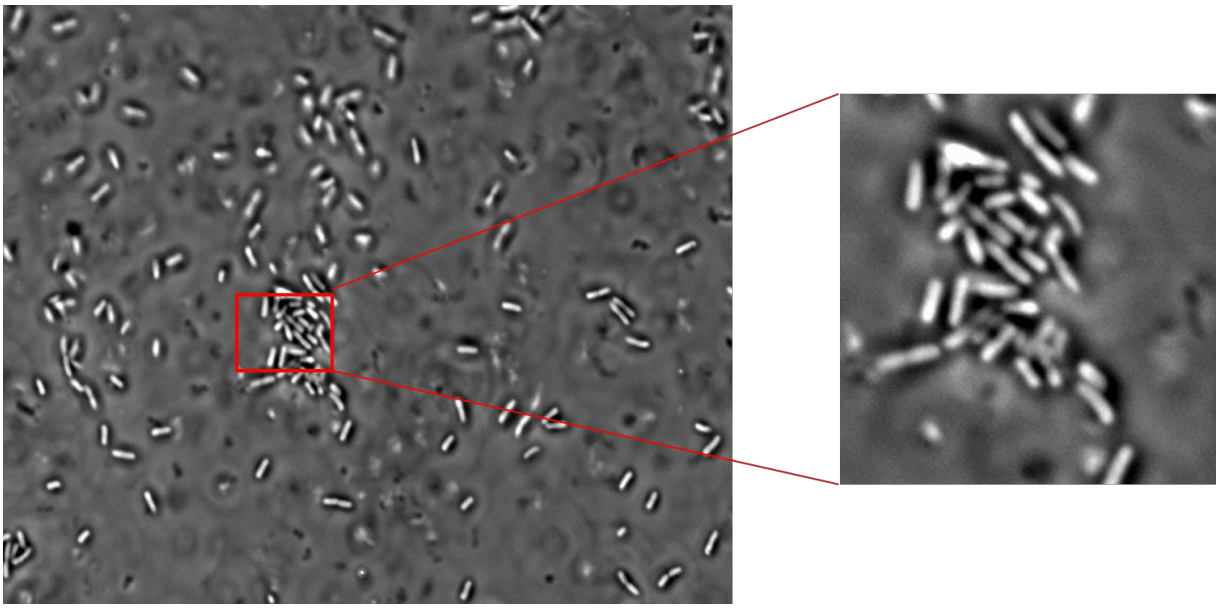

Figure S6: Micrograph of *Ochrobactrum sp FrEM 15651* cells by light microscope (Axioskop Plus2, ZEISS, Germany (×100 resolution- oil emulsion), AxioVision 4.1

Attempts of glyphosate degradation with Ochrobactrum anthropi *GPK3*

Preliminary biodegradation experiments were conducted with two pure strains *Ochrobactrum antropia* GPK 3 and *Achromobacter sp*. The bacterial strains were kindly shared by Dr. Alexey A. Leontievsky from G.K. Skryabin Institute of Biochemistry and Physiology of Microorganisms, Russian Academy of Sciences. We carefully cultured the pure strains with the protocol provided to us. Unfortunately, attempts to use the pure strains to degrade glyphosate were unsuccessful. In the first attempt, the *Ochrobactrum antropia* GPK 3 strain degraded half of the glyphosate and then the glyphosate concentration remained unchanged. Surprisingly, the bacterial biomass increased (cell growth) over time (monitored by Optical density OD 560nm) indicating growth on glutamate without further breakdown of glyphosate. This observation (growth of *Ochrobactrum antropia* GPK 3 without breakdown of glyphosate) was reproduced in five independent cultivation experiments. Biodegradation experiments with *Achromobacter sp* showed a similar observation. Figure S6 shows the biodegradation of glyphosate and the bacteria growth curve. To check for strain contamination over time, we conducted 16S RNA gene sequencing. The amplified DNA gene sequence showed that the strains were *Ochrobactrum antropia* GPK 3 and *Achromobacter sp.* Therefore, we concluded that the bacterial strain grew on glutamate (carbon source) even without the need of glyphosate. The reason may be that it was able to use trace phosphate sources (cleaning detergents for our laboratory glass ware) that might have been present and were difficult to eliminate.

In response to these unsuccessful degradation experiments with the strains provided, *Ochrobactrum sp.* strain FrEM was subsequently isolated from agricultural soil as described in the manuscript. With this new isolate, the degradation experiments of the study were conducted.

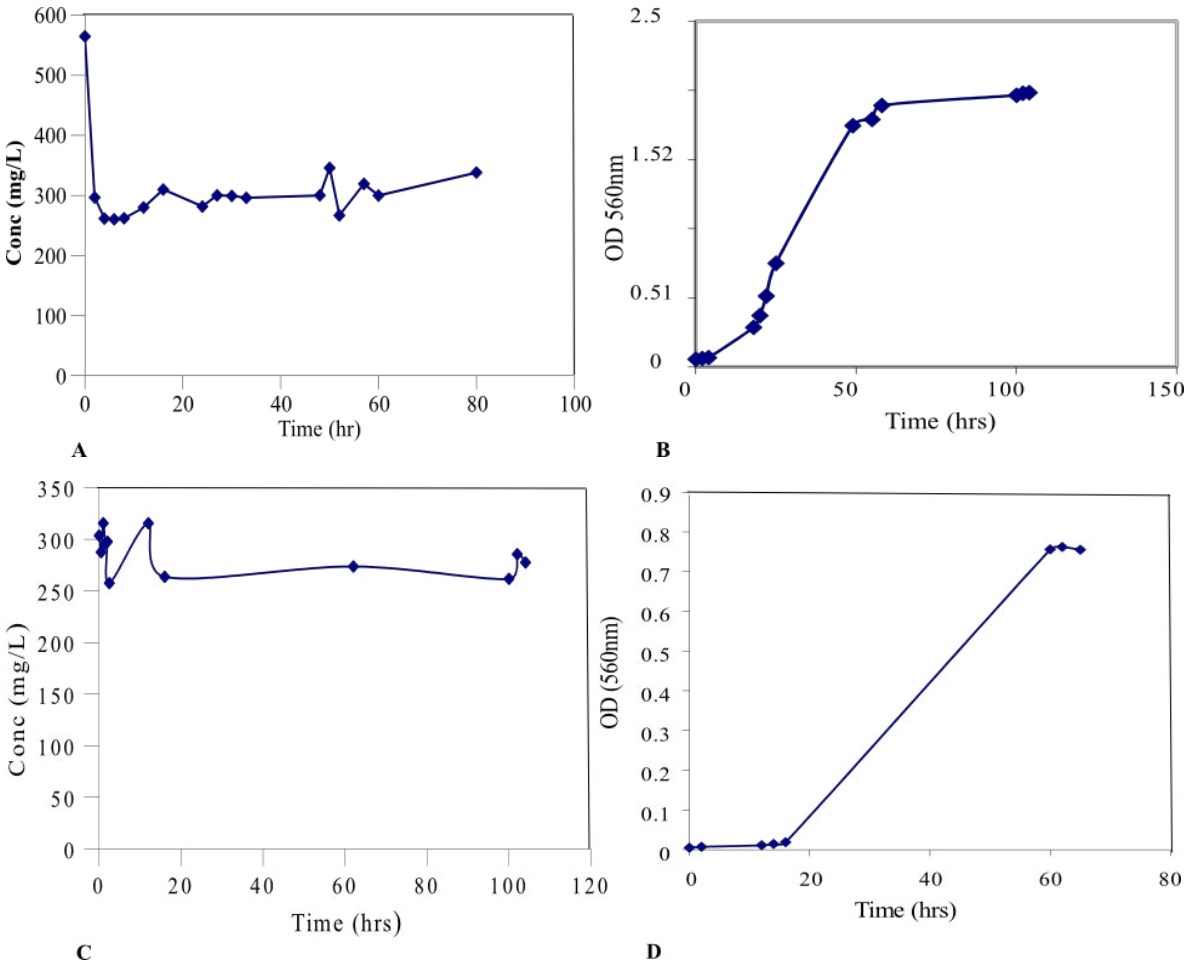

Figure S7: Panel A Degradation of glyphosate by *Ochrobactrum antropia* GPK 3 when grown in MS1 medium containing 3 mM glyphosate as the only phosphorous source. **Panel B** Measured bacterial growth (OD 560 nm) over time. **Panel C** Degradation of glyphosate by ***Achromobacter sp*** when grown in MS1 medium containing 1.5 mM glyphosate as the only phosphorous source. **Panel D** Measured bacterial growth (OD 560 nm) over time.

Graphic Art

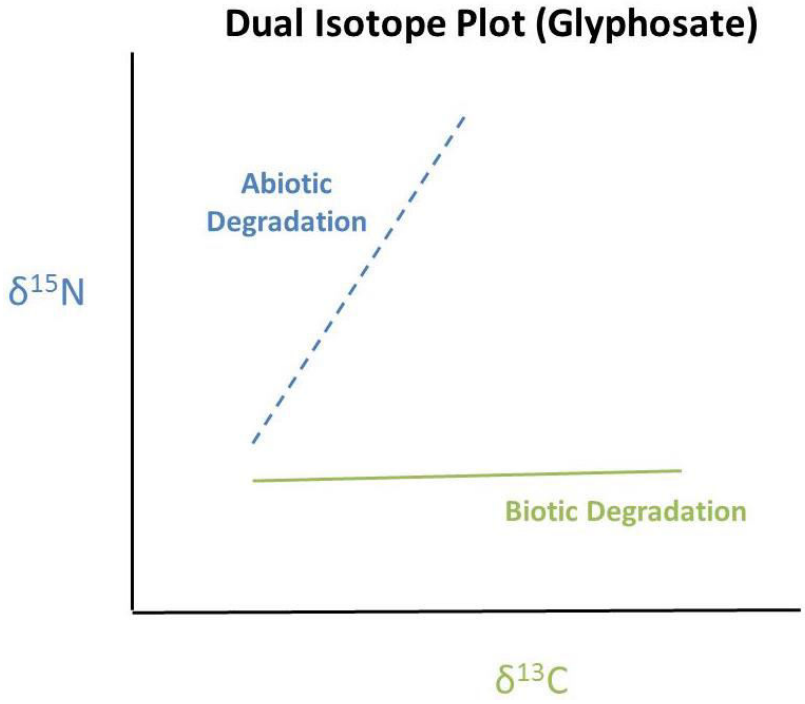

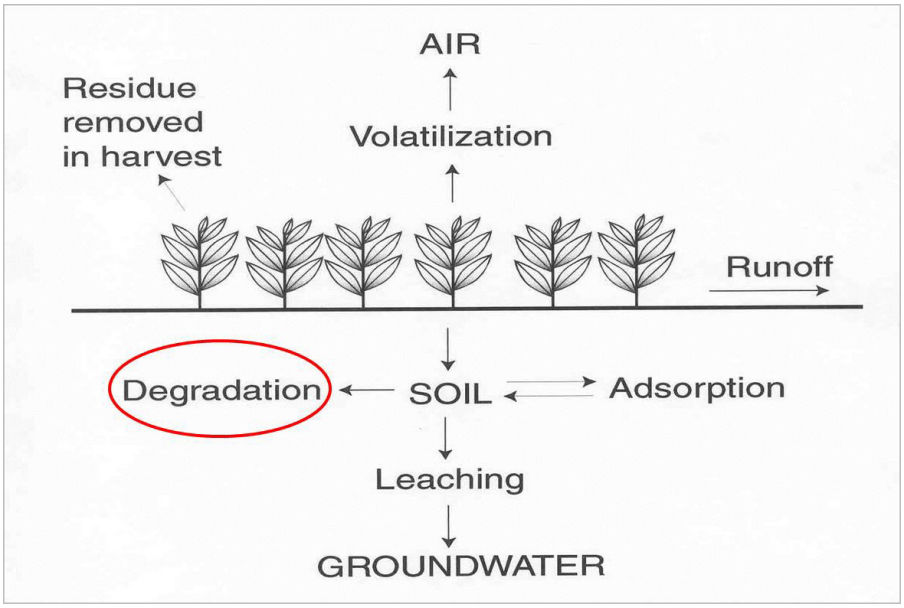

AIII Figure S8: Schematic representation of Pesticides released into the environment subjected to various physical, chemical and biological processes. Processes that determine the fate of pesticides in the environment.

Appendix IV: Chapter 4- SI

Supporting Information

Extraction of Glyphosate and AMPA from Water with Activated Alumina: Parameter Optimization and Preliminary Isotope Measurements

Emmanuel O. Mogusu and Martin Elsner

Contents

AIV: Figure S1: carbon isotope effect at equilibrium concentration during the sorption glyphosate on activated alumina, goethite and quartz

AIV: Figure S2: Elution of adsorbed glyphosate on alumina with potassium dihydrogen phosphate**,** ammonium carbonate and ammonium hydroxide

AIV: Table S1. Transitions parameters measured for glyphosate quantification and conformation

AIV: Figure S3. Chromatogram of direct glyphosate standard (at 100 μgL^{-1}) measured by LC/MS-MS

AIV: Table SII. Transitions parameters measured for glyphosate quantification and conformation

AIV Figure S4: chromatogram of glyphosate-FMOC first blue peak (13.4 min) and AMPA-FMOC 2^{nd} light blue peak (14.9 min) at 1 mgL^{-1} concentration

AIV: Figure S5. Langmuir adsorption isotherm model for activated alumina and goethite

AIV: Figure S6. Picture of the glyphosate extraction setup with packed activated alumina

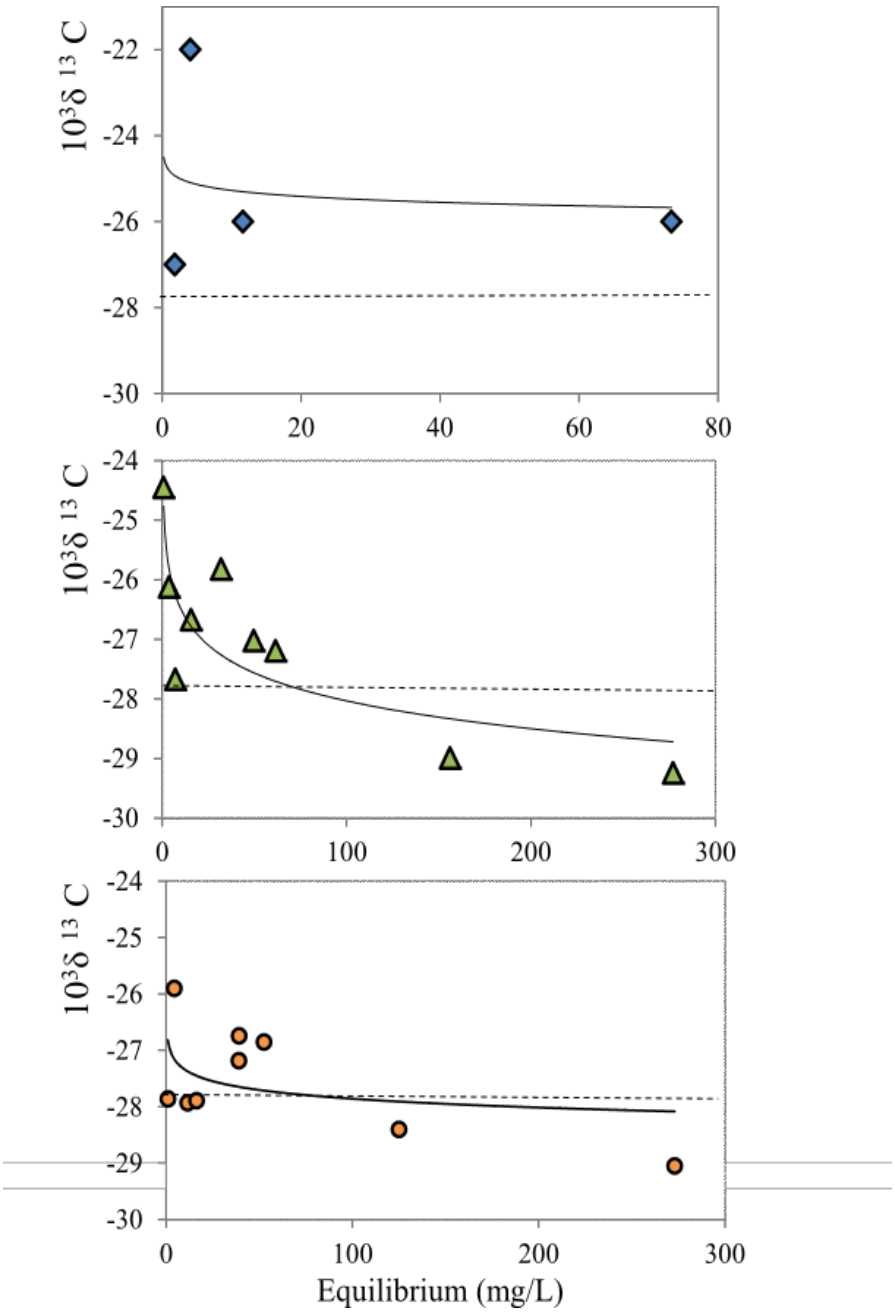

AIV: Figure S1: Panel (a) carbon isotope effect at equilibrium concentration during the sorption glyphosate on activated alumina **Panel (b)** carbon isotope effect during the sorption glyphosate on goethite and **Panel (c)** carbon isotope effect during the sorption glyphosate on quartz. The dashed lines represent the standard glyphosate carbon isotope values measure with EA-IRMS.

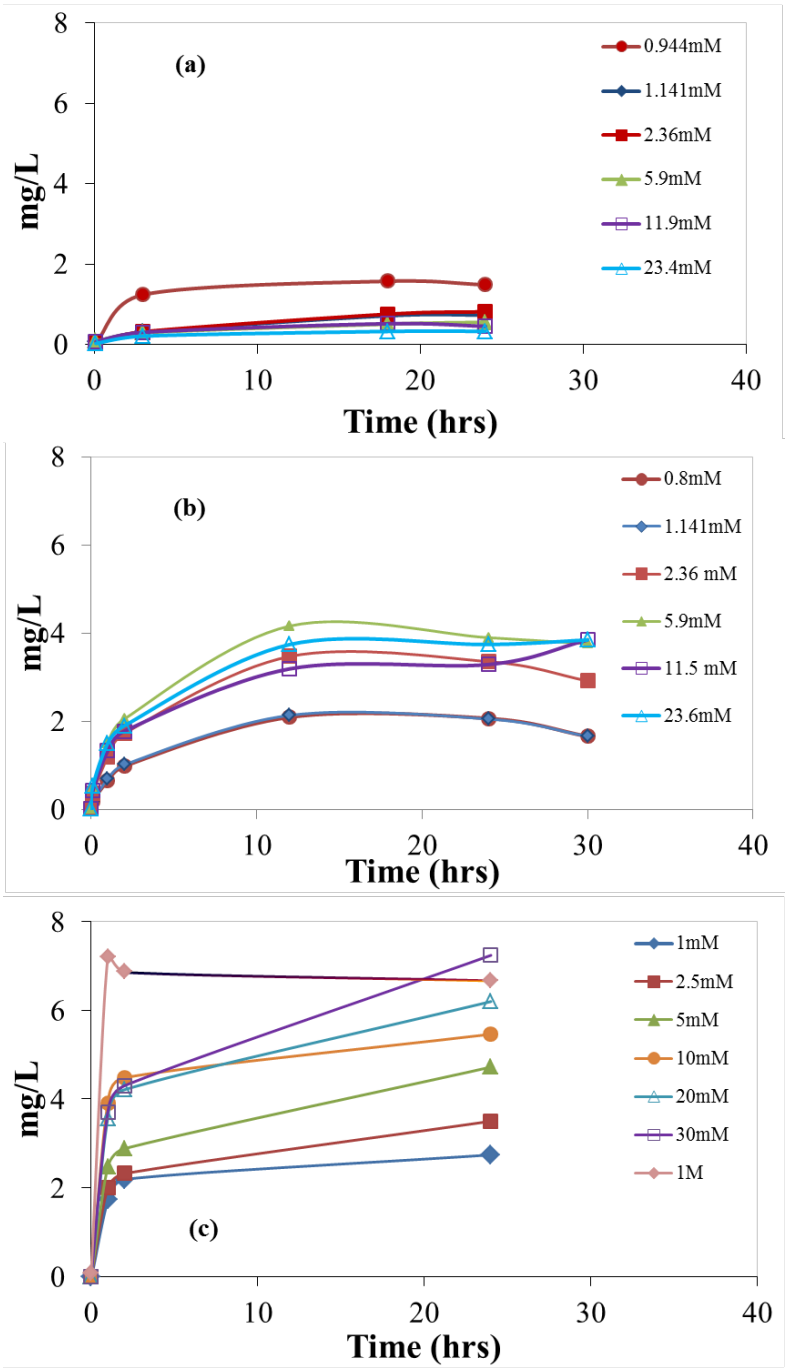

AIV: Figure S2: Panel (a) Elution of adsorbed glyphosate on alumina with potassium dihydrogen phosphate. **Panel (b)** Elution of adsorbed glyphosate on alumina with ammonium carbonate and **Panel (c)** Elution of adsorbed glyphosate on alumina with ammonium hydroxide.

Derivatization of glyphosate with FMOC-Cl

The quantification of glyphosate was performed on a LC/MS-MS (liquid chromatograph coupled to a tandem mass spectrometer) after a derivatization step with FMOC-Cl in alkaline medium [151,82]. Briefly, 0.5 ml of 4 mM borate buffer were mixed with 3 ml of glyphosate solution in 15 ml polypropylene centrifuge tubes. After that, 0.5 ml of 6.5 µM FMOC-Cl solution were added and the mixture was shaken on an overhead shaker. After 2 hrs of reaction, 4 ml of dichloromethane (DCM) were added and the mixture was centrifuged at 3000 g for 10 minutes to separate DCM from water (immiscible). DCM is used to extract excess FMOC-Cl which interferes with mass spectrometric measurements. A similar treatment was done for glyphosate laboratory standards which were used for calibration.

Analyte	Precusur ion *m/z*	Product ion *m/z*	ime (se	DP	EP	CE	CXP	CEP
Glyphosate	170	Q: 87.9	150	146	11	13	14	10
Glyphosate	170	q: 59.95	150	50	8	11.8	25	8
Glyphosate	170	q: 42	150	50	10	11.8	37	6

Q: transition used for quantification q: transition used for confirmation
DP:Declustering potential EP:Entrance potential CE:Collission energy CXP:Collission cell exit potential rod offset
CEP:Collission cell entrance potential

AIV: Table S1. Transitions parameters measured for glyphosate quantification and conformation

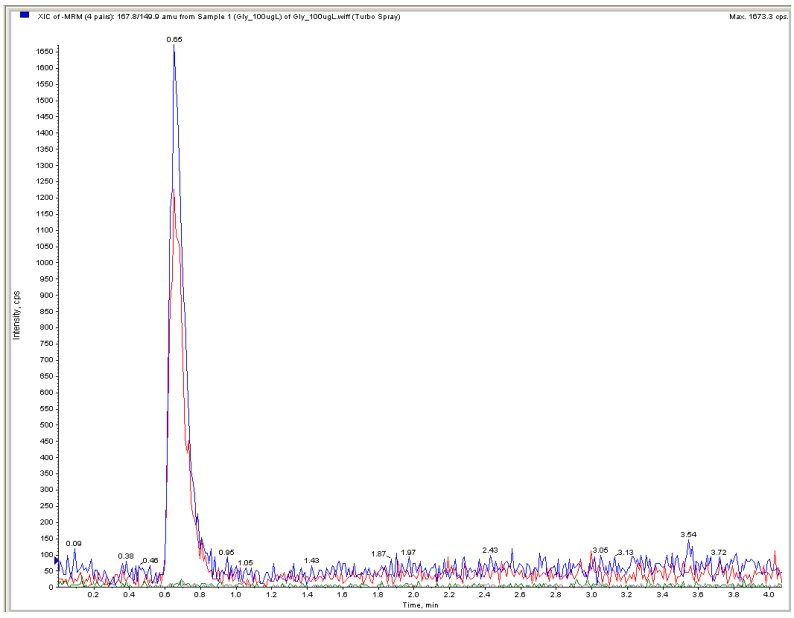

AIV: Figure S3. Chromatogram of direct glyphosate standard at 100 μgL^{-1} ($Q_{m/z}$ = 87.9) measured by LC/MS-MS

Analyte	Precusur ion (m/z)	Product ion *(m/z)*	Time (sec)	DP	EP	CE	CXP	CEP	RO_2
Glyphosate-FMOC	389.9	Q: 168	150	-21	-3.7	-14	-4	-22	10
Glyphosate-FMOC	389.9	q: 150	150	-41	-3	-34	0	-22	10
Glyphosate-FMOC	167.8	q:150	150	-46	-9	-8	0	-12	11
Glyphosate-FMOC	167.8	q: 80.9	150	-46	-9	-20	0	-12	9
AMPA-FMOC	332.5	Q: 109.9	150	-6	-5.5	-10	-2	-	-
AMPA-FMOC	109.8	q: 81.1	150	-21	-8	-16	0	-	-
1,2 ^{13}C ^{15}N Glyphosate-FMOC	389.9	Q: 171	150	-21	-3.7	-14	-4	-22	10

Q: transition used for quantification q: transition used for confirmation
DP:Declustering potential EP:Entrance potential CE:Collission energy CXP:Collission cell exit potential rod offset
CEP:Collission cell entrance potential RO_2:collision cell

AIV: Table SII. Transitions parameters measured for glyphosate quantification and conformation

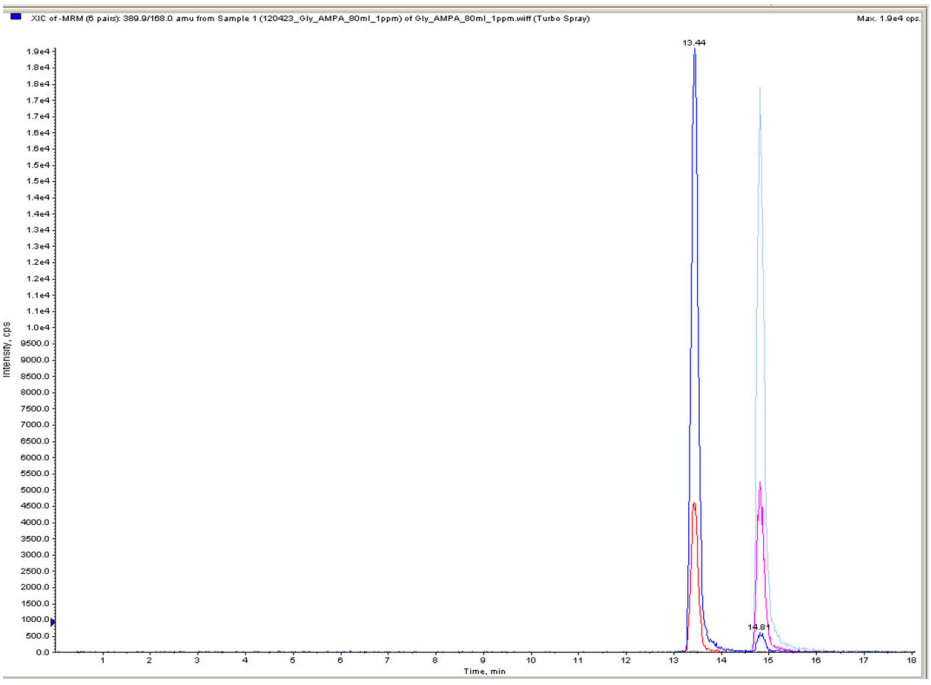

AIV Figure S4: chromatogram of glyphosate-FMOC first blue peak at 13.4 min ($Q_{m/z}$ = 168) and AMPA-FMOC 2nd light blue peak at 14.9 min ($Q_{m/z}$ = 150) at 1 mgL^{-1} concentration

Isotopic mass balance calculations

Carbon isotope mass balance

In Figure 4-5 (a), the non adsorbed glyphosate fraction was approx. 0.2 that corresponded to carbon isotope ratio of -27‰. The input carbon isotope ratio was -28.9 ‰. Using equation 4-3, the $\delta^{13}C$ values of adsorbed glyphosate would be -29.3 ‰ which corresponds to a decrease by 0.4‰.

$$\delta\ ^{13}C^{0} = \delta\ ^{13}C^{A} \times F^{A} + \delta\ ^{13}C^{NA} \times F^{NA}$$

Nitrogen isotope mass balance

In a similar way, the non adsorbed glyphosate fraction was approx. 0.2 that corresponded to carbon isotope ratio of 5‰. The input carbon isotope ratio was -0.3 ‰. The $\delta^{15}N$ values of adsorbed glyphosate would be -1.6 ‰ which corresponds to a decrease by 0.8‰.

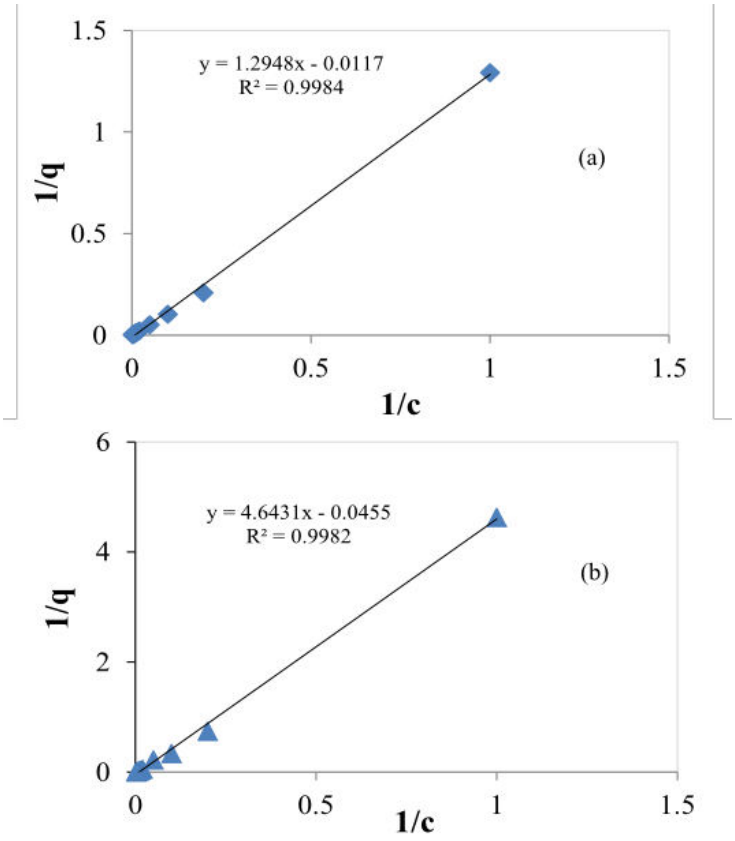

AIV: Figure S5. Panel (a) Langmuir adsorption isotherm model for activated alumina Panel (b) Langmuir adsorption isotherm model for goethite

AIV: Figure S6. Picture of the glyphosate extraction setup with packed activated alumina

Appendix V: CURRICULUM VITAE/LEBENSLAUF

Name	Emmanuel Onyonka Mogusu
Date of birth	18 .02.1983
Place of birth	Nairobi, Kenya
Address	Ingolstädter Landstr. 1, D-85764 Neuherberg, MUNICH
Nationality	Kenyan
Occupation	Research Scientist

Oct 2011-Sept 2015	PhD Student (Environmental Analytical Isotope Chemistry) - EBERHARD KARLS UNIVERSITÄT TÜBINGEN in collaboration with the institute of groundwater Ecology (Helmholtz-center of research- Munich) Thesis title: "**Compound Specific Isotopic Analysis to Investigate Sources and Degradation of Glyphosate**".
April- Sept 2011	German Language course – Goethite Institute Mannheim (A.1, A.2, B.1, B.2.2)
April –April 2011	**Assistant Lecturer**- teaching at Mwenge University College Tanzania. Preparation of lecture classes and organize chemistry practical.
July – April 2010	**Assistant Lecturer**- teaching at Bugema University Kampala, Uganda. Preparation of lecture classes and organize chemistry practical.
April 2008 – July 2009	**Part-time Lecturer-** as an instructor at Mount Kenya University. Organize practical experiments and lecture classes.

Education

June 2005 – Dec 2007	**Masters of Science (Msc) in Analytical Chemistry-** Periyar University Salem India. Major subjects: Analytical chemistry Instrumentation & Environmental chemistry. Minor Subject: physical, organic & in-organic chemistry (Grade: Distinction).
Jan – April 2007	Research project dissertation: "**Physiochemical parameters of sugar effluent from Sakty sugar factory (Erode, India) and its effect on ground water**"
June 2002- June 2005	**Bachelor of Science (Bsc)** – Karnataka University Dharward India. Major Subjects: Chemistry, Botany & Industrial microbiology (Grade: Distinction).
1999- 2001	Kenya Certificate of Secondary Education (KCSE) **Grade B plain**

Awards

- **Fellowship with the Duetscher Akademisher Austausch Dienst (DAAD) -** Date of award April 2011- to conduct my PhD thesis – Helmholtz research center. This also included a 6 month German Language course
- **Travel grant** – HELENA graduate school to attend Goldschmidt conference 2014 – Sacramento USA
- **Poster Prize- "($^{13}C/^{12}C$ and $^{15}N/^{14}N$) Dual Element Isotope Analysis of Glyphosate and its Metabolite AMPA to Distinguish sources and Degradation"** – Wasser Conference 2015-Schwerin
- **Travel grant-** Wasserchemishe Gesellschaft (German water Chemistry Society) – to attend Wasser Conference 2015-Schwerin

Research contributions

Publications

- **E. O. Mogusu**, B. Wolbert, M. Jochmann, D. Kujawinski, M. Elsner; *Dual Element ($^{15}N/^{14}N$, $^{13}C/^{12}C$) Isotope Analysis of Glyphosate and AMPA by Derivatization-Gas Chromatography Isotope Ratio Mass Spectrometry (GC/IRMS) Combined with LC/IRMS* Analytical Bioanalytical Chemistry 17 April 2015 **Paper in Forefront**
- **E. O. Mogusu**, B. Wolbert, M. Jochmann, M. Elsner; *Compound-specific Isotope Fractionation during Biodegradation of Glyphosate with Ochrobactrum sp. FrEM*. In preparation to Environmental Science & Technol letters

Conferences

- **Poster:** *Compound-specific nitrogen isotope analysis of glyphosate and AMPA by derivatization – gas chromatography - isotope ratio mass spectrometry* **ASI** conference (**German Association for Stable *Isotope* Research**) *Braunschweig* Germany 8th -10th September 2013
- **Presentation:** *$^{13}C/^{12}C$ and $^{15}N/^{14}N$ isotope analysis of glyphosate during oxidative degradation by MnO_2* – **International conference -Goldschmidt 2014** Sacramento CA USA 8th - 14th June 2014
- **Poster**: *$^{15}N/^{14}N$ isotope fractionation indicates deprotonation during glyphosate oxidative degradation at MnO_2 surface.* **International Symposium for biogeochemical interaction** in soil at Helmholtz Gemeinshaft, Leipzig Germany 8th - 12th October 2014
- **Poster***: $^{13}C/^{12}C$ isotope fractionation of glyphosate during biodegradation with soil isolated bacteria.* **Arbeitgemendshaft Stabile isotope (ASI)** at Helmholtz research center, Munich Germany 15th -19th October 2014
- **Poster***: "($^{13}C/^{12}C$ and $^{15}N/^{14}N$) Dual Element Isotope Analysis of Glyphosate and its Metabolite AMPA to Distinguish sources and Degradation" -* ***Wasser 2015 conference*** *Jahrestagung der* Wasserchemishe Gesellschaft Schwerin 12th – 15th May Germany 2015